



THE UNIVERSITY *of* EDINBURGH

This thesis has been submitted in fulfilment of the requirements for a postgraduate degree (e.g. PhD, MPhil, DClinPsychol) at the University of Edinburgh. Please note the following terms and conditions of use:

This work is protected by copyright and other intellectual property rights, which are retained by the thesis author, unless otherwise stated.

A copy can be downloaded for personal non-commercial research or study, without prior permission or charge.

This thesis cannot be reproduced or quoted extensively from without first obtaining permission in writing from the author.

The content must not be changed in any way or sold commercially in any format or medium without the formal permission of the author.

When referring to this work, full bibliographic details including the author, title, awarding institution and date of the thesis must be given.

Phosphate sensing and signalling in
Arabidopsis thaliana

Xin Tian

Doctor of Philosophy

The University of Edinburgh

2013

Abstract:

Phosphate (Pi) deficiency is a global problem for food production. Plants have evolved complex mechanisms to adapt to low Pi. We focused on the initial aspects of adaptation to low Pi - perception and immediate-early responses to changes in external Pi.

To examine whether a labile repressor controls expression of the high affinity Pi transporter, *Pht1;1*, we performed electrophoretic mobility shift assays (EMSA) but observed only weak protein-DNA binding activity using extracts from *Arabidopsis* suspension cultures or seedlings. The regulatory role of different regions in *Pht1;1* promoter was dissected by promoter deletion analysis, using *uidA* as a reporter. We identified two domains important for regulation: sequences between -1898 bp and -932 bp are important for induction of *Pht1;1* in low Pi; the intron in the 5'UTR impacts *Pht1;1* expression in the young part of both primary and lateral root apices.

A complementary approach to identify repressors of Pi starvation responses was pursued: We identified ZAT18, a putative transcription factor, as a candidate repressor. ZAT18 contains an EAR motif, a repressor domain in plants; the expression of ZAT18 responds to Pi starvation. Using transgenic lines with promoter::ZAT18-VENUS constructs, we studied its expression, localization and abundance in different levels of Pi availability: ZAT18 is mainly expressed in the nucleus of *Arabidopsis* root hair cells. Its accumulation was induced by 4 day Pi starvation.

We also performed a microarray analysis to examine global gene expression levels during Pi starvation and rapid recovery. Our data indicated that 258 genes were induced and 188 genes were suppressed during Pi starvation. For most of these genes, responses were reversed after 4 hour Pi recovery. Further study of these genes will help to define targets of the early Pi starvation-signalling pathway.

I declare that the work presented in this thesis is my own and it has not been submitted in any previous application for a degree or qualification. Any contribution made by other parties is clearly acknowledged.

Acknowledgement

First, I would like to express my sincere gratitude to Dr. Peter Doerner, who is not only my supervisor but also dear friend. Three years' PhD study in Doerner group was really productive and exciting with all the guidance and encouragement from Peter. Whenever I met the troubles in my research, Peter was always there to help me and give me advice. He taught me how to face the difficulties and how to approach the problems in a scientific way, which is truly helpful in my way to be a real scientist. I treasure all the moments that we spent together to discuss projects, design experiments and analyze results, from where I felt his enthusiasm and motivation in doing scientific research that deeply influenced me. I could not have imaged having a better supervisor of my PhD study.

I wish to give my thanks to the present and past members of Doerner group for their help in my daily life in the lab, and providing a home-like atmosphere in the office. Also, many thanks to all the members in big lab and all the people who help me in Rutherford Building. Thanks to Dr. Florian Halbritter for helping me with the analysis of the microarray data.

I would like to say a heartfelt thank you to my parents for all their love and always believing in me and encouraging me to pursue my dream. I wish to give my special thanks to my wife, Jun Wu, for her unwavering support of my studying abroad. Without her love and encouragement, I could not complete my PhD.

In the end, I gratefully acknowledge Darwin Trust for funding my study in Edinburgh.

Abbreviation

APase	Acid phosphatase
ATP	Adenosine triphosphate
cDNA	Complementary DNA
CHX	Cycloheximide
Col-0	Ecotype (wild type)
cpm	Counts per minutes
CTAB	Cetyltrimethylammonium bromide
Cyt	Cytochrome
DAVID	The Database for Annotation, Visualization and Integrated Discovery
DEPC	Diethyl pyrocarbonate
DGDG	Digalactosyldiacylglycerol
DNA	Deoxyribonucleic acid
dNTP	Deoxynucleotide Triphosphate
DTT	Dithiothreitol
EDTA	Ethylenediaminetetraacetic acid
EMSA	Electrophoretic mobility shift assay
GFP	Green fluorescent protein
GUS	β -glucuronidase
HEPES	4-(2-hydroxyethyl)-1-piperazineethanesulfonic acid
KIN	Kinetin
LB	Luria-Bertrani medium
LN2	Liquid nitrogen
MES	2-morpholinoethanesulfonic acid
MGDG	Monogalactosyldiacylglycerol
MS	Murashige and Skoog medium
mRNA	Messenger RNA
NCBI	National Center for Biotechnology Information
NEB	New England Biolab
SQDG	Sulfoquinovosyldiacylglycerol

ORF	Open reading frame
P	Phosphorous
P1BS	PHR1 binding site
PCR	Polymerase chain reaction
PHR1	Phosphate starvation response 1
Pi	Phosphate
PSR	Phosphate starvation responsive
RNA	Ribonucleic acid
rcf	Relative centrifugal force
RSA	Root system architecture
RT	Reverse transcription
T-DNA	Transfer DNA
TAIR	The Arabidopsis information center
TE	Tris HCl Ethylenediaminetetraacetic acid
UV	Ultra violet
WT	Wild type

Table of Contents

1. Introduction	1
1.1 Importance of P to plants	1
1.2 Low availability of Pi in the soil	1
1.3 Phosphate transporters in plants	2
1.3.1 The Pht1 transporter family	2
1.3.2 Other phosphate transporters in plants	6
1.4 Plant response to low Phosphate	7
1.4.1 Modification of root system architecture (RSA)	7
1.4.2 Secretion of organic acid and acid phosphatase	9
1.4.3 Biochemical changes under Pi deficiency	10
1.4.4 Changes in gene expression under Pi deficiency	11
1.5 Regulators involved in Pi starvation responses	13
1.5.1 PHR1 (Phosphate Starvation Response 1)	13
1.5.2 microRNA 399	14
1.5.3 PHO2	14
1.5.4 AtIPS1 and At4	16
1.5.5 AtSIZ1	17
1.5.6 ZAT6	18
1.5.7 WRKY6 and WRKY75	19
1.6 A potential repressor in Pi signaling pathway	20
2. Materials and methods	25
2.1 Plant material	25
2.2 Plant growth	25
2.2.1 <i>Arabidopsis</i> seed sterilization	25
2.2.2 Media for plant growth and Pi starvation treatment	25
2.2.3 Plant growth condition	28
2.3 Phosphate starvation treatment and inhibitor treatment	28
2.3.1 Phosphate starvation treatment with <i>Arabidopsis</i> seedlings	28
2.3.2 Phosphate starvation treatment and inhibitor treatment with <i>Arabidopsis</i> suspension cell culture	30
2.4 DNA analysis	31

2.4.1 PCR amplification.....	31
2.4.2 Plant genomic DNA preparation with CTAB method for PCR purpose	31
2.4.3 Recombinant DNA construct	32
2.4.4 Transformation of <i>Escherichia coli</i> competent cell.....	32
2.4.5 Plasmid DNA isolation with boiling method.....	32
2.4.6 Plasmid DNA isolation with commercial Kit	33
2.4.7 Transformation of <i>Agrobacterium tumefaciens</i> competent cell.....	33
2.4.8 Vector construction for <i>Pht1;1</i> promoter deletion analysis	34
2.5 Transcriptional analysis	35
2.5.1 RNA isolation from plant materials	35
2.5.2 DNase treatment of RNA samples.....	35
2.5.3 Reverse transcription reaction.....	36
2.5.4 Quantitative Real-time PCR	36
2.6 Arabidopsis transformation by floral dip method	37
2.7. GUS histochemical assay	38
2.8. Electrophoretic mobility shift assay	38
2.8.1 Probe labeling and purification.....	38
2.8.2 Total protein isolation from plant material	39
2.8.3 Protein-DNA binding reaction.....	39
2.8.4 Visualization of protein-DNA complex.....	39
2.9 Microarray analysis	40
3. Electrophoretic mobility shift assays show weak binding activity of unknown proteins to the <i>Pht1;1</i> promoter.....	41
3.1 Introduction.....	41
3.2 Results.....	44
3.2.1 EMSA experimental system setup.....	44
3.2.2 Test protein-DNA binding activity between <i>Pht1;1</i> promoter and unknown proteins.....	48
3.2.3 Sequence difference of the <i>Pht1;1</i> promoter in Col-0 and Ler background.....	57
3.3 Discussion	61
4. Early transcriptional responses to phosphate starvation in <i>Arabidopsis</i>	64

4.1 Introduction.....	64
4.2 Results.....	64
4.2.1 Expression kinetics of phosphate starvation responsive genes in <i>Arabidopsis</i> suspension cell cultures during Pi deprivation.....	64
4.2.2 Expression kinetics of phosphate starvation responsive genes in <i>Arabidopsis</i> seedlings during Pi deprivation.....	73
4.3 Discussion.....	78
5. <i>AtPht1;1</i> promoter deletion.....	82
5.1 Introduction.....	82
5.2 Results.....	83
5.2.1 Construction of a promoter deletion series for <i>AtPht1;1</i>	83
5.2.2 Histochemical staining analysis of <i>uidA</i> expression driven by full-length <i>Pht1;1</i> promoter in <i>Arabidopsis</i> roots	84
5.2.3 Deletion of fragments affected expression of reporter gene in <i>Arabidopsis</i> roots under both Pi sufficient and Pi deficient condition.....	87
5.2.4 The intron in the 5'UTR regulates the spatio-temporal expression of <i>Pht1;1</i> gene expression	90
5.3 Discussion.....	91
6 <i>Zat18</i> is a new regulator in phosphate starvation response	94
6.1 Introduction.....	94
6.2 Results.....	96
6.2.1 Identification of <i>Zat18</i> as a transcriptional regulator, possibly a repressor	96
6.2.2 Low Pi induces <i>Zat18</i> expression and increases <i>ZAT18</i> accumulation in <i>Arabidopsis</i> roots.....	100
6.3. Discussion	102
7. Transcriptomic analysis of gene expression in Col-0 wild type roots under different Pi conditions	104
7.1 Introduction.....	104
7.2 Results.....	107
7.2.1 Experimental design.....	107
7.2.2 Overview of regulated gene expression in <i>Arabidopsis</i> seedling roots identified by microarray analysis.....	108

7.2.3 Expression profiles of Pi starvation responsive (PSR) genes during Pi recovery	109
7.2.4 Comparison across different microarray datasets.....	114
7.2.5 A robust list of rapid Pi responsive marker genes.....	116
7.3 Discussion.....	121
8. Summary and Discussion.....	124
9. References	130
List of tables.....	141
List of figures.....	141
Appendix1	144

1. Introduction

1.1 Importance of P to plants

Phosphorus (P) is one of 17 essential mineral elements required for plant growth and development (Bielecki, 1973), of which the oxyanion phosphate is the only form that plants can utilize. Phosphorus also participates in many cellular processes, including energy conservation, carbon assimilation, photosynthesis, respiration, and regulation of a number of enzymes. As structural component of macromolecules, phosphate forms the basic skeleton of DNA and RNA. The bridging form of the P diester is also abundant in phospholipids of biomembranes. Many phosphate esters are intermediates in metabolic pathways of biosynthesis and degradation. Another pivotal role that phosphorus plays is the control of cell signalling pathways through phosphorylation of proteins and lipids during plant responses to developmental and environmental cues (Marschner, 1995). Thus, the availability of phosphorus in soil can have a profound effect on plant growth, development and crop productivity.

1.2 Low availability of Pi in the soil.

Although the total amount of P in the soil may be high, it is often present in unavailable forms. For plants, the oxyanion phosphate (Pi) is the only form of phosphorous they can assimilate. However, many soils throughout the world are Pi-deficient, and even in the more fertile soils, the Pi concentration of the soil solution is rarely higher than 10 μM (Bielecki, 1973). In most soils, the concentration ($\sim 2 \mu\text{M}$) of available Pi in soil solution is several orders of magnitude lower than that in plant tissues (5–20 mM) (Marschner, 1995).

The level of Pi in soil solution is regulated mainly by its interaction with organic or inorganic surfaces. In soils, up to 30%–80% phosphorus is present in organic forms, of which phytic acid (inositol hexaphosphate) is usually a major component (Richardson, 1994). The organic form of phosphorus must be mineralized to the inorganic form before it becomes available to plants. However, the inorganic form of phosphorus is easily precipitated with common cations like calcium (Ca), magnesium (Mg), iron (Fe) and aluminum (Al), which render it unavailable to plants. Plants must also compete with microorganisms to obtain Pi under nutrient-limiting

conditions. Therefore, the low concentration of Pi in the soil solution is a major factor limiting growth in many natural ecosystems.

1.3 Phosphate transporters in plants

Plants cells are separated from the environment by plasma membranes. To acquire Pi, plants need to transport Pi across the plasma membrane through a series of high-affinity Pi transporters, which are membrane-associated proteins. In *Arabidopsis*, four Pi transporter families, designated Pht1, Pht2, Pht3, and Pht4, were identified (Poirier and Bucher, 2002; Guo *et al.*, 2008). Among them, members of the Pht1 family are high-affinity Pi/H⁺ symporters located in the plasma membrane. Pht1 transporters function to acquire Pi from the rhizosphere because most of them are expressed in root epidermal cells, whereas other PHT families are located in the endomembrane systems.

1.3.1 The Pht1 transporter family

The first two phosphate transporters, AtPT1 and AtPT2, were isolated in *Arabidopsis* by screening a cDNA library prepared from phosphate-starved root samples (Muchhal *et al.*, 1996). Their polypeptides shared over 70% identity to each other and a high degree of amino acid similarity to high-affinity phosphate transporters in yeast and fungus. Both of transporters were sufficient to complement the phenotype of the *pho84* yeast mutant that lack high-affinity Pi transporter. Since then, a few more phosphate transporters were identified in many plant species, including MtPT1 and MtPT2 in *Medicago truncatula* (Liu *et al.*, 1998), LePT1 and LePT2 in *Lycopersicon esculentum* (Daram *et al.*, 1998; Liu, 1998), StPT1 and StPT2 in *Solanum tuberosum* (Leggewie *et al.*, 1997), PIT1 in *Catharanthus roseus* (Kai *et al.*, 1997).

In *Arabidopsis*, a total of nine closely related members, *Pht1;1* to *Pht1;9*, were identified by BLAST searches against the *Arabidopsis* whole genome (Table1.1). Expression pattern analysis showed that these transporters are predominantly expressed in plant root tissues, except for *Pht1;6* (Mudge, *et al.*, 2003), which is expressed mainly in anthers. *Pht1;1* and *Pht1;4*, previously known as *AtPT1* and *AtPT2*, respectively, have the highest expression in Pi-starved roots. Over-expression of *Pht1;1* in tobacco cell cultures increased Pi uptake and thus enhanced cell

proliferation when Pi was limited (Mitsukawa *et al.*, 1997). The Pi uptake rate of *Pht1;1* T-DNA knockout mutants is reduced to 80% of the wild-type level under low Pi conditions and 60% of the wild-type level under Pi sufficient conditions (Shin *et al.*, 2004). The decrease in Pi uptake results in lower Pi content in the shoots of *pht1;1* mutants. This confirms the importance of *Pht1;1* in Pi acquisition under both Pi-sufficient and Pi-deficient conditions. However, although *pht1;4* mutants also display a 23–43% reduction in Pi uptake under low Pi conditions, the Pi content in *pht1;4* mutants is similar to that in wild type plants (Misson *et al.*, 2004; Shin *et al.*, 2004). The authors concluded that PHT1;4-dependent Pi uptake may not be a limiting factor for growth. Nevertheless, the *pht1;1/pht1;4* double mutant has a significant decrease in Pi uptake and accumulation of shoot Pi under both Pi-sufficient and Pi-deficient conditions, which indicates that the effect of *Pht1;1* and *Pht1;4* knockout is additive (Shin *et al.*, 2004). Because of low internal Pi concentrations, Pi starvation symptoms were accelerated in the *pht1;1/pht1;4* plants when Pi was limited. In parallel with the studies in *Arabidopsis*, in tomato, Pi uptake and biomass were reduced in a transposon-insertion line defective in a Pi transporter, LePT4 (Xu *et al.*, 2007).

Table1.1 Pht1 family in *Arabidopsis*

Gene name	Protein entry code	Former name(s)
<i>ARATH; Pht1;1</i>	At5g43350	<i>PHT1, APT2, AtPT1</i>
<i>ARATH; Pht1;2</i>	At5g43370	<i>PHT2, APT1</i>
<i>ARATH; Pht1;3</i>	At5g43360	<i>PHT3, AtPT4</i>
<i>ARATH; Pht1;4</i>	At2g38940	<i>PHT4, AtPT2</i>
<i>ARATH; Pht1;5</i>	At2g32830	<i>PHT5</i>
<i>ARATH; Pht1;6</i>	At5g43340	<i>PHT6</i>
<i>ARATH; Pht1;7</i>	At3g54700	-
<i>ARATH; Pht1;8</i>	At1g20860	-
<i>ARATH; Pht1;9</i>	At1g76430	-

These nine Pht1 phosphate transporter genes are located on chromosome 1, 2, 3, 5 respectively. Interestingly, *Pht1;1*, *Pht1;2*, *Pht1;3*, and *Pht1;6* are clustered within 24,200 bp on chromosome 5, suggesting that several gene duplication events might occur during the molecular evolution of the Pht1 gene family. Phylogenetic analysis showed that *Pht1;1* and *Pht1;2* were most closely related, which suggested they might share a common ancestral gene and were evolutionary younger than *Pht1;6* (*Fig. 1.1*) (Poirier and Bucher, 2002).

Structural analysis of Pht1 family transporters across different plant species showed high similarity (Raghothama, 1999; Poirier and Bucher, 2002). Based on computational analysis, their secondary structures are predicted to have twelve hydrophobic domains presumably spanning the plasma membrane, a hydrophilic N and C terminus localized in the cytoplasm and a large hydrophilic loop between trans-membrane spanning domains 6 and 7 (Poirier and Bucher, 2002).

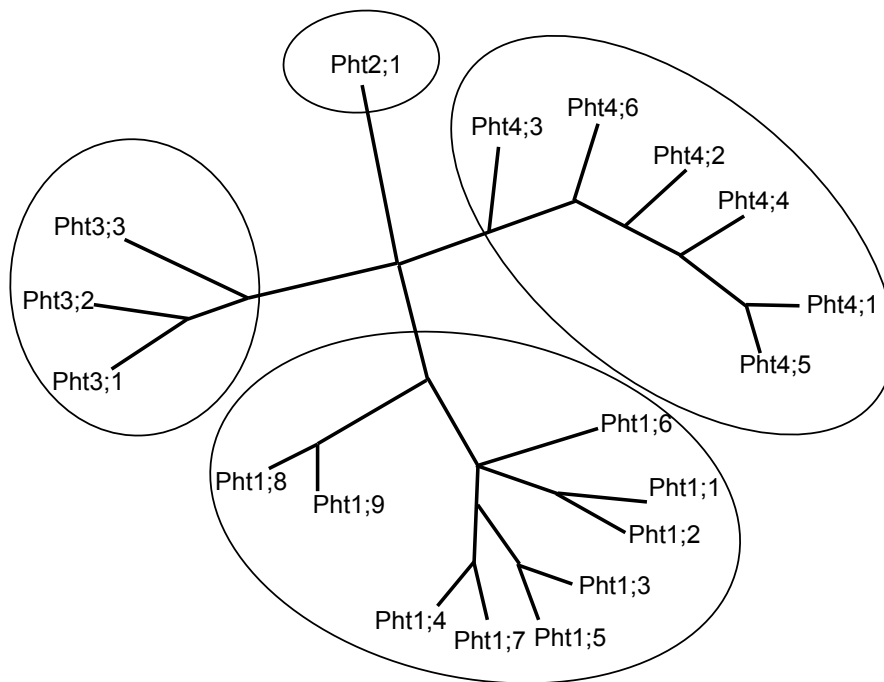


Fig.1.1 Phylogenetic analysis of *Arabidopsis* phosphate transporter protein sequences. The map is updated with online tool (<http://phylogeny.lirmm.fr/phylo.cgi/index.cgi>) based on the result published by Poirier and Bucher in 2002 (Poirier and Bucher, 2002).

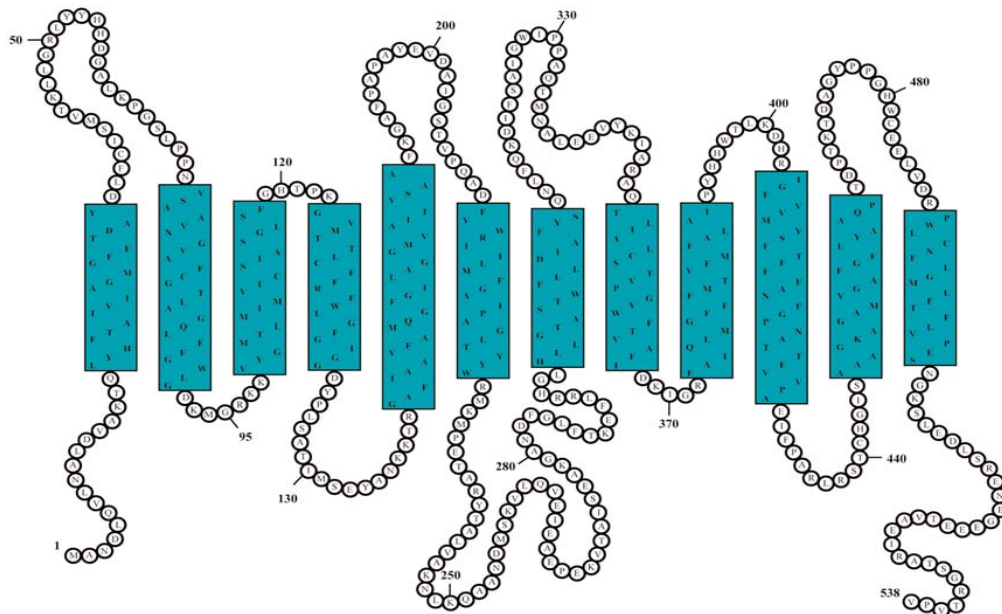


Fig.1.2 Predicted topology of the tomato Pht1;1 (LePT1) Pi transporter (Daram *et al.*, 1998) typical for Pht1;1 proteins, with 12 transmembrane helices, a cytoplasmic N and C terminus and a long cytoplasmic loop between transmembrane helices 6 and 7. Numbers indicate amino acids with the start methionine marked as number 1.

1.3.2 Other phosphate transporters in plants

In *Arabidopsis*, three more Pht transporter families were identified other than the Pht1 family, namely Pht2, Pht3 and Pht4 (Poirier and Bucher, 2002). The Pht2 transporter family has only one member in *Arabidopsis*, Pht2;1, which is a low affinity Pi transporter. The expression pattern of *Pht2;1* determined by RNA hybridization showed that its expression was mainly in green leaves while barely detected in roots (Daram *et al.*, 1999). Localization analysis by using PHT2;1-GFP fusion protein showed that the protein was localized in chloroplasts (Versaw, 2002). Study of null mutant *pht2;1-1* plants indicated that PHT2;1 may function in reallocation of Pi between shoots and roots. Under Pi-limited conditions, *pht2;1* mutant plants exhibited reduced Pi content (52–70% of the wild-type level), while increased shoot Pi concentration (129–156% of wild-type level). Moreover, the redistribution of Pi between old and young leaves is impaired in *pht2;1-1*. By contrast, over-expression or suppression of the *PHT2;1* orthologues in potato does not change the leaf Pi content and Pi allocation (Rausch *et al.*, 2004). Whether *PHT2;1* plays different roles in different plant species requires further study.

The Pht4 transporter family has 6 members identified in *Arabidopsis*, designated as *Pht4;1* through *Pht4;6*. Computational analysis indicated Pht4 proteins were structurally related to animal proteins that comprise the SLC17/type I Pi transporter family. PHT4 transporters were shown to predominately localize in plastids in leaves (Roth *et al.*, 2004; Guo *et al.*, 2008). More specifically, PHT4;2 and PHT4;5 were localized to chloroplast, shown by GFP fusion protein, while PHT4;6-GFP co-localized with a Golgi marker (Guo *et al.*, 2008). Complementation of PHT4 transporters into yeast Pi transport defective mutant showed that all members were capable of mediating Pi transport. Arsenate, a structural analog of Pi, can compete for the transport activity of PHT4 transporters, but not glutamate, chloride, sulfate or nitrite, which indicated the specificity for Pi (Guo *et al.*, 2008). However, the specific function of PHT4 transporters in plant cells is still poorly understood.

PHO1 is another kind of Pi transporter. The *pho1* mutant has normal Pi uptake and root Pi concentrations, but lower shoot Pi concentration, indicating that PHO1 may participate in Pi loading into the xylem and the subsequent translocation of Pi from

the roots to the shoots (Poirier *et al.*, 1991). The PHO1 protein was later revealed to harbor a hydrophilic N-terminal SPX (SYG1/Pho81/XPR1) tripartite domain followed by a six-trans-membrane spanning domain of EXS at the C-terminus (Hamburger, 2002; Wang *et al.*, 2004). Of note is that proteins with the SPX domain in *Saccharomyces cerevisiae* play important roles in Pi transport or sensing or in sorting Pi into endo-membranes (Lenburg and O'Shea, 1996). PHO1 is expressed predominantly in the vascular cells of roots and may contribute to the xylem loading of Pi (Hamburger, 2002), although the Pi transport activity of PHO1 has not been demonstrated.

1.4 Plant response to low Phosphate

As a nonrenewable resource, Pi deficiency has become a global problem (Bielecki, 1973; Raghothama, 1999). In response to persistently low levels of available Pi in the rhizosphere, plants have developed highly specialized mechanisms to acquire and utilize Pi from the environment (Table 1.2) (Raghothama, 1999).

Table 1.2 Multiple responses of plants to phosphate deficiency

Morphological responses

Increased root:shoot ratio; changes in root morphology and architecture; increased root hair proliferation; root hair elongation; accumulation of anthocyanin pigments; proteoid root formation; increased association with mycorrhizal fungi

Physiological

Enhanced Pi uptake; reduced Pi efflux; increased Pi use efficiency; mobilization of Pi from the vacuole to cytoplasm; increased translocation of phosphorus within plants; retention of more Pi in roots; secretion of organic acids, protons and chelators; secretion of phosphatases and RNases; altered respiration, carbon metabolism, photosynthesis, nitrogen fixation and aromatic enzyme pathways

Biochemical

Activation of enzymes; enhanced production of phosphatases, RNases and organic acids; changes in protein phosphorylation, activation of glycolytic bypass pathway

Molecular

Activation of genes (RNases, phosphatases, phosphate transporters, Ca-ATPase, vegetative storage proteins, β -glucosidase, PEPCase and novel genes such as *TPSII*, *Mt 4*)

1.4.1 Modification of root system architecture (RSA)

Root system architecture (RSA) refers to the complexity of root system spatial configurations that arise in response to soil conditions. It includes root morphology,

topology and distribution patterns (Lynch, 1995; Lynch *et al.*, 2005). Modification of root growth and architecture is a well-documented response to Pi starvation (Bonser *et al.*, 1996; Williamson *et al.*, 2001). Under Pi deficient conditions, a typical hallmark of the plant response is the increased root-to-shoot ratio, which enhances the total surface area available for soil exploration and acquisition of nutrients to maintain plant growth. Plants with a more branched root system that is efficient in uptake are well suited to exploit soil Pi.

In the study with common bean (*Phaseolus vulgaris*), Bonser *et al* have shown that bean plants grown on low phosphate change the angle of growth of basal roots in favor of outward rather than downward growth, which facilitate acquisition of P from the topsoil (Bonser *et al.*, 1996). Adaptations that enhance acquisition of P from topsoil are important because phosphate availability is greater in surface soils or near-surface horizons than in the subsoil. In *Arabidopsis*, high phosphate supply stimulates primary root growth while inhibit lateral root density and suppress lateral root elongation (Linkohr *et al.*, 2002). However, growth on low Pi media results in a redistribution of root growth from the primary root to lateral root. Reduced primary root elongation under low Pi condition was accompanied by increased lateral root density and growth (Williamson *et al.*, 2001).

In low phosphate conditions, increased root hair density and elongation is an essential trait in RSA modification. Root hairs are tubular-shaped cells specialized for nutrient uptake (Gilroy and Jones, 2000). In P-deficient soil, the length and density of *Arabidopsis* root hairs increase massively, expanding the root's surface area from 0.21 mm²/mm root under P-sufficient conditions to 1.44 mm²/mm root under P-starvation conditions, with the root hairs constituting 91% of the root's total surface area (Bates and Lynch, 1996).

Formation of cluster roots (proteoid roots) under Pi deficiency is another well-characterized response in plants. Cluster roots are formed in most members of Proteaceae and other species adapted to habitats of extremely low Pi fertility (Louis *et al.*, 1990; Skene, 2000; Adams *et al.*, 2002). Formation of cluster roots is the result of a highly coordinated modification of root development and biochemistry. Cluster roots are composed of bottlebrush-like clusters of rootlets covered with a super-

dense of root hairs that develop on lateral roots (Keerthisinghe *et al.*, 1998). The secretion of organic acids is increased from cluster roots to aid the release of Pi from Ca, Fe, and Al phosphate, via chelation of the metal. In addition, phosphatase production is also increased to release the Pi from organic complexes (Tadano *et al.*, 1993).

In most vascular land plants, the root system can be widely colonized by arbuscular mycorrhizal (AM) fungi from soil, which provide an efficient way to increase the mineral nutrition of the plant. In this symbiotic system, the AM fungi rely on the plants as their carbon source. In exchange, the fungi enhance plant growth by increasing the uptake of nutrients, particularly the acquisition of phosphorus from environment. Previous studies showed that the influx of P into roots colonized by mycorrhizae can be 3 to 5 times higher than that in non-colonized (NC) roots (Smith and Read, 1997). In soil, the AM fungi grow extensively to form a complicated hyphal network that can efficiently uptake Pi. As the individual fungal hyphae have a much smaller diameter than roots, these can grow through narrower soil pores and increase the soil volume explored. In the plants, the fungus invades the roots through the growth of the hyphal germ tube. Once inside the cortex cells, the fungus differentiates to form a highly branched structure called an arbuscule, which is then enveloped by a specialized membrane known as periarbuscular membrane. This highly-developed structure provides a very effective pathway by which P is scavenged from large volumes of soil and rapidly delivered to cortical cells within the root, bypassing direct uptake by the root epidermis. Several studies have shown that the Pi depletion zone around plant roots was larger in AM plants than NC plants (Bolan, 1991).

1.4.2 Secretion of organic acid and acid phosphatase

In many ecosystems, the low availability of Pi is a major factor determining plant productivity. As most P exists in immobile form, it has to be solubilized before being taken up by plant roots. Under Pi deficiency, plants secrete increased amounts of organic acid into the environment and alter rhizosphere chemistry to release free Pi to the soil. When grown in low Pi conditions, cluster roots of white lupin synthesize and exude 20- to 40- fold more malate and citrate, which allows chelation of Al^{3+} ,

Fe^{2+} , Ca^{2+} , and subsequent displacement of Pi from its bound and precipitated form (Johnson *et al.*, 1996; Keerthisinghe *et al.*, 1998).

In soils, a large portion of Pi may be present in organic forms. The organic P complexes need to be broken down by enzymatic activity before the inorganic Pi is released into the rhizosphere. A universal response by plants to Pi deficiency is the synthesis and secretion of acid phosphatase (APase). These phosphatases produced by plants may be involved in degradation of organic P-complexes. The first APase identified in *Arabidopsis* was AtACP5, which is a type 5 purple acid phosphatase (del Pozo *et al.*, 1999). Molecular studies on AtACP5 showed it has 338 amino acids, including a 31 amino acid N-terminal extension with characteristics of a membrane targeting signal peptide. AtACP5 expression is highly induced in both root and shoot under Pi deficient conditions. However, there is at present no evidence that AtACP5 protein is secreted, which indicates the function of AtACP5 is more involved in internal P remobilization than Pi acquisition. The first truly secreted APase identified in *Arabidopsis* is AtAPse (Haran *et al.*, 2000). The gene is highly induced by Pi deficiency. When fused to GFP fluorescent protein as reporter, GFP was detected in root exudates of Pi-starved plants.

1.4.3 Biochemical changes under Pi deficiency

Changes in biochemical processes commonly occur during Pi deficiency. In response to Pi limitation, many plants show remarkable flexibility in adjusting metabolic rates and utilizing alternative metabolic pathways. The levels of ATP and all of the nucleotides are significantly reduced during Pi starvation of plant cell cultures and P_{pi} (pyrophosphate), which is maintained at high levels, may function as an autonomous energy donor. During Pi starvation, enzymes that do not require nucleotide phosphates or Pi as substrate(s) are activated. These enzymes are considered to be adaptive enzymes of the glycolytic pathway during Pi starvation, and they are involved in “bypass reactions” that circumvent Pi and adenylate-requiring steps in glycolysis, thus permitting carbon metabolism to proceed during Pi starvation. Pi limitation also causes significant modification of the lipid composition in membranes. In response to P-deficiency, thylakoid membranes show decreased amounts of phospholipids accompanied by increased levels of the sulfolipid

sulfoquinovosyldiacylglycerol (SQDG) and galactolipid digalactosyldiacylglycerol (DGDG) membrane lipids. In *Arabidopsis*, SQD1 and SQD2 catalyze the two steps in the sulfolipid synthesis pathway. It has been shown that the expression of both SQD1 and SQD2 is induced during P-deficiency. Moreover, mutation in SQD2 impairs *Arabidopsis* growth under Pi starvation conditions (Yu *et al.*, 2002). Similarly, the accumulation of enzymes involved in biosynthesis of galactolipid was also increased during Pi starvation (Awai *et al.*, 2001; Kobayashi *et al.*, 2004). Monogalactosyldiacylglycerol (MGDG) is the simplest form of galactolipids, which constitutes up to 50% of thylakoid membrane lipids in chloroplasts. MGDG is also the substrate for the biosynthesis of digalactosyldiacylglycerol (DGDG); therefore, the MGDG synthases become the key enzymes in biosynthesis of galactolipids. In *Arabidopsis*, three functional MGDG synthases, MGD1, MGD2 and MGD3, have been identified and classified into type-A (MGD1) and type-B (MGD2 and MGD3) enzymes according to their amino acid identity (Awai *et al.*, 2001). During Pi starvation, the type-B enzymes (MGD2 and MGD3) were dramatically up regulated (Awai *et al.*, 2001). Mutation analysis also showed that the MGD3 was the main isoform in membrane lipid remodeling during Pi starvation (Kobayashi *et al.*, 2004).

1.4.4 Changes in gene expression under Pi deficiency

The expression of many genes is changed in response to Pi starvation. Changes to the accumulation and secretion of different proteins/enzymes are a good indicator of extensive changes in gene expression. Phosphate starvation responsive (PSR) genes can be generally divided into 3 categories. The first category includes genes involved in mobilizing the Pi from inorganic/organic sources. In *Arabidopsis*, two of the well-characterized senescence-associated RNase genes (RNS1 and RNS2) were shown to be induced under Pi starvation conditions (Bariola *et al.*, 1994). The expression of the purple acid phosphatase encoding gene, *AtACP5*, is also enhanced in response to Pi starvation (del Pozo *et al.*, 1999). These enzymes could release Pi from nucleotides or other molecules in the extracellular space, including those derived from other organisms in the rhizosphere.

The second category mainly includes the phosphate transporter encoding genes. Up-regulation of phosphate transporters could facilitate increased Pi uptake from the

environment and Pi remobilization within the plant. In *Arabidopsis*, nine members of *Pht1* gene family were identified by genome analysis. Expression analysis showed that five genes were predominantly expressed in root, while transcripts of four genes were detectable in both root and shoot organs. Under P-deficiency, the expression of all nine genes was enhanced (Bari *et al.*, 2006). Similarly, expression of transporter genes from root of potato (StPT1, StPT2) (Leggewie *et al.*, 1997), *Medicago truncatula* (MtPT1, MtPT2) (Liu *et al.*, 1998), and tomato (LePT1, LePT2) (Daram *et al.*, 1998; Liu *et al.*, 1997) was induced during growth in Pi deficient environment.

The third category is comprised of regulatory genes involved in Pi starvation responses. MicroRNAs were recently identified as a novel class of regulators involved in many biological processes. Under Pi deficiency, miR399 is highly induced in *Arabidopsis* (Aung *et al.*, 2006). Further study identified that miR399 targets *PHO2*, an ubiquitin-conjugating E2 enzyme encoding gene (Aung *et al.*, 2006; Bari *et al.*, 2006). Mutation of *PHO2* caused 2- to 4-fold increase in the amount of Pi in leaves compared to wild type plants while Pi content in the root stays unchanged. Furthermore, the promoter of miR399 genes contains P1BS (PHR1-bind site) motifs, which indicate its regulation by PHR1, a central transcription factor in the Pi starvation signalling pathway. A recent study also reveals that PHO2 functions through targeting PHO1, a potential Pi transporter that loads Pi into xylem, for degradation (Liu *et al.*, 2012). In *Arabidopsis*, several transcription factors were identified to be induced by Pi starvation, including ZAT6 (Devaiah *et al.*, 2007a), WRKY75 (Devaiah *et al.*, 2007b), bHLH32 (Chen *et al.*, 2007), SPX1 (Duan *et al.*, 2008) etc.

In recent years, high-through-put profiling methods were applied to analyze global changes in gene expression under Pi deficiency. These genome wide analyses provide valuable information to understand the gene expression profiles at the whole transcriptome level. In 2005, Misson *et al.* (2005) performed microarray analysis on global gene expression in response to Pi starvation using the *Arabidopsis thaliana* whole genome Affymetrix gene chip (Misson *et al.*, 2005). The data revealed a coordinated induction and suppression of 612 and 254 Pi-responsive genes, respectively. Functional classification of some of these genes indicated their involvement in various metabolic pathways, ion transport, signal transduction,

transcriptional regulation, and other processes related to growth and development. Another microarray analysis conducted by Woo *et al.* in 2012 used a different experiment design. This study included *Arabidopsis* shoot and root samples separately, subjected to long Pi starvation followed by return to Pi replete conditions (Woo *et al.*, 2012). A total of 1257 genes detected by ATH1 probe-sets were differentially expressed in roots during either starvation or recovery, while 182 genes with changed expression were identified in shoots. By comparing two different technological platforms to determine transcriptome changes, they found that the majority of known Pi-responsive genes were initially responsive. An even more detailed analysis was applied to dissect the local and systemic transcriptional responses to Pi starvation in *Arabidopsis* roots (Thibaud *et al.*, 2010). They found 412 and 351 genes significantly up- or down-regulated by Pi starvation, respectively, among which 301 induced and 240 repressed genes were locally regulated.

1.5 Regulators involved in Pi starvation responses

1.5.1 PHR1 (Phosphate Starvation Response 1)

PHR1 was the first transcription factor identified that was strongly linked to plant Pi starvation responses (Rubio, 2001). The *phr1* mutant was isolated by a screen for plants with altered Pi starvation responses in a mutagenized population harboring a reporter gene specifically responsive to Pi starvation (*AtIPS1::GUS*). Mutation in *PHR1* results in a reduced induction of *AtIPS1::GUS* in response to Pi starvation, and also had a broad range of Pi starvation responses impaired, including the responsiveness of various other Pi starvation-induced genes and metabolic responses, such as an increase in anthocyanin accumulation. Further studies showed that *PHR1* encodes a member of MYB superfamily and PHR1 can bind to the P1BS (PHR1 binding sequence) *cis*-element (GNATATNC) of several PSR (Phosphate Starvation Responsive) genes (Rubio, 2001). Further work involved the analysis of a T-DNA knockout allele of *phr1* and PHR1-overexpressing *Arabidopsis* plants (Nilsson *et al.*, 2007). Over-expression of *PHR1* leads to an increased concentration of Pi in the shoots, together with the elevated expression of a range of Pi starvation-induced genes, including ones that encode a Pi transporter, phosphatase and RNase (Nilsson *et al.*, 2007). However, *PHR1* expression is not responsive to Pi starvation and it

controls only a small subset of Pi starvation responses, suggesting the existence of other regulators (Rubio, 2001).

1.5.2 microRNA 399

MicroRNA (miRNA) have been widely recognized as a novel type of regulator of gene expression in plants and animals. In *Arabidopsis*, miR399 was identified as the first microRNA that was involved in Pi starvation responses in 2005 (Fujii *et al.*, 2005). miR399 has six loci in the *Arabidopsis* genome. Its target was predicted to be a gene encoding a putative ubiquitin-conjugating enzyme (UBC) which was subsequently identified as PHO2 (Fujii *et al.*, 2005; Bari *et al.*, 2006). miR399 was specifically induced by low Pi, but not low K or N. Constitutive expression of miR399 suppressed the accumulation of UBC mRNA even under high Pi condition, which indicated the suppression was mediated by miR399. Further study confirmed that miR399 targeted UBC mRNA to regulate its expression, and the regulation required 5'UTR region of UBC mRNA. Plants that constitutively express miR399 could mimic the phenotype of *pho2* mutant in terms of over-accumulation of Pi in leaves and causing Pi toxicity.

1.5.3 PHO2

The *pho2* mutant was isolated by screening a ethyl methylsulfonate (EMS) mutagenized population in the Col-0 background for seedlings showing higher or lower P content (Delhaize and Randall, 1995). Two mutants, *pho2-1* and *pho2-2*, were identified by this screen, which exhibited Pi toxicity depending on transpiration rate. Growing either in hydroponic culture or on agar plates, the *pho2* mutant showed 2-5-fold higher Pi content in leaves than WT, while the Pi level in root remained unchanged (Delhaize and Randall, 1995). Moreover, *pho2* mutants displayed about a 2-fold greater Pi uptake rate than the wild type under Pi sufficient conditions (Dong *et al.*, 1998). Together, these data indicated that *pho2* mutants have not only a higher Pi uptake rate by the roots, but also a greater capability to translocate more Pi from root to shoot. Further study by Dong *et al.* suggested that the greater uptake rate in *pho2* mutant was possibly due to the shoots providing a constitutive Pi sink, because their data showed that the difference in root Pi uptake rate between *pho2* and WT disappeared when shoots were removed (Dong *et al.*, 1998). Micro-grafting

experiments revealed that a *pho2* root genotype is necessary and sufficient to lead to high Pi levels in the shoot (Bari *et al.*, 2006). *Pho2* was identified by map-based cloning as At2g33770, which encode an ubiquitin-conjugating E3 enzyme. The mutant contains a G to A mutation in At2g33770 that results in replacement of W⁶⁷¹ by a stop codon. The *pho2* mutation does not only affect Pi reallocation between root and shoot, but also affects the expression of a few Pi-starvation-inducible genes. Microarray analysis performed by Bari *et al.* showed that 12 genes in *pho2* reproducibly accumulate higher transcripts levels compared to WT under Pi sufficient conditions, many of which are classic Pi-starvation-inducible genes. A few more genes that are either not included or poorly represented in ATH1 microarray were tested by qRT-PCR analysis. The data showed that *IPS1*, *At4*, *Pht1;8* and *Pht1;9* expression profiles in *pho2* were attenuated in response to Pi. Under Pi sufficient condition, *Pht1;8* and *Pht1;9* expression levels remained higher compared to wild type plants, which could partially explain the higher Pi content in mutant leaves (Bari *et al.*, 2006).

Expression of PHO2 is ubiquitous, based on the analysis of over 720 ATH1 microarray experiments. This is also confirmed by qRT-PCR-based transcript measurements and by analyzing GUS reporter lines where the GUS gene is driven by a 1.8 kb PHO2 putative promoter sequence. Computational analysis of the PHO2 promoter revealed that 5'-UTR region contains 5 nearly identical, 21-nucleotides motifs that are complementary to microRNA399. Experimental data showed that moderate overexpression of miR399f in *Arabidopsis* results in moderate down-regulation of *PHO2* transcripts, while in strong over-expressers, PHO2 expression was reduced to an even lower level. This provides genetic evidence that miR399 species could regulate PHO2 expression (Bari *et al.*, 2006). Further analysis showed that PHO2 transcripts changed reciprocally to miR399 transcripts in Pi-deprived plants, which is consistent with previous data published by Fujii *et al.* (Mukatira *et al.*, 2001; Fujii *et al.*, 2005). Moreover, miR399 expression is under control of PHR1. A signalling pathway that connects PHR1 and PHO2 by abundance of miR399 has been established (Fig. 1.3), which regulates Pi dependent responses like re-allocation of Pi between roots and shoots (Bari *et al.*, 2006). In a more recent study, Liu *et al.* isolated two *pho2* suppressors carrying missense mutations in PHO1, designated

pho1-5 pho2 and *pho1-6 pho2* (Liu *et al.*, 2012). Their study showed that increased accumulation of PHO1 protein in *pho2* mutants was reduced in both suppressors. Data from cycloheximide and E-64 inhibitors treatments suggested that PHO1 degradation was PHO2 dependent. The two proteins were shown to be partially co-localized and physically interact in endo-membranes by transient expression analysis experiments with tobacco leaves, and UBC activity of PHO2 is required for PHO1 degradation. These data affirm PHO1 is a target of PHO2, and functions as a downstream component in the PHO2 signalling pathway (*Fig. 1.3*) (Liu *et al.*, 2012).

1.5.4 *AtIPS1* and *At4*

AtIPS1 and *At4* belong to a small gene family named *TPSII/Mt4* family. The members of this gene family have been identified in several plant species, including *TPSII* from tomato (Liu *et al.*, 1997), *Mt4* from *Medicago truncatula* (Burleigh and Harrison, 1997), *AtIPS1/At4* from *Arabidopsis* (Burleigh and Harrison, 1998; Martín *et al.*, 2000) and *OsPII* from rice (Wasaki *et al.*, 2003). *Mt4* was firstly isolated by a differential screen to identify genes showing altered expression during the interaction between *Medicago truncatula* and the vesicular-arbuscular mycorrhizal (VAM) fungus *Glomus versiforme* (Burleigh and Harrison, 1997). The expression of *Mt4* was down regulated in roots in response to Pi fertilization and colonization by arbuscular mycorrhizal (AM) fungi (Burleigh and Harrison, 1998). The orthologous gene in *Arabidopsis*, *At4*, was isolated by RNA gel blot using a 30-bp oligonucleotide probe, representing the sequence conserved between *Mt4* and the tomato homolog *TPSII*. *At4* is a single copy gene in *Arabidopsis* genome and its expression is highly induced by Pi deprivation (Burleigh and Harrison, 1998). A T-DNA insertion mutant, *at4*, displayed a reduction in Pi uptake relative to wild type plant. However, an increase in Pi allocation to the shoots was observed during Pi deprivation, which was even magnified in Pi transporter double mutants, *pht1;1Δ4Δ*. This suggested *At4* may function in Pi translocation between roots and shoots in *Arabidopsis* (Shin *et al.*, 2006). Northern blot analysis using the first 21nt of *At4* conserved sequence as probe, detected a ~22nt small RNA in RNA samples prepared from Pi starved root but not from samples of plant root under Pi sufficient conditions (Shin *et al.*, 2006). This implied that *At4* could be regulated by small RNAs on a post-transcriptional level.

AtIPS1 was isolated through differential screen aiming to identify key regulatory components in Pi starvation responses (Martín *et al.*, 2000). Sequence analysis indicated AtIPS1 belonged to TPSI1/Mt4 family. Its cDNA was predicted to contain only short ORFs with longest one to be 24 amino acids. Northern blot analysis showed AtIPS1 was strongly induced in both roots and shoots of plants under Pi starvation, and the induction was specific to Pi stress. This expression profile was also confirmed by analysis of an AtIPS1:GUS fusion expression. Interestingly, cytokinins, but not auxins, could suppress the response of AtIPS1 and other Pi responsive genes during Pi deprivation, including At4, AtPht1;1 and AtACP5. This indicated cytokinins could play a broader role than previously suspected in regulation of Pi-starvation responses (Martín *et al.*, 2000).

Sequence comparison showed a conserved 23nt motif existed in members of TPSI1/Mt4 gene family. This motif showed extensive complementary with miR399, but with critical mismatch including a bulge opposite positions 10–11 of the miRNA (Franco-Zorrilla *et al.*, 2007). It has been proved that sequence complementary in this region is strictly required for miRNA-guided cleavage of mRNA target. This indicated AtIPS1/At4 might affect the target mRNA degradation mediated by miR399 in *Arabidopsis* (Franco-Zorrilla *et al.*, 2007). Experimental data showed that AtIPS1 could directly interact with miR399, and suppressed the miR399 mediated PHO2 mRNA degradation. This inhibition of mRNA cleavage required the existence of mismatch in AtIPS1 mRNA. Hence, a mechanism named target mimicry was proposed. In the example of AtIPS1, miR399 and PHO2, AtIPS1 can not be cleaved by miR399 because of the minor mismatch in its mRNA sequence, but this mRNA provide a mimicry target which could inhibit the effect of miR399 on PHO2 mRNA (Franco-Zorrilla *et al.*, 2007). This model provided a new strategy that can be used to inhibit the activity of specific miRNAs.

1.5.5 AtSIZ1

The *siz1* mutant was originally isolated by screening a T-DNA insertion library in the *Arabidopsis gl1/sos3-1* background for new loci that affect NaCl response (Miura *et al.*, 2005). However, this mutant exhibited more pronounced Pi starvation responses than WT. Under Pi-limited conditions, the *siz1-1* mutant showed an

inhibition of primary root growth, an increase in lateral root and root hair growth, and a higher root/shoot fresh weight ratio than wild type plants. Further study also showed that the *siz* mutation altered expression profiles of Pi starvation-inducible genes, including *AtIPS1* and *AtRNS1*, which belong to *PHR1* regulon. Based on protein sequence analysis, SIZ1 was predicted to encode a putative SUMO E3 ligase, which was confirmed by both *in vitro* and *in vivo* assay. Miura *et al.* suggest that sumoylation of PHR1 controlled expression of Pi starvation-responsive genes (Miura *et al.*, 2005). However, *siz1* has pleiotropic phenotypes and it is not entirely clear whether its role in regulation in Pi-metabolism is specific.

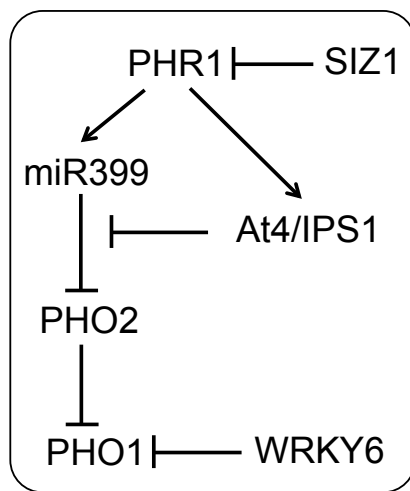


Fig. 1.3 An overview of Pi signalling pathway involving a complex network of transcriptional and post-transcriptional regulatory steps in *Arabidopsis*. Arrows denote positive effects, whereas lines ending with a short bar indicate negative effects.

1.5.6 ZAT6

ZAT6 (Zinc finger *Arabidopsis* 6, At5g04340) is a Cysteine2/Histidine2-Zinc finger transcription factor. Microarray analysis showed that the expression of ZAT6 was highly induced during Pi starvation (Misson *et al.*, 2005). Detailed RNA-blot data showed ZAT6 transcripts abundance increased to varying level in different tissues of mature plants during Pi deprivation, while the basal expression and induction of ZAT6 is even stronger in young seedlings. A ZAT6-GFP fusion protein indicates its nucleus localization irrespective of Pi availability. Sequence analysis showed that

ZAT6 has two C2H2 zinc finger motifs, a B-box motif that provides nucleus localization signal, an L-box, and a repressor domain DLN boxes. These data indicates that ZAT6 is a Pi responsive transcription factor that could possibly function as a transcription repressor (Devaiah *et al.*, 2007). Overexpression of ZAT6 leads to retardation of young seedling development and primary growth, increased secretion of acid phosphatase and increased accumulation of anthocyanin. In older plants, the root system architecture is significantly altered in ZOe (ZAT6 overexpression) plants with decreased primary root length and lateral root number but increased lateral root length. These changes lead to an increased root to shoot ratio, higher Pi uptake and accumulation. As a result of higher P content, the expression of an array of phosphate starvation inducible genes is reduced during Pi deprivation in ZOe plants compared to WT plants. Together, these data suggest ZAT6 plays important roles in regulation of Pi responses through controlling root growth.

1.5.7 WRKY6 and WRKY75

As a plant specific transcription factor superfamily, WRKY family members have been proved to regulate a broad range of biotic and abiotic responses. Their regulatory function is performed by their binding to W box motif on the promoter of target genes. WRKY75 is identified to respond to Pi starvation based on microarray data (Misson *et al.*, 2005). During Pi deprivation, WRKY75 transcript accumulation increased to varying level in different part of *Arabidopsis* plants (Devaiah *et al.*, 2007). When Pi is re-supplied to starved plants, a rapid decrease in elevated transcripts level was observed in 3 hours. This suggested WRKY75 is one of rapid induced genes that respond to altered Pi status. Localization analysis aided by GFP reporter showed that WRKY75 protein located in nucleus irrespective of Pi availability. Suppression of WRKY75 by RNAi silencing resulted in early accumulation of anthocyanin and down-regulation of several PSR genes including phosphatase encoding genes, *Mt4/TPSI*-like genes, and high-affinity Pi transporters. The RNAi silenced mutant also showed reduced Pi uptake during Pi starvation, suggesting WRKY75 functions as a positive regulator in a Pi responsive mechanism. Interestingly, in older RNAi plants, total Pi content of mutant is increased, possibly due to the fact that suppression of WRKY75 increased growth of lateral root and

number of root hairs (Devaiah *et al.*, 2007). Together, these data suggest dual function of WRKY75. On one hand, it could positively regulate plant responses to Pi starvation; on the other hand, it may function as a constitutive negative regulator in root architecture development irrespective of P-regime.

A further member of the WRKY gene family that was recently reported to affect phosphate starvation responses is WRKY6. Plants over-expressing *WRKY6* displayed higher sensitivity to low-Pi stress. The phenotype of *WRKY6*-OE plants is very similar as the *pho1* mutant under low Pi condition, including growth inhibition, anthocyanin accumulation and Pi accumulation in shoot. ChIP-qPCR assay indicated that WRKY6 directly bound to the W-box of *PHO1* promoter to control its expression. Under normal Pi supply conditions, overexpression of *WRKY6* down-regulated expression of *PHO1* gene, suggesting WRKY6 served as a negative regulator in controlling *PHO1* expression. And the regulation required the existence of certain W-box motifs on the promoter of *PHO1*. During Pi deprivation, a decrease of WRKY6 protein was detected by protein gel blot, which resulted in up-regulation of *PHO1*. Result from yeast-two-hybrid experiment and MG132 treatment both indicated the degradation of WRKY6 protein is possibly mediated by 26S proteasome pathway (Chen *et al.*, 2009). Together, these data suggested that WRKY6 could negatively regulate *PHO1* expression on transcriptional level, and the regulation is Pi-dependent.

1.6 A potential repressor in Pi signaling pathway

Although some components of Pi starvation signalling pathway have been identified, the overall pathways are still poorly understood. Besides, previous studies mainly focused on the identification of regulatory genes involved in Pi starvation responses followed by withdrawal of Pi. So far, all the components that have been identified mainly play their roles at the transcriptional level, which in terms of signalling, is already a late response. In another words, the early steps of phosphate signalling are still completely unknown, including phosphate receptor(s) and signal transduction proteins. Our group are particularly interested in dissecting the early events of the Phosphate signalling pathway, which will significantly contribute to our understanding of plant responses to Pi starvation.

To characterise the early Pi signalling system, previous work in our group, particularly by Fan Lai, a previous PhD student has focused on the response kinetics of several molecular markers to Pi perception in Pi-depleted *Arabidopsis* root and suspension cells. As shown in Fig.1.3, the expression of the *Pht1;1*, *At4* and *MGD3* was very rapidly suppressed by provision of Pi, indicating they were involved in the early events of Pi perception.

To further investigate Pi perception, the kinetics of gene expression after withdrawal of Pi was also examined. As shown in Fig.1.4A, the expression of *Pht1;1* was rapidly induced by transferring of *Arabidopsis* suspension cells from +Pi media to -Pi media in first 2-4 hours, and reduced in the following 4 hours. This result did not appear when transferring cells from +Pi media to fresh media with different concentration of Pi. The quantitative analysis of RNA blots in similar experiments with *Arabidopsis* seedlings confirmed this observation (Fig.1.4B). Analysis of sub-cellular distribution of Pi pools with ^{31}P -NMR has revealed that exposure of cells to Pi-deplete conditions initially results in a rapid drop in cytoplasmic Pi. Homeostasis by vacuolar reserves then occurs within a few hours, due to the kinetic properties of tonoplast transporters (Mimura, 1999). Therefore, the above observation suggests that *Pht1;1* RNA abundance responds directly to the changes of Pi concentration in the cytoplasm, but not the external Pi change.

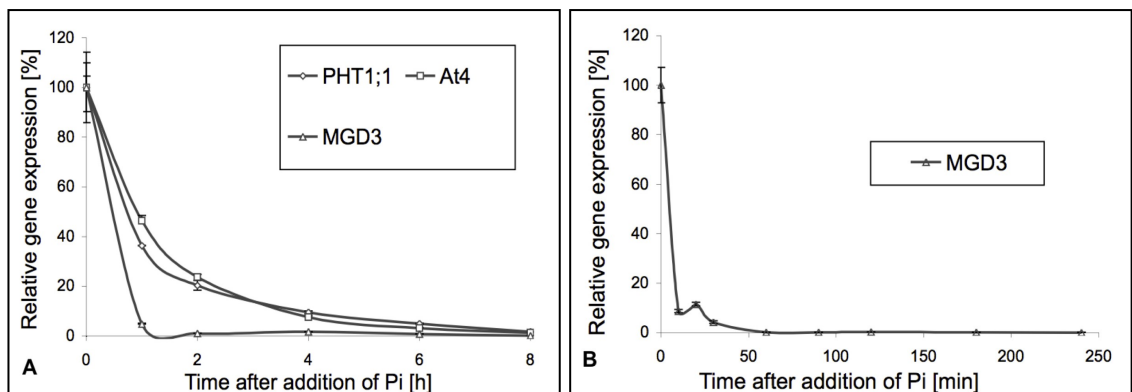


Fig 1.4. Gene expression kinetics of phosphate abundance-responsive genes in *Arabidopsis* suspension-cultured cells and roots. Phosphate starved suspension cells (A) and whole plant roots (B) were exposed to 10mM Pi. Changes in transcript abundance of three representative genes *At4*, *Pht1;1*, and *MGD3* were monitored in a time course by real-time PCR. Error bars indicate standard error of the mean (SEM) and are smaller than the symbol when not visible. (Lai, 2006)

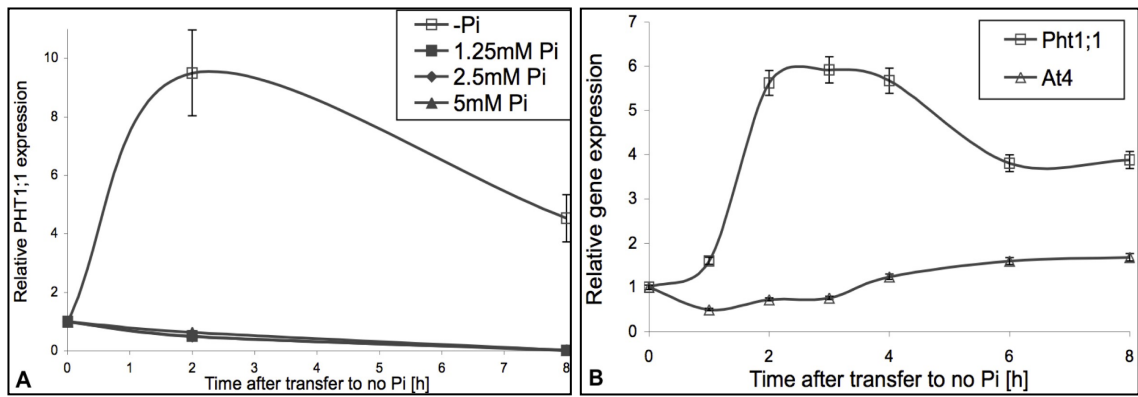


Fig. 1.5 *Pht1;1* RNA abundance directly responds to changes in cytoplasmic phosphate homeostasis. *Arabidopsis* cells or seedlings were in Pi media first, then washed with 1.0mM CaCl₂/MES and re-suspended in Pi-deplete media or corresponding media.

A: *Pht1;1* gene expression of *Arabidopsis* cell culture; gene expression were monitored in a time course by real-time PCR. Error bars indicate standard error of the mean (SEM). B: Northern blot shown the *Pht1;1* RNA abundance in *Arabidopsis* roots. Error bars show SEM. (Lai, 2006)

Recent work in plants have revealed a prevalence of negative regulation of plant hormone signalling networks by labile molecules susceptible to regulated protein degradation (Gazzarrini and McCourt, 2003). Meanwhile, in Pi-deplete conditions, the rapid down-regulation of our Pi responsive genes by provision of Pi suggests that the early responses of Pi signalling might under negative control.

Therefore, the expression of *MGD3*, *Pht1;1* and *At4* were examined in response to cycloheximide (CHX) which is a protein synthesis inhibitor. As shown in Fig.1.5, treatment of *Arabidopsis* cells with 20 μ M CHX in the presence of adequate Pi has no or only slight effects on *At4* or *MGD3* RNA levels, respectively. In contrast, *Pht1;1* gene expression dramatically increased in 2 hours after treatment with CHX, suggesting *Pht1;1* transcription is controlled by a labile repressor. Afterwards, different concentrations of CHX were applied to the cell culture together with 2.5mM Pi. It was obvious that the increased level of *Pht1;1* gene expression was dependent on the concentration of CHX. Therefore, it is hypothesized that a certain amount of labile repressor existed in the cell cytoplasm. After treating cells with CHX, protein synthesis was blocked and no more repressor could be produced, which result in reduced repressor concentration. Therefore, *Pht1;1* expression increased.

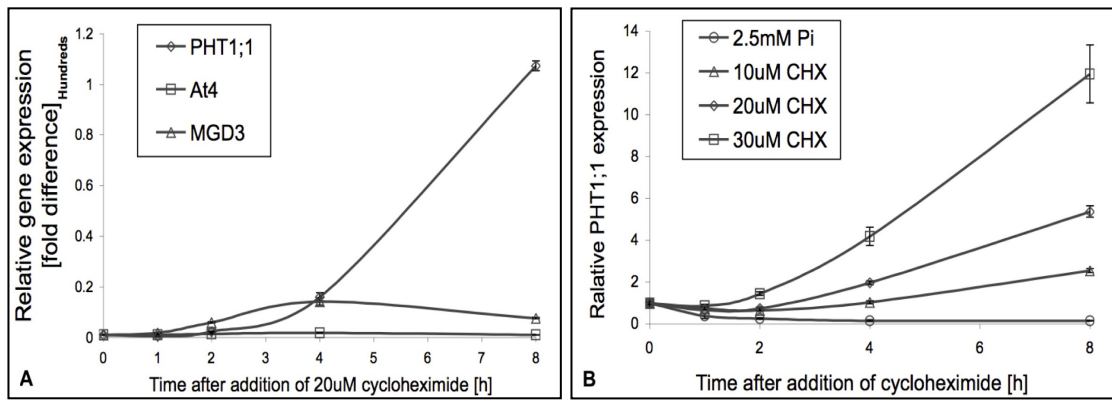


Fig.1.6 Gene expression of phosphate-responsive genes after exposure of *Arabidopsis* cells to cycloheximide (CHX). A: Pht1;1, At4 and MGD3 gene expression after providing 20 μ M CHX; B: Pht1;1 gene expression after adding 2.5 mM Pi with different concentrations of CHX to Pi-depleted cells. Gene expression was determined by real-time RT-PCR. Error bars show SEM. (Lai, 2006)

In eukaryotic cells, the ubiquitin-dependent proteasome pathway is one of the major mechanisms for the targeted degradation of proteins with short half-lives (Nawaz *et al.*, 1999). Thus, a few different protein degradation inhibitors were tested to examine whether ubiquitin-mediated proteolysis is involved in the early steps of Pi signalling. Among different inhibitors, only MG132 showed a distinctive effect on suppression of *Pht1;1* expression but not *MGD3* expression, when added to Pi starved suspension cells. As shown in Fig. 1.6A, addition of 100 μ M MG132 (a reversible, cell-permeable proteasome inhibitor) to Pi-deplete cell could mimic the effect of Pi in terms of suppressing *Pht1;1* expression, indicating *Pht1;1* RNA abundance might be controlled by the ubiquitin dependent degradation pathway.

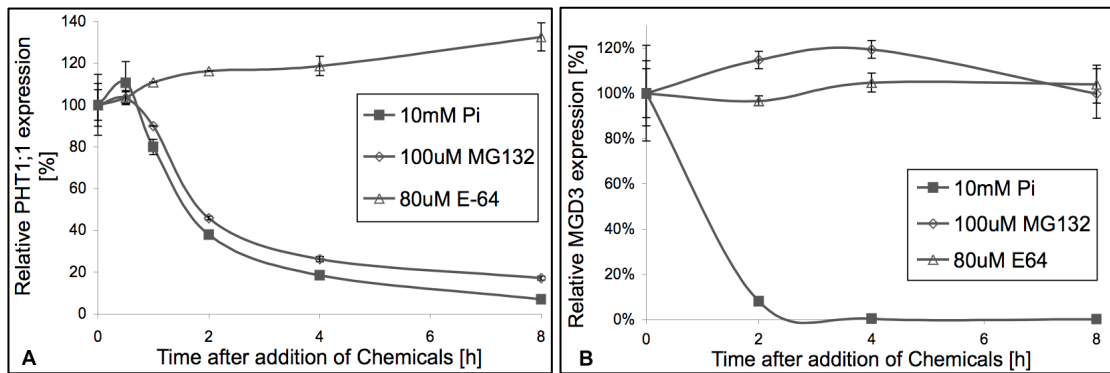


Fig. 1.7 Gene expression kinetics after exposure of Pi-deplete cells to protein proteolysis inhibitors (Lai, 2006)

A: Pht1;1 gene expression, B: MGD3 gene expression. Gene expressions were determined by real-time RT-PCR. Error bars shown SEM.

Through the above experiments, it has been shown that *Pht1;1* is a rapid Pi starvation responsive gene and is a good marker gene of the early steps of Pi signalling. CHX experiments suggest that *Pht1;1* expression was under negative regulation by a labile repressor protein whose stability is controlled by the availability of Pi. The data from MG132 treatment indicates the labile repressor could be susceptible to ubiquitin dependent protein degradation pathway. Based on this evidence, we propose a working model of the early Pi signalling. In this model, a certain amount of labile repressors exist in the plant cell which can regulate the expression of *Pht1;1* gene. Under Pi sufficient condition, repressors are relatively stable and could bind to the promoter of *Pht1;1*, which result in its low expression. When Pi availability changes to be low, a Pi signal is transduced to the repressors that could weaken their stability and result in their degradation through ubiquitin dependent pathway. Therefore, the *Pht1;1* promoter could be released from the repressor, and the expression is increased under Pi deficient conditions, which help plants uptake more Pi from the environment.

2. Materials and methods

2.1 Plant material

Arabidopsis plant and suspension cell culture system were used as main experimental materials in my research work. *Arabidopsis* ecotype Col-0 was used as wild type plant in all experiments. *Arabidopsis* suspension cell cultures were provided by Fry lab (Ler ecotype) and Aubert lab (Col-0 ecotype).

2.2 Plant growth

2.2.1 *Arabidopsis* seed sterilization

Arabidopsis seeds were surface-sterilized by soaking in 70% ethanol with 0.05% Tween-20 (v/v) for ~15 min with constant shaking at 37°C. Afterwards, the ethanol was removed and the seeds were rinsed with 95% ethanol twice, and then air-dried on autoclaved Whatman® filter papers in the sterile tissue culture hood. Dry seeds were collected into sterile Eppendorf tubes, re-suspended in 0.1% agar solution and stored in the dark at 4° C for 4 days for stratification.

2.2.2 Media for plant growth and Pi starvation treatment

In general, all plants were grown in half strength Murashige and Skoog (MS) medium (Murashige and Skoog, 1962) with minor modification. Plant growth media were titrated to pH 5.7 using 1 M KOH. The sucrose concentration was specific to individual experiments. Media were solidified with 0.5% (w/v) of micro-agar if necessary. For *Arabidopsis* suspension cell culture, full strength MS medium was used together with 0.5 mg/L NAA and 0.05 mg/L kinetin. pH value was titrated to 5.8 using 1 M KOH.

The media for Pi starvation treatment were prepared in the same way as the growth media except that the KH_2PO_4 was omitted.

Table 2.1 Full nutrient media for *Arabidopsis* seedling growth

Compounds	MW (g/mol)	Amount for 0.5x (mg/L)	Concentration for 0.5x (mM)
KNO ₃	101.11	950	9.4
CaCl ₂	110.99	166.01	1.5
NH ₄ NO ₃	80.04	825	10.31
MgSO ₄	120.37	90.27	0.75
KH ₂ PO ₄	136.09	204.14	1.5
H ₃ BO ₃	61.83	3.1	0.05
MnSO ₄ .H ₂ O	169	8.45	0.05
CoCl ₂ .6H ₂ O	237.93	0.0125	0.000055
ZnSO ₄ .7H ₂ O	287.54	4.30	0.015
CuSO ₄ .5H ₂ O	249.68	0.0125	0.00005
KI	166	0.415	0.0025
Na ₂ MoO ₄ .2H ₂ O	241.95	0.125	0.000515
FeNa ₂ EDTA	367.05	18.35	0.05

Table 2.2 Pi-free media for starvation treatment with *Arabidopsis* seedlings

Compounds	MW (g/mol)	Amount for 0.5x (mg/L)	Concentration for 0.5x (mM)
KNO ₃	101.11	1900.00	9.4
CaCl ₂	110.99	332.02	1.5
NH ₄ NO ₃	80.04	1650.00	10.31
MgSO ₄	120.37	180.54	0.75
H ₃ BO ₃	61.83	6.20	0.05
MnSO ₄ .H ₂ O	169	16.90	0.05
CoCl ₂ .6H ₂ O	237.93	0.025	0.000055
ZnSO ₄ .7H ₂ O	287.54	8.60	0.015
CuSO ₄ .5H ₂ O	249.68	0.025	0.00005
KI	166	0.83	0.0025
Na ₂ MoO ₄ .2H ₂ O	241.95	0.25	0.000515
FeNa ₂ EDTA	367.05	36.70	0.05

Table 2.3 Full nutrient media for *Arabidopsis* suspension cell culture growth

Compounds	MW (g/mol)	Amount for 1x (mg/L)	Concentration for 1x (mM)
KNO ₃	101.11	1900.00	9.4
CaCl ₂	110.99	332.02	1.5
NH ₄ NO ₃	80.04	1650.00	10.31
MgSO ₄	120.37	180.54	0.75
KH ₂ PO ₄	136.09	340.00	2.5
H ₃ BO ₃	61.83	6.20	0.05
MnSO ₄ .H ₂ O	169	16.90	0.05
CoCl ₂ .6H ₂ O	237.93	0.025	0.000055
ZnSO ₄ .7H ₂ O	287.54	8.60	0.015
CuSO ₄ .5H ₂ O	249.68	0.025	0.00005
KI	166	0.83	0.0025
Na ₂ MoO ₄ .2H ₂ O	241.95	0.25	0.000515
FeNa ₂ EDTA	367.05	36.70	0.05
Thiamine HCl	337.27	0.40	0.0012
myo-inositol	180.16	100.00	0.555
Sucrose	342.20	30,000	3% (w/v)

Table 2.4 Pi-free media for starvation treatment with *Arabidopsis* suspension cells

Compounds	MW (g/mol)	Amount for 1x (mg/L)	Concentration for 1x (mM)
KNO ₃	101.11	1900.00	9.4
CaCl ₂	110.99	332.02	1.5
NH ₄ NO ₃	80.04	1650.00	10.31
MgSO ₄	120.37	180.54	0.75
H ₃ BO ₃	61.83	6.20	0.05
MnSO ₄ .H ₂ O	169	16.90	0.05
CoCl ₂ .6H ₂ O	237.93	0.025	0.000055
ZnSO ₄ .7H ₂ O	287.54	8.60	0.015
CuSO ₄ .5H ₂ O	249.68	0.025	0.00005
KI	166	0.83	0.0025
Na ₂ MoO ₄ .2H ₂ O	241.95	0.25	0.000515
FeNa ₂ EDTA	367.05	36.70	0.05
Thiamine HCl	337.27	0.40	0.0012
myo-inositol	180.16	100.00	0.555
Sucrose	342.20	30,000	3% (w/v)

2.2.3 Plant growth conditions

Arabidopsis seedlings were grown at 22°C with a 16 h light / 8 h dark photoperiod in either liquid media or solid media. For any treatments with seedlings, the treatments always began at 3 hours after the seedlings entered daylight condition.

Arabidopsis plants for floral dipping transformation were germinated and initially grown at 22°C with an 8 h light / 16 h dark photoperiod for 5 weeks, and then transferred to a 22°C and 16 h light / 8 h dark photoperiod for the rest of life cycle.

Arabidopsis suspension cell cultures were kept at 22°C with either constant light or in constant dark conditions. For any treatments with cell culture, the experiments always started at 10:00 unless specified otherwise.

2.3 Phosphate starvation treatment and inhibitor treatment

2.3.1 Phosphate starvation treatment with *Arabidopsis* seedlings

Long-term phosphate starvation experiment with *Arabidopsis* seedlings

- *Arabidopsis* seeds were sterilized and kept in cold room (4°C) for 4 days before sowing in the media.
- On day one, 5 seeds were sowed into 10 ml liquid 1/2MS media with 1% sucrose in 250 ml flask. All flasks were kept on shaker with speed set up at 40 rpm.
- On day eight, the growth media was refreshed with 15 ml 1/2MS media with 1% sucrose.
- On day fourteen, the growth media was refreshed with 15 ml fresh 1/2MS media with 0.3% sucrose.
- On day eighteen, the growth media was removed. In half of the flasks, it was replaced with 1/2MS media (0.3% sucrose) without Pi to generate Pi starvation treated samples; and in the other half of flasks, it was replaced with 1/2MS media (0.3% sucrose) with 1.5 mM Pi to generate control samples.
- Time course started immediately after the media switch. Root samples were collected under different time-points. For each time point, samples were collected from 3 individual flasks for statistical analysis.

Short-term phosphate starvation experiment with *Arabidopsis* plants

- *Arabidopsis* seeds were sterilized and kept in cold room (4°C) for 4 days before sowing in the media.
- On day one, 5 seeds were sowed into 10 ml liquid 1/2MS media with 1% sucrose in 250 ml flask. All flasks were kept on a shaker with speed set at 40 rpm.
- On day eight, the media media was refreshed with 10 ml fresh 1/2MS media with 0.6% sucrose.
- On day fourteen, the old media was refreshed with 10 ml fresh 1/2MS media with 0.3% sucrose.
- On day eighteen, the old media was refreshed with 10 ml fresh 1/2MS media with 0.3% sucrose.
- On the following day, the old media was removed. The seedlings were washed with Pi-free 1/2MS media briefly, and then 10 ml fresh Pi-free 1/2 MS media was added. For control samples, the seedling were washed with 1/2MS media (1.5 mM Pi) and then refreshed with 1/2 MS media (1.5 mM Pi). Time-courses start right after addition of fresh +/- Pi media.
- Root samples were collected under different time-point. For each time point, samples were collected from 3 individual flasks for statistical analysis.

Phosphate recovery experiment with *Arabidopsis* plants

- *Arabidopsis* seeds were sterilized and kept in cold room (4°C) for 4 days before sowing in the media.
- On day one, 5 seeds were sowed into 10ml liquid 1/2MS media with 1% sucrose in 250 ml flask. All flasks were kept on shaker with speed set up at 40 rpm.
- On day eight, the growth media was refreshed with 15 ml fresh 1/2MS media with 1% sucrose.
- On day fourteen, the growth media was refreshed with 15 ml fresh 1/2MS media with 0.3% sucrose.
- On day eighteen, the growth media was replaced with 15 ml 1/2MS media (0.3% sucrose) without Pi to starve the seedlings. The media were refreshed every 2 days to ensure the seedlings have enough nutrients except for Pi.

- After 7-day's starvation, 1.5mM KH_2PO_4 (final concentration) was provided to the seedlings, and time-course started right after the re-supply of Pi.
- Root samples were collected at different time-points. For each time point, samples were collected from 3 individual flasks for statistical analysis.

2.3.2 Phosphate starvation treatment and inhibitor treatment with *Arabidopsis* suspension cell culture

Short-term phosphate starvation treatment with *Arabidopsis* suspension cells

- On day one, pipette 5 ml *Arabidopsis* suspension cell culture into 45 ml fresh media in 250 ml flasks. Keep shaking the flasks at 100 rpm at 27°C.
- On day four, 2 mM KH_2PO_4 (final concentration) was added into each flask.
- On day six, exchange the media for cell culture with fresh media, and dilute the suspension cells by half.
- On day seven, the suspension cells were washed with Pi-free media twice. The washing media were removed with vacuum filter device. After wash, the cells were transferred to a new flask with 100ml Pi-free media. Start time course and collect samples at different time-points. For each time point, 3 samples were collected for statistical analysis.

Cycloheximide (CHX) treatment with *Arabidopsis* suspension cells

- On day one, pipette 5 ml *Arabidopsis* suspension cell culture into 45 ml fresh media in 250 ml flasks. Keep shaking the flasks at 100 rpm at 27°C.
- On day four, 2 mM KH_2PO_4 (final concentration) was added into each flask.
- On day six, exchange the media for cell culture with fresh media, and dilute the suspension cells by half.
- On day seven, mix culture from two flasks and split equally into two fresh flasks. Add 20 μM CHX (final concentration) to one flask for treatment. Start time course after addition of CHX and collect samples at different time-points. For each time point, 3 samples were collected for statistical analysis.

MG132 treatment with *Arabidopsis* suspension cells

- On day one, pipette 5 ml *Arabidopsis* suspension cell culture into 45 ml fresh media in 250 ml flasks. Keep shaking the flasks at 100 rpm at 27°C.
- On day four, 2 mM KH₂PO₄ (final concentration) was added into each flask.
- On day six, exchange the media for cell culture with Pi-free media, and dilute the suspension cells by fourth.
- On day nine, mix culture from 3 flasks and split into three fresh flasks. Provide 100 µM MG132 and start time course. For each time point, 3 samples were collected for statistical analysis.

2.4 DNA analysis

2.4.1 PCR amplification

PCR primer pairs were designed with Primer 3 program (free on the internet <http://frodo.wi.mit.edu/>) for ordinary PCR amplification. Most of PCR reactions in my study were performed with the Crimson Taq system (NEB, M0324). For cloning purpose, Phusion® High-Fidelity DNA Polymerase (NEB, M0530) was used to ensure the correct DNA sequence. All PCR reactions followed the protocol from manufacturer.

2.4.2 Plant genomic DNA preparation with CTAB method for PCR purpose

Two or 3 young *Arabidopsis* rosette leaves (around 100 mg) were collected into a 1.5ml Eppendorf tubes with 2 steel beads. CTAB solution (2% cetyltrimethylammonium bromide (CTAB); 1.4 M NaCl; 100 mM Tris-HCl, pH 8.0; 20 mM EDTA; 0.2% β-mercaptoethanol) was pre-heated to 65°C and 500 µl solution were added to each tube. The tubes were mechanically homogenized for 3 min twice at 30 Hz using a Mixer Mill MM 300 (Retsch, Germany). All tubes were kept at 65°C for 30 minutes with occasional vortexing. 500 µl Chloroform:iso/amyl alcohol (24:1) was added to each tube and mixed well. The tubes were then centrifuged at 8,220 g for 10 minutes. The aqueous phase was recovered from each tube into fresh tubes. One volume of chloroform was added to each tube and mixed well. Samples were centrifuged at 8,220 g for 10 minutes. The aqueous phase was recovered into fresh tubes. One volume of isopropanol was added to each tube and mixed well. The

tubes were kept on ice for 30 minutes to precipitate DNA. The tubes were centrifuged at 12,000 rpm for 10min to pellet DNA. The supernatant was discarded and 500 µl 70% ethanol was added to wash the DNA. The tubes were centrifuged at 11,835 g for 10 minutes. The supernatant was discarded and the pellets were air-dried, and then dissolved in 200 µl low TE buffer (10 mM Tris-HCl, pH8.0; 0.1 mM EDTA). 2µl was used in a PCR reaction.

2.4.3 Recombinant DNA construct

PCR products after Phusion reaction were blunt-ended, and therefore need A-tailing reaction before further operation. For A-tailing reaction, 200 ng PCR product were mixed with 0.25 mmol dATP, 0.1 µl Crimson Taq and 4µl 5 x Crimson Buffer in 20 µl reaction system and kept at 68 °C for 30 minutes.

A-tailed PCR product could be used for ligation into vector. A standard ligation was performed using T4 DNA ligase (NEB, M0202) in the manufacturer's buffer and incubated as recommended. Target insert to vector DNA ratios were approximately 3:1.

During the construct preparation, DNA digestion with restriction endonuclease was used for different purposes. The reaction was carried out following the enzyme manufacture's protocol with the recommended buffer and incubation temperature.

2.4.4 Transformation of *Escherichia coli* competent cell

DNA ligation product or plasmid DNA were mixed with 100 µl *E. coli* DH5α competent cells, and kept on ice for 30 minutes. Cells were heat-shocked at 42 °C for 90 seconds, and placed on ice immediately for 2 minutes. 1ml LB media were added to cells and the culture was shaken at 37°C, 200 rpm for 1.5 hours for recovery. The cell culture was then centrifuged at 3,000 g for 1 minute. The majority of the clear supernatant was removed before cells were resuspended in the residual supernatant and spread on fresh, selective LB plates.

2.4.5 Plasmid DNA isolation with boiling method

A single bacterial colony was inoculated in 3 ml LB media with appropriate selective antibiotic, and grew overnight at 37°C, 250 rpm. One ml of the culture was centrifuged at 16,110 g for 3 min in an Eppendorf microcentrifuge tube. The

supernatant was discarded and the pellet was resuspended in 100 µl STET buffer (8% sucrose, 5% Triton-X 100, 50 mM EDTA, 50 mM Tris-HCl pH 8.0). Before the boiling step, 500 µl of ice-cold STET with 10mg/ml lysozyme was added to the tube and mixed well. The mix was boiled for 2 minutes, and then centrifuged at 11,835 g for 5 minutes. The slimy pellet was removed by a sterile toothpick. 500 µl isopropanol were added to the supernatant to precipitate the DNA. The tube was centrifuged at 16,110 g for 5 minutes. The supernatant was discarded. The pellet was washed with 70% ethanol twice, dried by speed vacuum and dissolved in 100 µl lo-TE (10mM Tris-HCl pH 7.5, 0.2mM EDTA) with 10 mg/ml RNaseA.

2.4.6 Plasmid DNA isolation with commercial Kit

5 ml LB medium containing the appropriate selective antibiotic were inoculated with 15 µl pre-culture, and grew overnight at 37 °C, 250rpm. Plasmid DNA was isolated with QIAprep Spin Miniprep kit (QIAGEN, Cat No. 27106). All steps followed the protocol from the kit with minor optimization.

2.4.7 Transformation of *Agrobacterium tumefaciens* competent cell

50 ml of YEB (10 g/L yeast extract, 10 g/L bacto-peptone, 5 g/L NaCl, pH to 7.5 with NaOH) was inoculated with 2 ml of an overnight culture of a single *Agrobacterium tumefaciens* GV3101 colony and incubated at 28°C with shaking. The culture was grown to OD600 about 0.5. The cells were collected by centrifuging at 2,000 g for 5 minutes at room temperature and re-suspended in 10 ml 0.15 M NaCl. This suspension was centrifuged at 2,000 g for 5 minutes and pellet was suspended in 1 ml of 20 mM ice-cold CaCl₂. The cells were frozen as 200 µl aliquots in liquid nitrogen and stored at -80°C.

300 ng plasmid DNA was mixed with 200 µl of thawed competent *Agrobacterium tumefaciens* GV3101 cells in 1.5 ml Eppendorf tube, which was then incubated on ice for 30 minutes. The tube was frozen in liquid nitrogen for 1 minute and thawed in 37 °C water bath. 1 ml of YEP medium was added to the tube and then incubated at 28°C shaker for 4 hours. Cell culture was centrifuged for 1 min at 3,000 g. The supernatant were discarded and the pellet was resuspended in 100 µl YEP medium. The concentrated culture were spread onto YEP plate with appropriate antibiotics.

The plates were kept in 28°C incubator for 48 hours. Glycerol stocks were made from appropriate clones, and stored at -80° C.

2.4.8 Vector construction for *Pht1;1* promoter deletion analysis

The truncated promoter sequences of *Pht1;1* gene were amplified with gene-specific primers (Table 2.5) from *Arabidopsis* wild type genomic DNA by PCR with Phusion polymerase (NEB, M0530). A schematic map for the constructs is shown in *Fig. 5.1*. To generate the promoter sequence without the intron, a long reverse primer was designed that comprised of 19 bp upstream of intron and 29 bp downstream. All promoter fragments were inserted into pGEM-T-easy vector for cloning. Afterwards, the promoter fragments were ligated upstream of the uidA reporter gene to generate the expression cassettes, which were then introduced into the binary vector pTV50^{hyg}. All clones were confirmed by DNA sequencing. The resulting plasmids were transformed into *Agrobacterium tumefaciens* strain GV3101.

Table 2.5 Primer sequences for *Pht1;1* promoter deletion construct

Primer sequence for Quantitative PCR		
<i>Pht1;1-FL</i>	Forward	5'GC GTCGAC GGCCTTTCTTTTCTTTGC ^{3'}
	Reverse	5'GCT CTAGAT GTTGTTTCGGCCATTTC ^{3'}
<i>Pht1;1-Δ1</i>	Forward	5'GC GTCGAC CCAACAAGATTAATACTACAAAC ^{3'}
	Reverse	5'GCT CTAGAT GTTGTTTCGGCCATTTC ^{3'}
<i>Pht1;1-Δ2</i>	Forward	5'GC GTCGAC AAAAATCATCCCATCTCACG ^{3'}
	Reverse	5'GCT CTAGAT GTTGTTTCGGCCATTTC ^{3'}
<i>Pht1;1-Δ13</i>	Forward	5'GC GTCGAC CATACGGAGGGAGTATTGATGA ^{3'}
	Reverse	5'GCT CTAGAT GTTGTTTCGGCCATTTC ^{3'}
<i>Pht1;1-Δ4</i>	Forward	5'GC GTCGAC TCAACTCTCCAGAGAAGTTCTTAATT ^{3'}
	Reverse	5'GCT CTAGAT GTTGTTTCGGCCATTTC ^{3'}
<i>Pht1;1-FLΔI</i>	Forward	5'GC GTCGAC GGCCTTTCTTTTCTTTGC ^{3'}
	Reverse	5'GCTCTAGATGTTGTTTCGGCCATTTCCTAGAGCTCTTAATC AGCTTGGCAGGA ^{3'}
<i>Pht1;1-Δ1ΔI</i>	Forward	5'GC GTCGAC CCAACAAGATTAATACTACAAAC ^{3'}
	Reverse	5'GCTCTAGATGTTGTTTCGGCCATTTCCTAGAGCTCTTAATC AGCTTGGCAGGA ^{3'}

2.5 Transcriptional analysis

2.5.1 RNA isolation from plant materials

100 mg plant materials were collected into 2 ml Eppendorf tubes with 2 steel beads and frozen in liquid nitrogen immediately. 1 ml TRIzol solution (38% Na-acetate equilibrated phenol; 1 M guanidine thiocyanate; 1 M ammonium thiocyanate; 0.1 M sodium acetate, pH 5.0; 5% glycerol) was added to each tube. Samples were then homogenized for 3 minutes twice at 30 Hz using a Mixer Mill MM 300 (Retsch, Germany). The tubes were left at room temperature for ≥ 15 minutes, and vortexed twice. All liquid was transferred to a fresh 1.5 ml Eppendorf tubes and 400 μ l chloroform was added to each tube. Samples were vigorously mixed by vortexing for 20 seconds, and then centrifuged at 16,110 g for 15 minutes at 4°C. The aqueous phase was recovered to a fresh 1.5 ml Eppendorf tube. To precipitate RNA, 250 μ l of 0.8 M sodium citrate/1.2 M NaCl and 500 μ l of isopropanol were added to each tube, and mixed vigorously by inverting. The tubes were left at room temperature for 10 minutes and then centrifuged at 16,110 g for 15 minutes at 4°C. The supernatants were discarded as completely as possible, and the pellets were washed with 75% ethanol followed by centrifugation at 16,110 g for 15 minutes at 4°C. The supernatant were removed and the pellets were air-dried in laminar flow hood for 30 minutes and dissolved in 200 μ l DEPC- H₂O. The tubes were kept in 65°C for 10 minutes, and then centrifuged at 16,110 g for 5 minutes at room temperature. The supernatant was recovered to a fresh tube and 60 μ l 10 M LiCl was added to each tube. The tubes were mixed by vortexing and kept on ice for overnight to precipitate RNA, and then centrifuged at 16,110 g for 15 minutes at 4 °C. The supernatant was removed carefully and 1 ml ice-cold 70% ethanol was gently added to the tube to wash RNA. Tubes were centrifuged at 16,110 g for 20 minutes at 4°C. The supernatant was removed and the pellets were air-dried in laminar flow hood for 30 minutes, and then re-suspended in 36 μ l 0.1 mM EDTA solution. The RNA concentrations were determined by NanoDrop.

2.5.2 DNase treatment of RNA samples

RNA samples prepared by the above method need to be treated with DNase to remove any remaining genomic DNA contamination before any further application

like reverse transcription reaction, qRT-PCR. To remove genomic DNA, Ambion TURBO DNase kit (Ambion, Inc.) was used. DNase digestion was performed with the RNase-free DNase set following the manufacturer's instruction.

2.5.3 Reverse transcription reaction

RNA samples after DNase treatment were qualified for reverse transcription (RT) reaction. RT reaction was performed with approximately 2 µg clean RNA by RevertAid first strand cDNA synthesis kit (Fermentas, #K1622) with a oligo(dT) primer. After reaction, 1st strand cDNA was generated in 10 µl volume. Another 90 µl sterile water was added to dilute the cDNA.

2.5.4 Quantitative Real-time PCR

First strand cDNA prepared following the above step could be used in quantitative Real-time PCR (qRT-PCR) analysis. 2 µl diluted cDNA was used as template in 15 µl qRT-PCR reaction also including 7.5 µl LightCycler® 480 SYBR Green I Master, 1 µl forward primer (4 µM), 1 µl reverse primer (4 µM) and 3.5 µl H₂O. Each PCR reaction was prepared in duplicate and then aliquot into 96 well plate. QPCR reactions were performed in LightCycler® 480 Real-Time PCR System (Roche). 483 nm and 533 nm filters were used for excitation and detection respectively. PCR reaction followed the protocol as: a, initial denaturation (95°C, 5 min); b, amplification (95°C, 10 sec; 58°C, 15 sec; 72°C, 15 sec); c, melting curve (95°C, 5 sec; 65°C, 1 min, continuous); d, cooling down (40°C, 30 sec).

To measure the efficiency of qPCR amplification, a standard curve was set up for each primer pair (Table 2.5). Ordinary PCR products from each primer pair were purified and diluted by 1:1000. The diluted product was used as 10⁰x sample. Another six 1:10 serial dilutions were prepared from 10⁰x sample (10⁻¹~10⁻⁶), and used as templates in qPCR amplification by LightCycler® 480 system (Roche). The efficiency for each primer pair was calculated by the protocol of “Abs Quant/2nd Derivative Max” and save as external standard curve. In the future experiments, standard sample (10⁻³x) was included for each qPCR amplification to ensure the accuracy.

In the qPCR test, the *eIF4a* gene was amplified as a reference to normalize each target gene. The eIF4a gene encodes the constitutively expressed eukaryotic protein synthesis initiation factor 4A (Metz et al., 1992). Calculation of the ratio of a target gene to the reference gene followed the protocol of “Advanced Relative Quantification” in LightCycler® 480 software V1.50.

Table 2.6 Primer sequences for amplification of cDNA by Quantitative PCR

Primer sequence for Quantitative PCR		
eIF4a (at3g13920)	Forward	5'TTCGCTCTTCTCTTTGCTCTC ^{3'}
	Reverse	5'GAACTCATCTTGTCCCTCAAGTA ^{3'}
Pht1;1 (at5g43350)	Forward	5'CTGCCAAGCTGATTAAGAGC ^{3'}
	Reverse	5'AAGGAGTTTCGTCACCAAGGAC ^{3'}
MGD3 (at2g11810)	Forward	5'TGCCACCGTACATGGTTC ^{3'}
	Reverse	5'TTGTCTTATTGGATTACTTTCTTTAGAG ^{3'}
At4 (At5g03545)	Forward	5'GGATGGCCCCAAACACAAG ^{3'}
	Reverse	5'TAAACCGGAAACAAAGTAAACACG ^{3'}
ZAT18 (at3g53600)	Forward	5'ATGTTTGGGACCGGTCAAGCTC ^{3'}
	Reverse	5'CCAAGATCTCCTTGCTGCTACTGC ^{3'}

2.6 *Arabidopsis* transformation by floral dip method

Two days before transformation, *A. tumefaciens* GV3101 carrying the binary vector helper plasmid was inoculated from frozen glycerol stock into 20 ml YEP medium (10 g/L yeast extract, 10 g/L bacto-peptone, 5 g/L NaCl, pH to 7.5 with NaOH). The culture was kept on shaker at 28°C with 200 rpm for overnight, which was then transferred into 500 ml of fresh YEP media with antibiotics for growth to OD₆₀₀=2. Bacteria were harvested by centrifugation (6,747 g, in SLC-4000 rotor at 15°C) and resuspend in 500 ml infiltration media (0.5x MS basal salt) with 200 µl Silwet. The aerial tissues of *Arabidopsis* plants were dipped in the bacteria suspension for ~2min and rested for 15 minutes. After transformation, plants were sealed with a transparent bag and kept for one overnight before removing.

Seeds were harvested from transformed plants and then selected on 0.5x MS medium containing 0.5% Agar with either 40 µg/ml hygromycin or 50 µg/ml kanamycin. After ~2 weeks, transgenic plants were transferred to soil and grown in growth room under conditions of 22°C and 16h light / 8h dark photoperiod.

2.7. GUS histochemical assay

Histochemical *in situ* localization of GUS expression was performed in transgenic *Arabidopsis* plants according to standard procedures with some modifications (Jefferson, 1987; Jefferson et al., 1987). *Arabidopsis* young seedlings grown in liquid media were used for the staining assay. 3~5 Seedlings were transferred to microplates and submerged in 3 ml Solution I (50 mM sodium phosphate buffer, pH 7.2, 0.3% formaldehyde, 0.5 mM potassium ferricyanide, 0.5 mM potassium ferrocyanide, 1 mM EDTA, 1% Triton X- 100), and subjected to a vacuum to remove any air. After 60 min incubation, specimens were washed twice with 3 ml rinse solution (50 mM sodium phosphate buffer, pH 7.2, 0.5 mM potassium ferricyanide, 0.5 mM potassium ferrocyanide, 1 mM EDTA), and then replaced with staining solution (50 mM sodium phosphate buffer, pH 7.2, 0.5 mM potassium ferricyanide, 0.5 mM potassium ferrocyanide, 1% Triton X-100, 2mM 5-bromo-4-chloro-3-indolyl-β-d-glucuronide (X-Gluc)). Samples were incubated at 37°C for several hours to overnight (depending on the tissue type and colour development rate). Chlorophyll was removed with an increasing ethanol series. Samples were observed as whole mounts in 20% ethanol, 20% glycerol.

2.8. Electrophoretic mobility shift assay

2.8.1 Probe labeling and purification

DNA fragments generated by PCR reaction were used for probe labeling reaction. One pmol 5'-end (calculated with online software <http://www.promega.com/biomath/calc05.htm>) was added in 20 µl labeling reaction including 1x T4 Polynucleotide Kinase Buffer, 10 unit T4 Polynucleotide Kinase (M0201S from NEB), 1 µl [γ-³²P] ATP. The reaction was incubated at 37°C for 30 minutes. The labeling product was mixed with 2 µl NaAcetate (3M, pH5.2), 3 µl LPA and 75 µl ethanol (100%). The mixture was kept on ice for 30 minutes, and then centrifuged at 13,890 g for 10 minutes. All the supernatant were removed, and the

pellet was washed with 100 μ l ethanol (80%) twice before drying out at 50 °C for 1 hour. To dissolve the pellet, 97.5 μ l low TE (10 mM Tris-HCl, pH 8; 0.1 mM EDTA) were added followed with 2.5 μ l KCl. The radioactivity of probe was measured by scintillation counting.

2.8.2 Total protein isolation from plant material

Plant material (12g) was thoroughly pulverized in LN₂-chilled mortar and pestle. After boiling off the LN₂, the powder was added to 6 ml of ice-cold EB1 buffer (100 mM Tris HCl pH 8.5, 1 M NaCl, 10 mM MgCl₂, 10% glycerol, 1 mM benzamidine, 0.5% insoluble PVPP, 7 mM β -mercaptoethanol, 1 mM NaF, 100 μ M AEBSF) in a beaker. When sample was thawed, material was mixed gently to generate good slurry. The material was transferred to a 50 ml Falcon tube and centrifuged 60 min at 47,800 g at 4°C. The supernatant was recovered to a beaker and adjusted to 50% saturation with solid ammonium sulfate. The sample was stirred on ice for 30 min to precipitate protein and then centrifuged at 3,615 g for 30 min at 4°C. The supernatant was discarded and the pellet was re-suspended in 700 μ l bufferA (50 mM Tris HCl pH 8.5, 50 mM NaCl, 0.5 mM EDTA, 10% glycerol, 1 mM benzamidine, 7 mM b-mercaptoethanol, 1 mM NaF, 100 μ M AEBSF). The sample was dialyzed in dialysis buffer (50 mM Tris HCl pH 8.5, 50 mM NaCl, 0.5 mM EDTA, 10% glycerol, 7 mM b-mercaptoethanol, 50 μ M AEBSF, 1 mM NaF) overnight, and then frozen in LN₂ and stored at -80°C.

2.8.3 Protein-DNA binding reaction

A binding reaction contains 1x EMS buffer (20mM HEPES, 50mM KCl, 1mM EDTA, 1mM DTT, 2ng/ μ l BSA, 15% Glycerol), 0.5 μ g poly dI:dC and 10 μ g protein extract. After gently mix, 2000 cpm end-labeled probe was added to the binding reaction and incubated at 25°C for 30 min.

2.8.4 Visualization of protein-DNA complex

Four percent polyacrylamide gel (19:1, acrylamide:bisacrylamide) was prepared and prewarmed by running in 0.5x Tris-glycine buffer for 60 minutes at 50 V prior to the addition of samples. The mixture of the binding reaction was then loaded onto the gel, and run in 0.5x Tris-glycine buffer for ~2 hour. The gel running system was placed in an icebox to avoid over-heating. Afterwards, the gel was briefly rinsed with

de-ionized H₂O, and placed on three sheets of Whatman® filter paper, and then wrapped with plastic film. The gel was dried under vacuum with heat. The filter paper was autoradiographed for overnight with storage phosphor screen, which will be scanned with Storm 860 Phosphor Imager.

2.9 Microarray analysis

RNA samples from *Arabidopsis* roots were prepared following the steps described in 2.5.1. 9µg of high quality RNA sample was used for cDNA synthesis with Invitrogen SuperScript Double-Stranded cDNA Synthesis Kit. Double strand cDNA was then labeled with Cyc3 using the NimbleGen One-Color DNA Labeling Kit. The labeled cDNA was hybridized to Nimblegen *Arabidopsis* 12x135k Array for 16 hours at 42°C. After hybridization, the arrays were washed according to the manufacturer's protocol. All steps during microarray experiment strictly followed the NimbleGen Arrays User's Guide V6.0. The arrays were scanned with Axon GenePix 4400A, and the signal values were obtained and normalized using NimbleScan software V2.6.

The Nimblegen 12x135k array contains ~13500 probe-sets that cover 37118 RNA transcripts from the *Arabidopsis* genome based on the annotation of TAIR9.0. Microarray data analysis was performed with Limma package (Smyth, 2005) incorporated within R software for background correction, quantile normalization, statistics calculation and expression estimate computation. Differentially expressed genes were identified based on fold change in expression and a significant p value threshold (over two fold change and p value < 0.05). GO enrichment analysis was performed with DAVID (<http://david.abcc.ncifcrf.gov/>).

3. Electrophoretic mobility shift assays show weak binding activity of unknown proteins to the *Pht1;1* promoter

3.1 Introduction

In higher plants, gene expression is often regulated by interactions between specific transcription factors (TFs) and *cis-acting* elements in promoter regions. Transcriptional regulation is of great importance in controlling gene expression under different circumstances. In plants, many transcription factors have been identified and their functions in regulating gene expression in a broad range of biological processes are well documented.

In *Arabidopsis*, a few transcription factors have been identified as regulators in Pi starvation responses. Among these TFs, AtPHR1 is the first and only transcription factor proved to directly control the expression of Pi starvation responsive (PSR) genes (Rubio, 2001). In the *phr1* mutant background, the activity of the β -glucuronidase (GUS) reporter gene driven by the *AtIPS1* promoter was reduced during Pi deprivation. Sequence analysis indicated that PHR1 encoded a member of the MYB superfamily of DNA binding proteins. The binding activity of PHR1 was confirmed by electrophoretic mobility shift assays (EMSA). The results indicated that PHR1 bound to the GNATATNC motif of the *AtIPS1* promoter to activate gene expression. Therefore, this motif is named as PHR1-binding sequence (PIBS). Sequence BLAST searches suggested that the PIBS motif was present in many PSR genes including *Pht1;1*, *IPS1/3*, *ACP5*, etc. PHR1 homologues have been identified in other species including OsPHR1 and OsPHR2 in rice, and PSR in green algae.

Previous studies on *Pht1;1* expression kinetics in response to Pi starvation and different inhibitors performed in our lab, allowed us to propose a model for regulation of *Pht1;1* (see Chapter 1, section 1.6). In this model, a certain amount of labile repressor is proposed to exist in plant cells to regulate the expression of *Pht1;1*. The regulation could be performed by repressor protein directly binding to the promoter of *Pht1;1*, or interacting with other *Pht1;1* promoter binding proteins. This labile repressor is constitutively under protein synthesis and degradation. Under Pi

sufficient conditions, the concentration of labile repressor is balanced to be high enough to inhibit *Phl1;1* expression. During Pi deprivation, the labile repressor would perceive the Pi starvation signal, and become more accessible to the protein degradation mechanism. The increased degradation results in reduced concentration of labile repressor. Therefore, the labile repressor would release the inhibition of *Phl1;1*. The up regulation of *Phl1;1* could then help the plant adapt to the Pi starvation conditions.

To prove this model, an important piece of evidence would come from protein-DNA binding assays to demonstrate the existence of one or several proteins that could bind to the promoter region of *Phl1;1*. Similar methods have been utilized to analyze *Phl1;4* and *AtIPSI* regulation. In 2001, Mukatira et al. showed that an unknown protein could bind to the promoter of *Phl1;4* and *AtIPSI* by EMSA (Mukatira *et al.*, 2001). The binding evidently existed under Pi sufficient conditions but disappeared in Pi starvation conditions. These data provided us with the confidence to perform EMSA to test protein-DNA binding between the potential unknown protein from Pi sufficient plants and the promoter of *Phl1;1*.

As an in vitro assay, EMSA has been proved to be a powerful tool to detect the interactions between protein and nucleic acids. The assay is usually performed in two steps. Firstly, the binding reaction is set up manually by addition of radiolabeled probes and protein extracts into a customized binding buffer. After a certain time of incubation, the result is visualized by running the reaction onto a non-denaturing polyacrylamide gel. The detection of binding activity is based on the observation that the electrophoretic mobility of a protein-nucleic acid complex is typically less than that of the free nucleic acid. In practice, the result of EMSA would be affected by a few factors. Therefore, for a study of a particular interaction, several variables should be considered including design of the nucleic acid target, binding reaction conditions and electrophoresis conditions. Normally, a short nucleic acid target is a good design, especially when the binding protein has low sequence-specificity. The protein-nucleic acid interactions are usually sensitive to the mono- or divalent salt concentrations and pH. In binding reaction, inclusion of a carrier protein, such as BSA, could improve the stability of some protein-nucleic acid complexes during electrophoresis. Another important additive is carrier DNA, which could avoid the

non-specific binding of proteins to the target sequence. Optimally, the sequence of carrier DNA should bear little resemblance to the specific binding site. For unknown target sequence, it is best to test different types of carrier DNA. Commonly used carrier DNAs include poly(dA-dT) and poly(dI-dC). The running buffer system can also affect the final result of EMSA. Among popular buffers, Tris-glycine system has several advantages. The higher ionic strength makes recirculation of buffer unnecessary. The bands tend to be sharper than that in low ionic strength buffers. Moreover, a smaller amount of carrier DNA is required to abolish the non-specific binding activity in higher-ionic-strength buffer.

In this chapter, EMSA was performed to test the protein-DNA binding activity using *Phl1;1* promoter fragments as probes. The results are described and discussed here.

3.2 Results

3.2.1 EMSA experimental system setup

The utility of EMSA is underscored by the many proteins that have been characterized using this assay. It has become clear that there is no single protocol that works best for all proteins. Therefore, the conditions for EMSA need to be optimized for my project. As discussed above, EMSA was used to test the interaction between the promoter of *Pht1;4* and unknown nuclear proteins (Hudson *et al.*, 1993; Mukatira *et al.*, 2001). In these experiments, two regions of the *Pht1;4* promoter specifically bound nuclear protein factors from Pi-sufficient *Arabidopsis* plants. I decided to first recapitulate the published experiments and therefore, I decided to set up the EMSA experiment with probes designed from promoter fragments of *Pht1;4*.

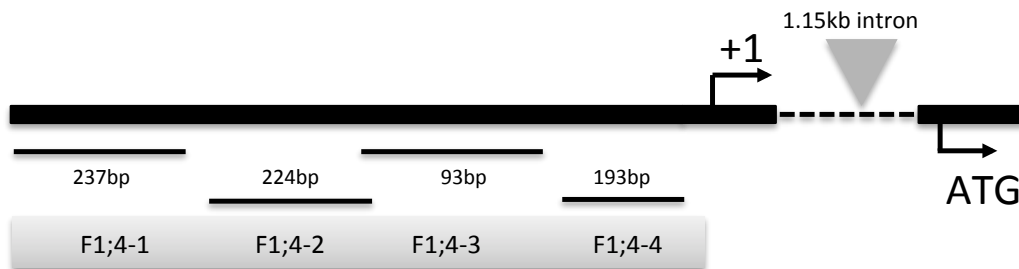


Fig. 3.1 Map of the different promoter fragments of *Pht1;4* used in EMSA assays. The location of an intron and the transcription start site (1+) and translation start site (ATG) are also shown.

As shown in Fig. 3.1, four fragments from *Pht1;4* promoter were chosen as probes. Sequence specific primers were designed to amplify the different fragments. PCR reactions were performed with Phusion polymerase (M0530S, NEB). PCR products were purified with the Qiagen PCR purification kit, and end-labeled with [γ - 32 P]-ATP. After the labeling reaction, the probes were purified, and the radioactivity was measured by scintillation counting. In the following protein-DNA binding reactions, 20,000 cpm of probes were always used unless specified otherwise. Total protein extract was prepared from either *Arabidopsis* roots or *Arabidopsis* suspension cell culture. The binding buffer included 10 mM HEPES (pH 7.9), 50 mM KCl, 1 mM EDTA, 1 mM DTT, 15% v/v glycerol, 2 ng/mL BSA and the electrophoresis was carried out in a 4% w/v polyacrylamide (39:1 acrylamide:bisacrylamide) gel, cast in

1 x Tris-glycine buffer (25mM Tris-base, 190mM Glycine, 1mM EDTA pH8.3), and run in 1 x Tris-glycine buffer.

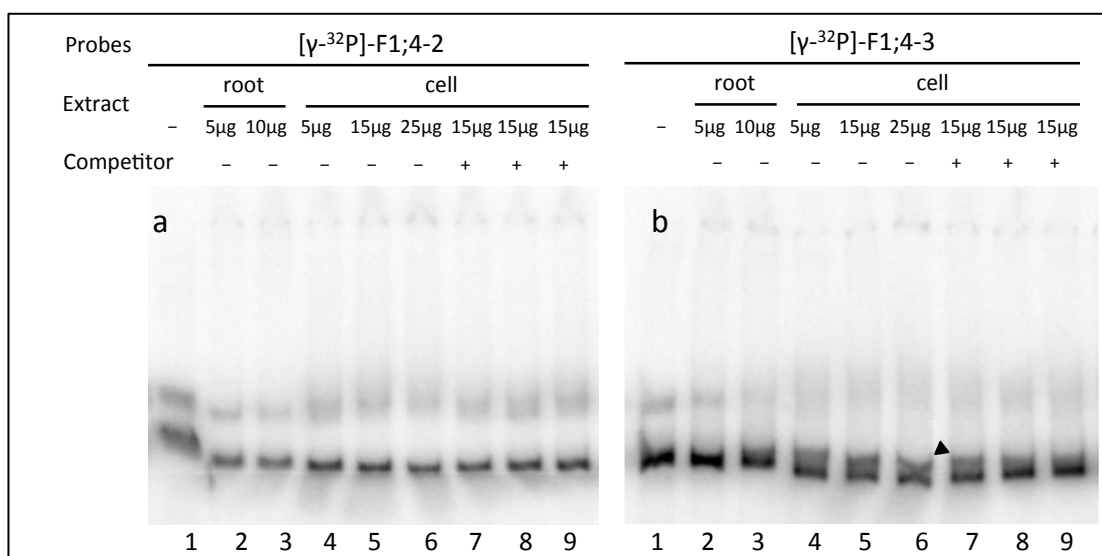


Fig. 3.2 EMSA using radio-labeled F1;4-2 (a) and F1;4-3 (b) fragments and total protein extracts from *Arabidopsis* roots and suspension cell cultures grown under +Pi conditions.

Lane 1: free probes as control, lane 2: probe with 5 μ g root extract, lane 3: probe with 10 μ g root extract, lane 4: probe with 5 μ g cell extract, lane 5: probe with 15 μ g cell extract, lane 6: probe with 25 μ g cell extract, lane 7: probe with 15 μ g cell extract and unlabeled F1;4-1 as competitor, lane 8: probe with 15 μ g cell extract and unlabeled F1;4-2 as competitor, lane 9: probe with 15 μ g cell extract and unlabeled F1;4-3 as competitor.

In the first experiment, probes of F1;4-2 and F1;4-3 were used in protein-DNA binding assays with protein extracts from *Arabidopsis* roots and suspension cells. As shown in Fig. 3.2a, the free probe contained a faint, more slowly-migrating band, which was also present in the samples with added protein. In Fig. 3.2b, another shifted band was observed in lane4~lane8, even though it was very close to the free probe. In this preliminary test, only F1;4-3 could generate a band that was not present in free probe (Fig. 3.2b). This suggested that F1;4-3 might work better than F1;4-2 as a positive control probe. However, the band migration was not as much as expected, which indicated that the EMSA condition needed optimization. To optimize the EMSA conditions, several adjustments were tested.

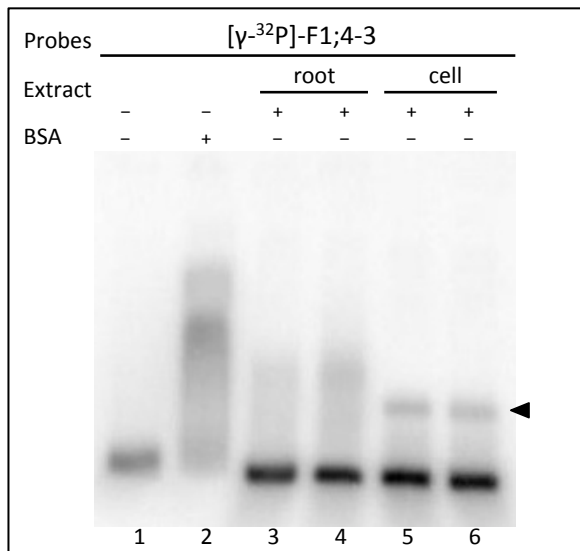


Fig. 3.3 EMSA using radio-labeled F1;4-3 fragments and total protein extracts from *Arabidopsis* roots and suspension cell cultures grown in +Pi conditions. Shifted bands were indicated by arrowhead.

Lane 1: free probe as control, no BSA in binding reaction, lane 2: free probe control, 2ng/ μ l BSA in binding reaction, lane 3: probe with 5 μ g root extract before dialysis, lane 4: probe with 5 μ g root extract after dialysis, lane 5: probe with 5 μ g cell culture extract before dialysis, lane 6: probe with 5 μ g cell culture extract after dialysis. From lane 3 to lane 6, no BSA is added in binding reaction.

The effect of BSA: BSA is normally suggested as a carrier protein in binding reaction to minimize non-specific losses of binding proteins during solution handling. In previous experiment (Fig. 3.2), BSA was included in the binding reaction. As the result was not ideal, I tested the effect of removing BSA from binding reaction. As shown in Fig. 3.3, F1;4-3 was used as probe in binding reactions with protein extracts, either before dialysis (Fig. 3.3 lane 3 & lane5) or after dialysis (Fig. 3.3 lane 4 & lane 6), from *Arabidopsis* roots or suspension cells. All reactions were set up without BSA except for one of the negative controls (Fig. 3.3, lane2). A shifted band was observed when protein extracts from *Arabidopsis* cell culture was included in binding reaction. This suggested that removal of BSA might help to stabilize the formation of protein-DNA complex in my experiment. However, the intensity of bands here was weak. To further optimize the condition, I decided to test the effect of salt concentration, which was an important factor that could affect the result of EMSA.

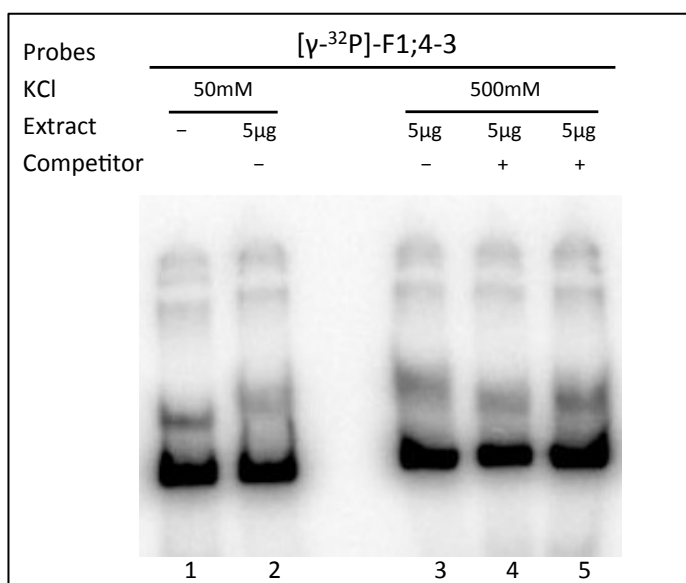


Fig. 3.4 EMSA using radio-labeled F1;4-3 fragments and total protein extracts from *Arabidopsis* suspension cell cultures grown in +Pi conditions.

Lane 1: free probes as control, 50 mM KCl in binding reaction, lane 2: probe with 5 μ g cell extract, 50 mM KCl in binding reaction, lane 3: probe with 5 μ g cell extract, 500 mM KCl in binding reaction, lane 4: probe with 5 μ g cell culture extract, 20x unlabeled F1;4-2 added as competitor, 500 mM KCl in binding reaction, lane 5: probe with 5 μ g cell culture extract, 20x unlabeled F1;4-3 added as competitor, 500 mM KCl in binding reaction

The effect of salt: Salt concentration is another factor that affects protein-DNA binding. As the properties of the potential binding protein are unknown, different salt concentrations were tested. In my experiment, KCl was used as the basal salt in binding reactions. As shown in Fig. 3.4, reaction in lane 2 and lane 3 were set up under 50 mM and 500 mM KCl conditions, respectively. In both cases, there was a faint band visible (Fig. 3.4, lane 2 and lane 3). However, this band was comparable to the band in free-probe-control (Fig.3.4, lane 1). Besides, addition of competitor, either unlabeled F1;4-2 or F1;4-3 (Fig.3.4, lane4 and lane 5), did not have any effect on the shifted band in lane 3. Together, these results indicated that slower migrating bands were not due to protein-DNA binding.

From the above results, the probes from *Pht1;4* promoter did not give the expected band migration as shown in the study of Mukatira *et al.* (2011). This could be due to different growth conditions for the plant materials used for the protein extracts. To take a step forward, I decided to take the risk of testing protein-DNA binding between the *Pht1;1* promoter and *Arabidopsis* protein extracts.

3.2.2 Test protein-DNA binding activity between *Pht1;1* promoter and unknown proteins

To test whether I could identify protein(s) that bind to the promoter of *Pht1;1* gene, five probes were prepared for the EMSA experiment. As shown in Fig. 3.5, five fragments were designed starting from 1056 bp upstream of transcription start site. To get the best result, the length of all the fragments were designed as between 200 bp-350 bp with ~25 bp overlapping region between adjacent fragments. All fragments were amplified with Phusion PCR polymerase (M0530S, NEB).

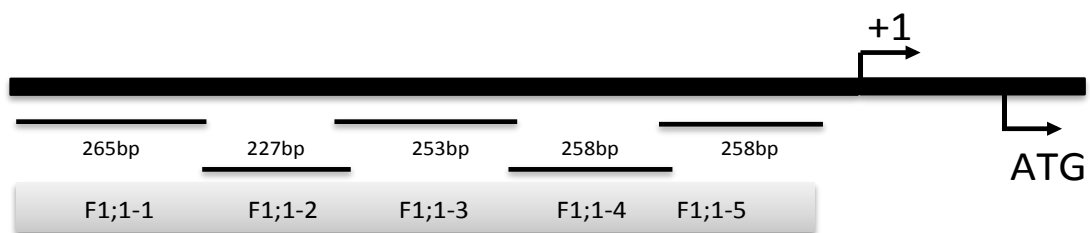


Fig. 3.5 Map of the different promoter fragments of *Pht1;4* used in EMSA assays. The location of an intron and the transcriptional start site (1+) and translational start site (ATG) are also shown.

PCR products were purified with Qiagen PCR purification kit, and end-labeled with [γ - 32 P] ATP. After labeling reaction, the probes were purified, and the radioactivity was measured by scintillation counting. In protein-DNA binding reactions, 20,000 cpm of probes are always used unless specified. Total protein extract was prepared from either *Arabidopsis* roots or *Arabidopsis* suspension cell culture. The binding buffer included 10 mM HEPES (pH 7.9), 50 mM KCl, 1 mM EDTA, 1 mM DTT, 15% v/v glycerol, 2 ng/mL BSA and the electrophoresis was carried out in a 4% w/v polyacrylamide (39:1 acrylamide:bisacrylamide) gel, cast in 1 x Tris-glycine buffer (25mM Tris-base, 190mM Glycine, 1mM EDTA pH8.3), and run in 1 x Tris-glycine buffer.

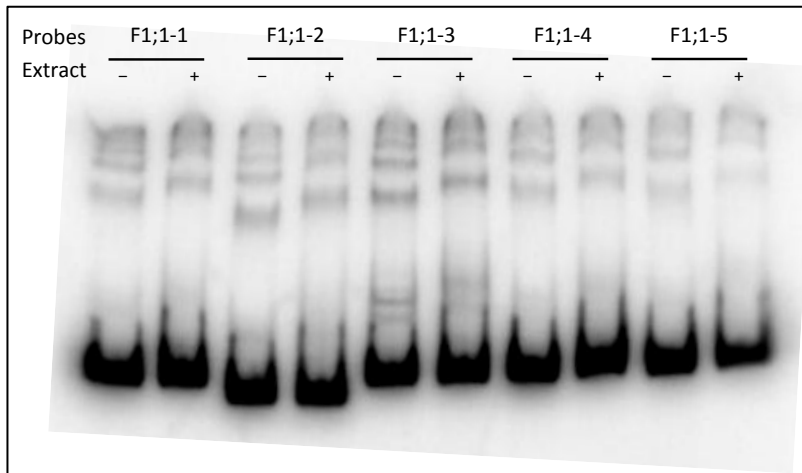


Fig. 3.6 EMSA using radio-labeled F1;1-1~5 fragments and total protein extract from *Arabidopsis* suspension cell cultures grown under +Pi condition. Labeled probes were incubated with 5 µg protein extract from cell culture (+). Negative control (-) was set up with labeled probes only.

In the first assay, all five probes were tested with total protein extracts from *Arabidopsis* cell culture. As shown in Fig. 3.6, there was not a clear shifted band in samples with protein added compared to negative controls. This indicated that there was not any protein-DNA complexes formed under current EMSA condition, or the current condition was not suitable for the visualization of the complexes. Considering that the expected band would be formed by a labile repressor protein binding to the target, it was possible that the potential protein-DNA complex was very sensitive to the experimental conditions. Therefore, I repeated the EMSA assays with different adjustments to optimize the conditions.

The effect of carrier DNA: Carrier DNA, such as poly(dI-dC)·poly(dI-dC) or poly(dA-dT)·poly(dA-dT), plays important roles in EMSA experiment. Usually, a protein sample will contain more than one nucleic acid binding activity, especially for a crude protein extract. When the secondary binding activity exists, it could unspecifically bind to the labeled probes and cause false positives. Addition of carrier DNA to binding reaction could reduce the chance of unspecific binding. For unknown proteins, it is always good to test the effect of different carrier DNAs. As shown in Fig. 3.7, a smear band (Fig. 3.7, pointed by arrowhead) appeared for all five probes when carrier DNA, poly(dI-dC)·poly(dI-dC), was removed from binding reaction. This indicated the carrier DNA did have an effect on the protein-DNA binding in my experiment. However, removal of carrier DNA increased the chance

for formation of non-specific protein-DNA complexes. Therefore, further tests were needed to distinguish whether the smear bands were formed by specific protein-DNA binding.

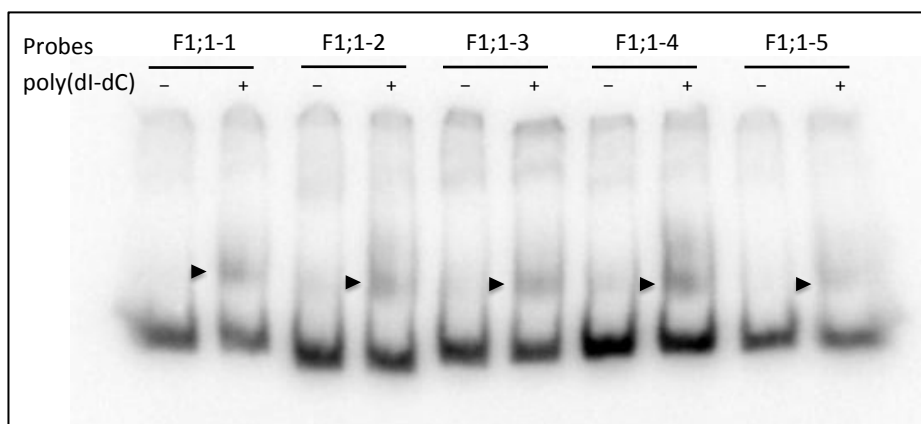


Fig. 3.7 EMSA using radio-labeled F1;1-1~F1;1-5 fragments and total protein extract from *Arabidopsis* suspension cell culture from +Pi condition. Smear bands were indicated by arrowhead. Labeled probes were incubated with 5 μ g protein extract from cell culture. The reactions were set up in binding buffers either with poly(dI-dC) (+) or without poly(dI-dC)(-).

In parallel with the EMSA experiments, the promoter sequence of *Phl1;1* was analyzed by SCOPE (<http://genie.dartmouth.edu/scope/>), with the aim to identify *cis*-elements. The results from this analysis suggested that the majority of potential, over-represented motifs were located in fragment 3 and 4, namely F1;1-3 and F1;1-4 (data not shown). Therefore, these 2 probes were chosen for further experiments. In the next assay, I decided to test the effect of different amount of salt included in binding reactions as the protein-DNA binding activity was proved to be sensitive to salt concentration.

The effect of salt: Salt concentration has been proved to affect the EMSA result significantly (Schneider-Poetsch *et al.*, 2010; Hudson *et al.*, 1993). Although the K^+ concentration is in the range of 80 mM to 200 mM in plant cells (Walker *et al.*, 1996), we tested a broader range of concentrations in order to find out the best conditions for *in vitro* protein-DNA binding. To test the effect of salt concentration in my experiments, protein-DNA binding reactions were set up in 50 mM, 200 mM

and 500 mM KCl buffer (Fig. 3.8). In reactions, different types of carrier DNA were also included. To limit the heating of the gel, the gel running system was incubated in an icebox. As shown in Fig. 3.8, two shifted bands appeared when reactions were set up in 500 mM KCl conditions (indicated by arrowhead), with one clear band close to the free probe and the other faint one with lower mobility (Fig. 3.8 a&b, lane 7~9). poly(dI-dC)·poly(dI-dC) and poly(dA-dT)·poly(dA-dT) did not seem to have a big effect on the band migration (Fig. 3.8 a&b, lane 8&9), when compared to the reaction without carrier DNA (Fig. 3.8 a&b, lane 7). However, in lower KCl concentrations, only the faint band appeared (Fig. 3.8 a&b, lane 1&4, indicated by star). Meanwhile, addition of carrier DNA reduced the capability of the protein binding to probe (Fig. 3.8 a&b, lane 2&3, lane 5&6). This indicated the unknown protein-DNA complex was likely more stable under higher salt concentration. To confirm the result, a repeat experiment was performed with probe F1;1-3 and F1;1-4, but only under 500 mM KCl condition (Fig. 3.9). As negative control, the reaction was set up with only probes, either F1;1-3 (Fig. 3.9, lane 1) or F1;1-4 (Fig. 3.9, lane 4). As shown in Fig. 3.9, two bands migrated from free probes compared to negative control, which were similar to shifted bands in the last experiment (Fig. 3.8). However, the result was not easily reproducible. As shown in Fig. 3.10, the two bands disappeared (Fig. 3.10, lane 2&3) in this repeat originally aiming to introduce competition (Fig. 3.10, lane 4&5). For probe F1;1-4, the only band showed in lane 7 where the reaction was set up without carrier DNA.

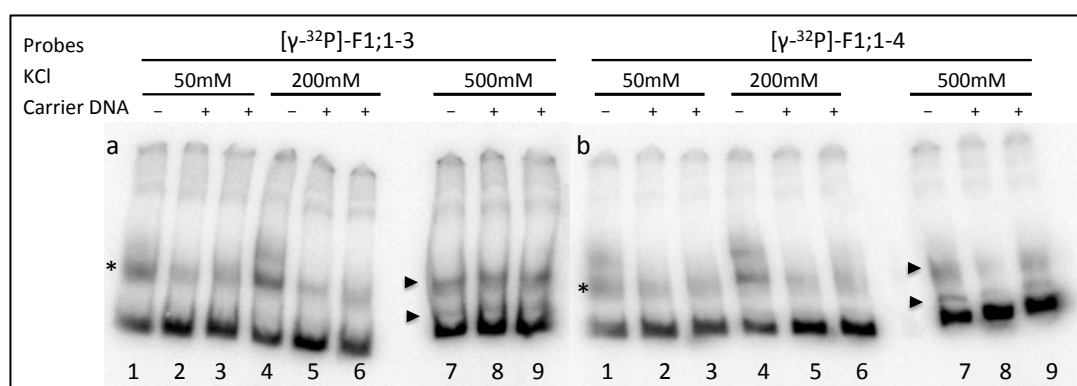


Fig. 3.8 EMSA using radio-labeled F1;1-1-3 (a) or F1;1-4 (b) fragments and total protein extracts from *Arabidopsis* suspension cell cultures grown in +Pi conditions. The shifted bands were indicated by star (lane1~6) or arrowheads (lane 7~9). The reaction was set up in binding buffers with different KCl concentrations (as indicated in the figure). poly(dA-dT) was added in reactions of lane 2, lane 5 and lane 8. poly(dI-dC) was added in reactions of lane 3, lane 6 and lane 9.

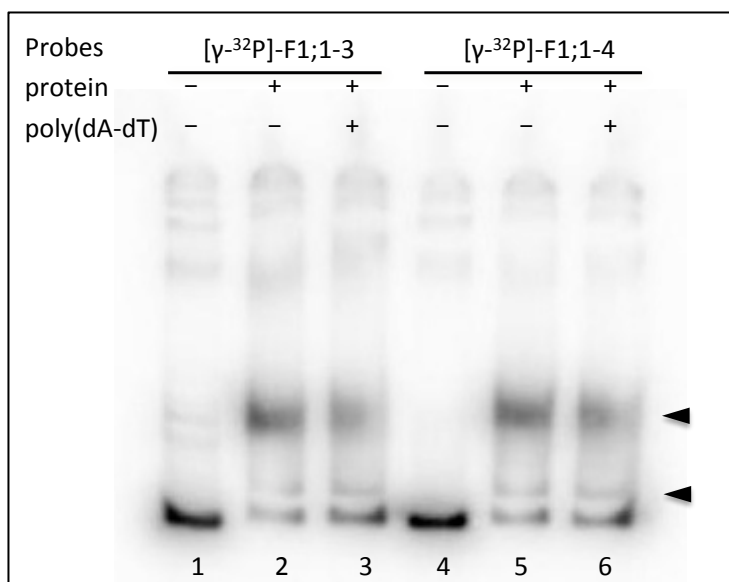


Fig. 3.9 EMSA using radio-labeled F1;1-3 (a) or F1;1-4 (b) fragments and total protein extract from *Arabidopsis* suspension cell cultures grown in +Pi conditions. The reaction was set up in binding buffers with 500 mM KCl. poly(dA-dT) was added in reactions of lane 3 and lane 6.

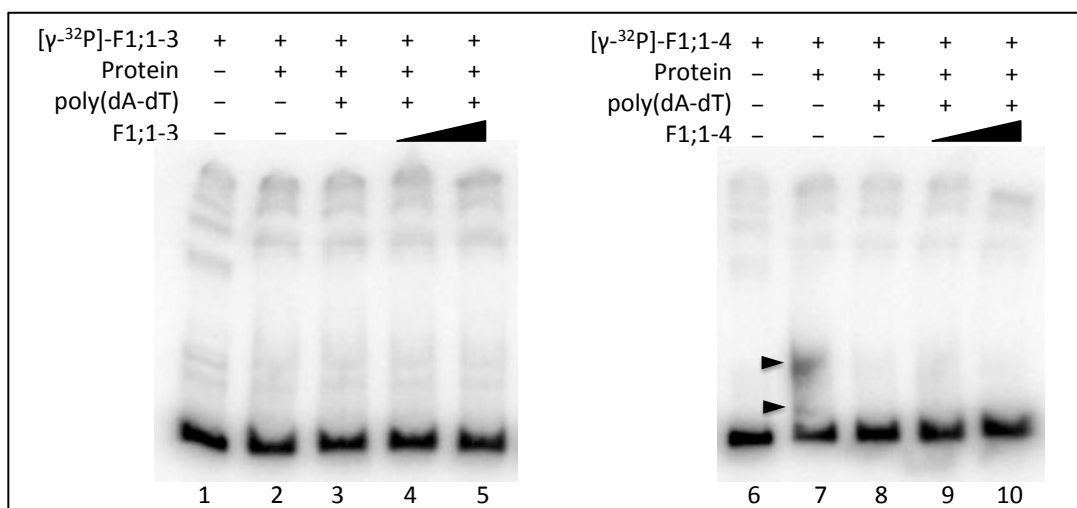


Fig. 3.10 EMSA using radio-labeled F1;1-3 (a) or F1;1-4 (b) fragments and total protein extract from *Arabidopsis* suspension cell culture grown in +Pi conditions. The reaction was set up in binding buffers with 500 mM KCl. Competition was introduced in lanes 4&5 and lanes 9&10.

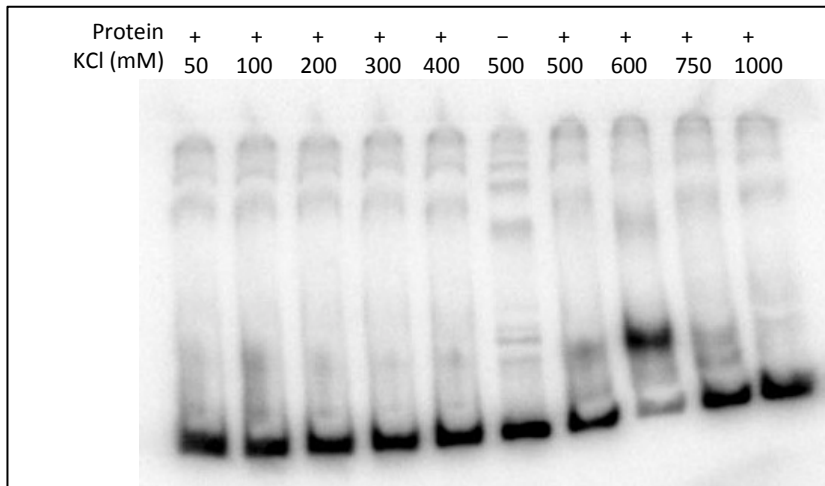


Fig. 3.11 EMSA using radio-labeled F1;1-3 fragment and total protein extract from *Arabidopsis* suspension cell cultures grown in +Pi conditions. The reaction was set up in binding buffers with different KCl concentration (as shown in figure).

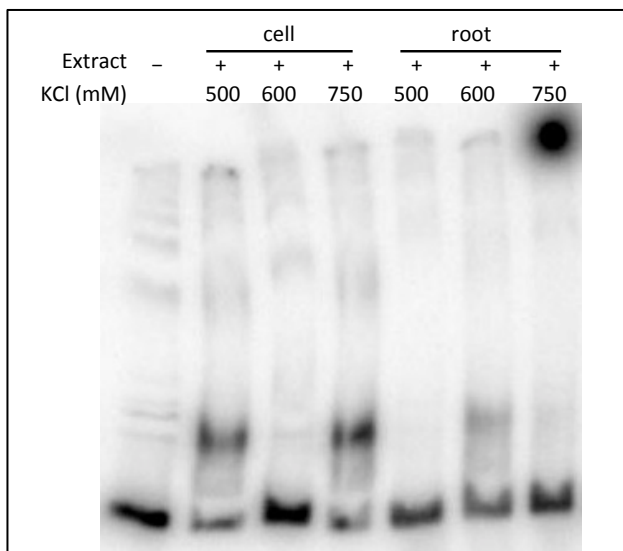


Fig. 3.12 EMSA using radio-labeled F1;1-3 fragment and total protein extract from *Arabidopsis* suspension cell culture and roots grown in +Pi conditions. The reaction was set up in binding buffers with different KCl concentrations (as shown in figure).

To identify the best salt condition, protein-DNA binding reactions were performed with F1;1-3 under more detailed salt concentrations (*Fig. 3.11*). Interestingly, a stronger shifted band appeared under 600 mM KCl condition while the bands under 500 mM and 750 mM KCl were relatively weaker. However, opposite result was obtained in next repeat where the bands were stronger under 500 mM and 750 mM

KCl (*Fig. 3.12*). Together, these data suggested that high salt concentration might have positive effect on stabilizing the protein-DNA complex. However, the best salt concentration was hard to determine because of the variable formation of protein-DNA complexes.

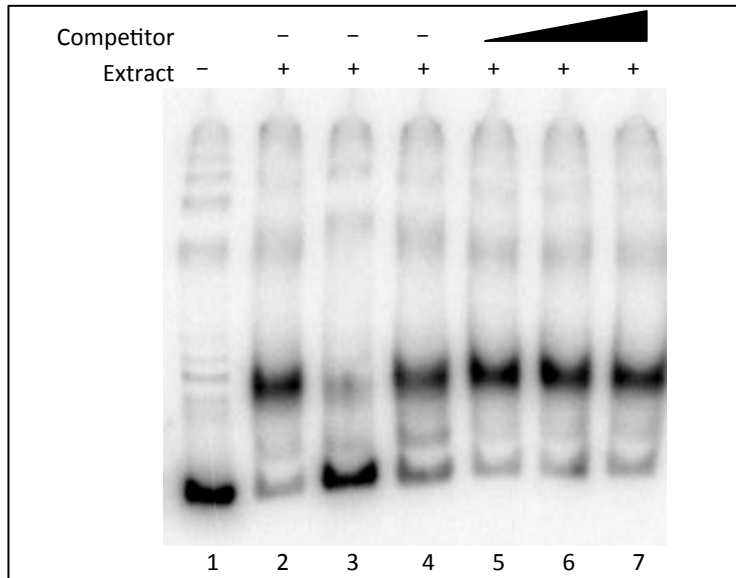


Fig. 3.13 EMSA using radio-labeled F1;1-3 fragment and total protein extract from *Arabidopsis* suspension cell culture grown in +Pi condition.

Lane 1: reaction with probe only as negative control; lane 2: probe with 5 µg proteins incubated in binding buffer for 10 min; lane 3: probe with 5 µg proteins incubated in binding buffer for 35 min; lane 4: 5 µg proteins were added to binding buffer and incubated for 20min, and then probes were added and incubated for another 20min; lane 5~lane 7: the reaction were prepared in same way as in lane 4 except that increasing amount of unlabeled F1;1-3 were added in the binding buffer as competitors.

The order effect of addition of protein and probes: In typical EMSA protocols, it is always suggested that protein should be added as the last component of the binding reaction. This will ensure that proteins could with equal probability encounter the radiolabeled probes and carrier DNA, thus the result would be more convincing. As the protein-DNA complex was not reproducible in my experiment, I decided to test the effect of adding protein before probes. As shown in *Fig. 3.13*, the two shifted bands were observed when protein was added into binding reaction before probes (*Fig.3.13, lane4*). The intensity of shifted bands in lane 4 was much stronger than those in lane 3 where the addition of components in reaction mixture followed typical protocol. When different concentrations of unlabeled F1;1-3 are added as

competitor, the band close to free probe became weaker, which suggested the binding of probes was competed by unlabeled fragment. In this experiment, another adjustment was included to test the effect of incubation time. In all previous experiments, the binding reaction was always incubated for at least 30 min at 30°C. However, the shifted bands, especially the upper band, are stronger when the reaction mixture was incubated for only 10 min (*Fig. 3.13, lane2*). This indicated that extension of incubation time might destabilize the protein-DNA complex.

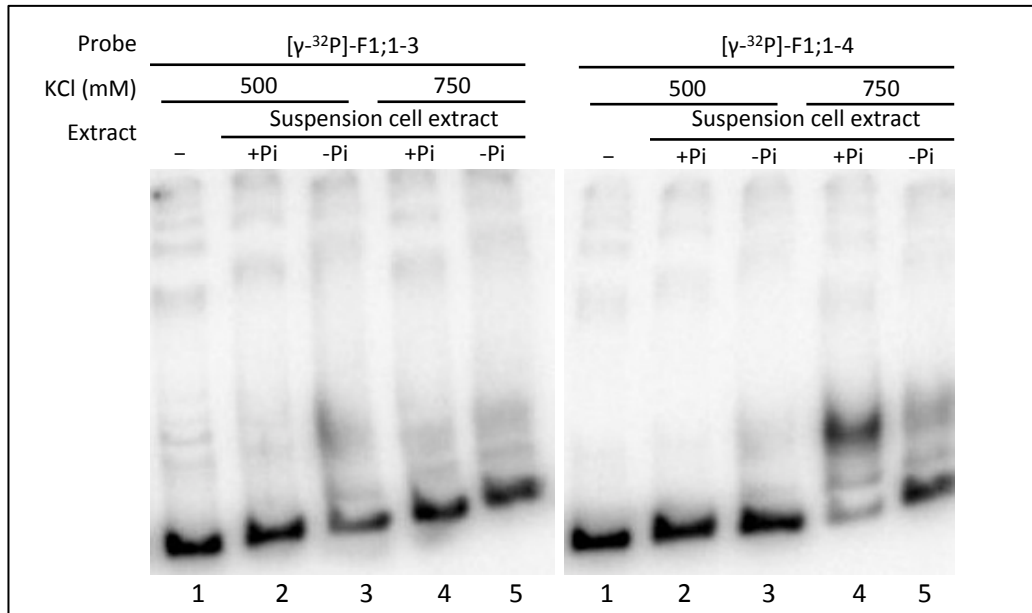


Fig. 3.14 EMSA using radio-labeled F1;1-3 (a) and F1;1-4 (b) fragments and total protein extract from *Arabidopsis* suspension cell culture grown in Pi sufficient (+Pi) or Pi deficient (-Pi) conditions.

The binding reactions were set up in either 500mM KCl (lane 1 ~ lane 3) or 750mM KCl buffer (lane 4 and lane 5). All reactions were set up by firstly adding the protein extract into binding buffer; after incubation for 20min, the probes were added and incubated for another 20min.

Proteins from +Pi and -Pi conditions: In our proposed model, a labile repressor could bind to the promoter of *Pht1;1* and further suppress its expression under Pi sufficient condition. This binding would become weak and fragile in response to Pi starvation. Therefore, protein extracts from +Pi and -Pi conditions were tested in EMSA experiment. As shown in *Fig. 3.14b*, the upper band showed higher intensity (lane9) when +Pi protein extract was used for binding reaction. This suggested the upper band could be the protein-DNA complex between labile repressor and probe. However, this band is expected to exist for both F1;1-3 and F1;1-4 with +Pi protein

extract, which has been shown in previous experiments (*Fig. 3.9, Fig. 3.10*). The observed loss of the retarded band further indicated that the binding between the potential labile repressor and promoter was weak.

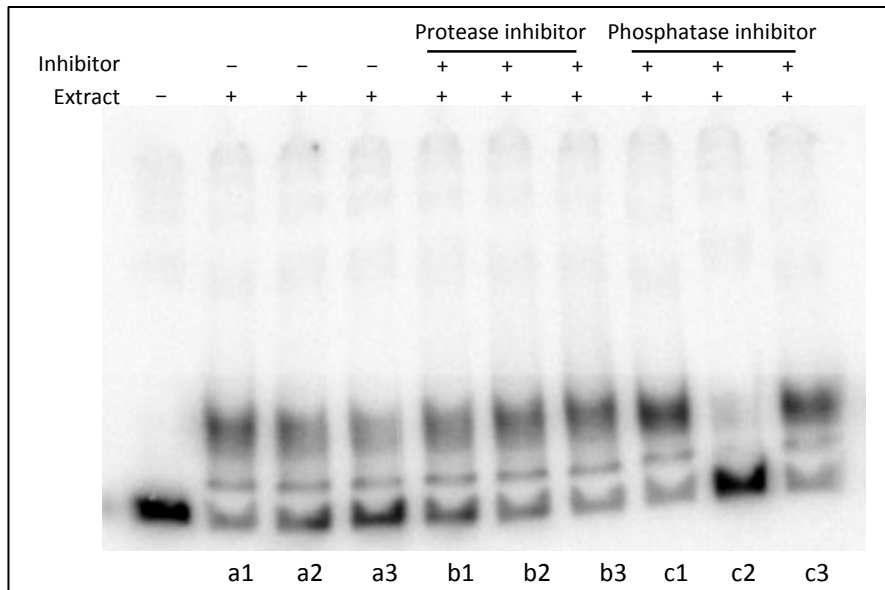


Fig. 3.15 EMSA using radio-labeled F1;1-3 fragment and total protein extract from *Arabidopsis* suspension cell culture.

The reactions were prepared in triplicates. All reactions were set up by firstly adding the protein extract into binding buffer; after incubation for 20min, the probes were added and incubated for another 20min. In lane b1~b3, protease inhibitor was included in binding buffer; in lane c1~c3, phosphatase inhibitor was included in binding buffer.

The effect of inhibitors: As proposed in the model, the potential repressor is labile and constitutively degraded, even in Pi sufficient conditions. The degradation of the repressor is possibly mediated by the ubiquitin-proteasome proteolysis pathway. Therefore, proteolysis inhibitors and phosphatase inhibitors were separately added in binding reaction. As shown in *Fig. 3.15*, each reaction was prepared in triplicate. Compared to the negative control, most of the binding reactions generated protein-DNA complexes. However, the addition of proteolysis and phosphatase inhibitors did not show much effect on the results. It did not help to stabilize the complex better than the normal condition (*Fig.3.15, lane a1~ a3*). Meanwhile, there was not any formation of new complexes compared to normal condition. This further indicated the weak binding between the unknown proteins and *Phl1;1* promoter fragments visualized in my experiment.

3.2.3 Sequence difference of the *Pht1;1* promoter in Col-0 and Ler background

As mentioned above, a model was proposed for the regulation of *Pht1;1* in early response to Pi starvation. (see Chapter1, section 1.6) This model was based on the responsive kinetics of *Pht1;1* during Pi deprivation and its response to CHX and MG132 inhibitor treatment. The key experiments to set up the model were mainly performed with an *Arabidopsis* suspension cell culture system. However, the cell culture line died afterwards, and the suspension cell culture used in EMSA experiments was obtained from a different source. Therefore, genotyping the cell culture line would be important.

To do this, the gene specific primers designed for EMSA experiments based on Col-0 background was firstly tested in genotyping PCR. Fortunately, one primer pair can distinguish the Col-0 and Ler ecotype. This primer pair was designed to amplify F1;1-2 and should generate a 227 bp fragments from *Pht1;1* promoter in Col-0 background (Fig. 3.5). Interestingly, it could produce a much larger fragment, which was around 280 bp in Ler background (Fig. 3.16, lane 2). As shown in Fig.3.16, the cell culture line used in EMSA proved to be Ler ecotype as it produced the same sized band as Ler plant (Fig. 3.16, lane 3). Considering the difference between Col-0 and Ler, it is important to have the sequence information of *Pht1;1* promoter in Ler background. We searched all the available databases, but unfortunately, no sequence information was publicly available at the moment. Therefore, another approach was resorted to. We used the primers for the full length promoter designed for Col-0 *Pht1;1* promoter deletion analysis (see details in Chapter 5) to amplify from genomic DNA from suspension cells as template. A larger PCR product (data not shown) was obtained and we sequenced this product to get the Ler *Pht1;1* promoter sequence. Sequence comparison between Col-0 and Ler ecotype was performed with ClustalW software (Appendix 1). The result showed that *Pht1;1* promoter sequence was quite different between Col-0 and Ler background. Compared to Col-0, there was a 785 bp insertion in the *Pht1;1* promoter sequence in Ler background. This large insertion could make the regulation of *Pht1;1* different between Col-0 and Ler plants. After this aspect of my project was completed, the *Arabidopsis* 1001 genome project commenced, which aims to provide the genome information from many accessions of *Arabidopsis thaliana*. We checked the polymorphisms in *Pht1;1* promoter

sequence in other *Arabidopsis* accessions. Interestingly, a few accessions showed similar variation in the *Phl1;1* promoter as observed in the Ler accession (Fig. 3.17). The 1001 genome project has not been completed yet. Therefore, we expect more accessions showing similar variation in the *Phl1;1* promoter sequence. Further experiments to examine *Phl1;1* regulation in these accessions would be interesting and helpful to reveal the function of these genetic variations.

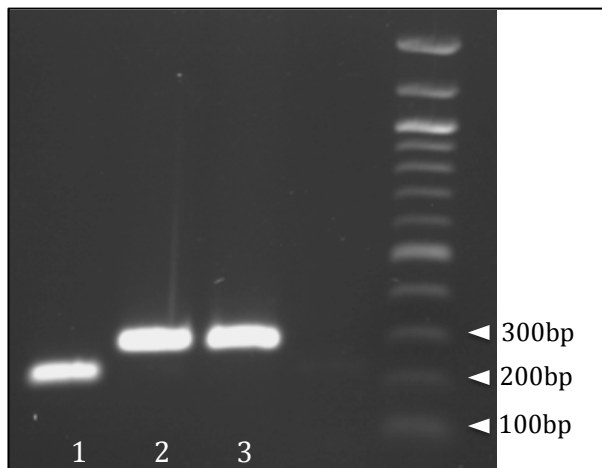


Fig.3.16 Genotyping PCR result with F1;1-2 primers. Lane1 and lane2 load the PCR product with Col-0 and Ler genomic DNA as template, respectively. Lane3 load the PCR product with suspension cell genomic DNA as template.



Fig. 3.17 Several *Arabidopsis* accessions showing similar genetic variations in the *Pht1;1* promoter sequence as that in Ler accession.

Promoter sequence is defined as 2000 bp upstream of translation start site.

Polymorphisms were visualized by comparison to the Col-0 accession.

A SNPs -- Red line

C SNPs -- Blue line

G SNPs -- Green line

T SNPs -- Yellow line

1 bp deletions -- Black line

Unsequenced regions -- .. (dot) or grey area

3.3 Discussion

In response to Pi starvation, the expressions of many genes are changed to facilitate plant adaption to the different environment. Among these genes, *Phl1;1* and *Phl1;4* are of great importance as they function as the main Pi transporters in *Arabidopsis* roots (Shin *et al.*, 2004). During Pi deprivation, *Phl1;1* and *Phl1;4* are significantly up-regulated to increase the uptake of Pi from the environment (Bari *et al.*, 2006). However, their regulation is still poorly understood. Until now, only P1BS motifs have been identified in the promoters of these two genes, which suggests their expression could be regulated by PHR1 on the transcriptional level.

In a previous study by our group, *Phl1;1* expression exhibited a transient peak within 4 hours in response to Pi starvation. Further analysis by utilizing cycloheximide (CHX) and MG132 indicated that *Phl1;1* could possibly be regulated by a labile repressor in this early response event. To identify the potential labile repressor, EMSA was firstly performed to reveal the existence of protein-DNA complexes between the *Phl1;1* promoter and unknown proteins under Pi sufficient conditions.

To set up the EMSA system, DNA fragments from the *Phl1;4* promoter were designed as probes. Among the four different probes (Fig. 3.1), F1;4-2 and F1;4-3 contained the protein-binding region showed in the study by Mukatira *et al.* (Mukatira *et al.*, 2001). However, our experiments showed different results, when compared to data from Mukatira *et al.* In our assay, a gel shift of the probe only appeared when F1;4-3 was used in protein-DNA binding assay (Fig. 3.3). But the shifted band was not reproducible in repeated experiments (Fig. 3.4 and Fig. 3.5). The reason for the difference could be due to the different materials used in the EMSA assays. In the study of Mukatira *et al.*, protein extracts from 12-day old seedlings were used in EMSA. However, in our experiment, the shifted band only appeared when protein extracts from *Arabidopsis* suspension cell cultures were used in binding reactions. Therefore, cell cultures were used as main source for protein extracts in repeat experiments. The difference between our result and published data would also indicate the difference in gene regulation between *Arabidopsis* plants and specific suspension cell culture lines.

To advance my project, probes designed from *Pht1;1* promoter were directly tested in EMSA assay (Fig. 3.6). Meanwhile, the promoter sequence was also analyzed by online software aiming to identify potential protein binding motifs. The analysis indicated that F1;1-3 and F1;1-4 could possibly contain such motifs. Therefore, these two probes were mainly used in the following EMSA experiments. To optimize the condition for EMSA, several adjustments were tried. From results, we found that both probes could form protein-DNA complexes, which were relatively stable under higher salt concentrations (Fig. 3.9). The stability of the complexes was not significantly affected by addition of carrier DNA (Fig. 3.9 and Fig. 3.10). However, the binding was not stable and reproducible in repeat experiments (Fig. 3.11). Surprisingly, the stability of protein-DNA complexes seemed to increase by: a, reducing the incubation time of the binding reaction; b, adding protein before probes into the binding reaction (Fig. 3.13). Addition of protease and phosphatase inhibitors did not increase the complex stability (Fig. 3.15). Together, these data suggested there may exist an unknown protein that could bind to the promoter of *Pht1;1* gene, but the binding was very unstable under *in vitro* conditions. Moreover, the protein-DNA complex visualized by EMSA in some experiments, may not be between a labile repressor and the promoter, as the shifted band appeared irrespective of Pi availability (Fig. 3.14).

The failure of EMSA to detect the potential repressor-DNA complex could be caused by several reasons. Firstly, EMSA is an *in vitro* method to detect protein-DNA binding activity. It works well when proteins can strongly bind to the DNA sequence. However, the potential labile repressor may only weakly bind to *Pht1;1* promoter, even *in vivo* in Pi sufficient conditions. The *in vitro* setup of the experiment may already break the potential complex. Secondly, the model for the labile repressor was proposed based on previous data, which were obtained by using a different cell culture line. However, that cell culture line died afterwards, and the cell culture line used in EMSA assays here was obtained from a different source. Suspension cell cultures are derived from a specific plant tissue, and different lines may show different behavior, and thus have different gene regulation. As the key experiments for model were not repeated with current cell culture line, we did not know whether the current cell culture line could reproduce the previous data (Lai, 2006). Therefore,

we can't deny the fact that the current cell culture may not show negative regulation of *Pht1;1*. Besides, the current cell culture line is genotyped to be Ler ecotype and the whole sequence of *Pht1;1* gene is significantly different between Col-0 and Ler ecotype. It could be very possible that regulation of *Pht1;1* gene is different between different *Arabidopsis* ecotypes. Therefore, to carry on this project, we decided to take a step backwards and repeat the key experiment with current plant materials and try to recapitalize the previous data to consolidate the model for labile repressor.

4. Early transcriptional responses to phosphate starvation in *Arabidopsis*

4.1 Introduction

Transcriptional changes in response to Pi starvation have been well documented. A few marker genes were identified to be highly inducible following the removal of Pi (Burleigh and Harrison, 1998; Martín *et al.*, 2000; Rubio, 2001; Shin *et al.*, 2004; Bari *et al.*, 2006). Previous studies in our group have examined expression kinetics of several Pi starvation responsive genes during Pi deprivation (Lai, 2006). As a result of these studies, a model was proposed for the immediately early response of *Phl1;1* gene expression based on several key experiments with a *Arabidopsis* suspension cell culture system (see Chapter 1, section 1.6).

In last chapter, EMSA was performed aiming to produce the initial evidence that could support this regulatory model for *Phl1;1* expression. However, the result was not satisfying. To continue the work, I decided to repeat those key experiments to check marker gene expression and recapitulate previous data in the currently available plant materials. Here, I mainly focused on two marker genes, which were the high affinity Pi transporter encoding gene *Phl1;1* (At5g43350) and the monogalactosyl-diacylglycerol (MGDG) synthase encoding gene *MGD3* (At2g11810). Previous studies in our group have shown that these two marker genes could rapidly respond to Pi cues (Lai, 2006). In my experiments, two types of plant material were used, namely a new *Arabidopsis* suspension cell culture and *Arabidopsis* young seedlings. Quantitative Real-time PCR (qRT-PCR) was performed to quantify the expression of marker genes and the results were described and discussed in this chapter.

4.2 Results

4.2.1 Expression kinetics of phosphate starvation responsive genes in *Arabidopsis* suspension cell cultures during Pi deprivation

Previous studies in our lab have shown that the suspension cell culture system was a highly efficient experimental system to study plant responses to nutrient stress at the molecular level. This system responds to external changes in Pi availability more

rapidly and consistently than seedlings, which could facilitate the study of the early Pi signalling. Besides, the cell culture system does not involve signal transduction or phosphate transport between individual cells, which make it a good system for the study local, cell autonomous signalling mechanisms. However, the cell culture lines that had been used previously in the lab died due to a failure of the temperature control system in the culture room, and the culture in use now was obtained from a different source, as the original culture's source was not available anymore. Therefore, the expression kinetics of marker genes was examined in the new cell culture line.

4.2.1.1 Pht1;1 & MGD3 expression kinetics during early Pi starvation treatment

To test the expression kinetics of marker genes during Pi starvation, *Arabidopsis* suspension cells grown in full nutrient media for 7 days were transferred to Pi-free media. qRT-PCR were performed with samples collected following a short time course after transfer. Oligonucleotide sequences for primers used in qRT-PCR were obtained from Fan's PhD thesis (Lai, 2006). Sequence comparison confirmed that all primers were designed based on Col-0 genomic sequence. Surprisingly, the qRT-PCR did not generate any signals for the *Pht1;1* gene. To confirm this result, a regular PCR reaction was performed with *Pht1;1* qRT-PCR primer pair. As shown in Fig. 4.1, the *Pht1;1* primer pair could generate the expected band from Col-0 root and Ler root cDNA samples, but not from suspension cell cDNA samples. As mentioned in last chapter, the cell culture line in use was confirmed to be Ler ecotype. The results from the above PCR reactions indicated that the Pht1;1 might express at very low level in this specific cell culture line. Additionally, the PCR generate a stronger band with cDNA samples from Col-0 roots than that from Ler roots, which suggest the differences in *Pht1;1* coding region between Col-0 and Ler ecotype. Therefore, the coding region of *Pht1;1* from the Ler genome was sequenced (Appendix 1). The result showed that the second nucleotide of *Pht1;1* forward primer was not complementary to the Ler *Pht1;1* cDNA sequence, and thus could cause the inefficient amplification in qRT-PCR reaction.

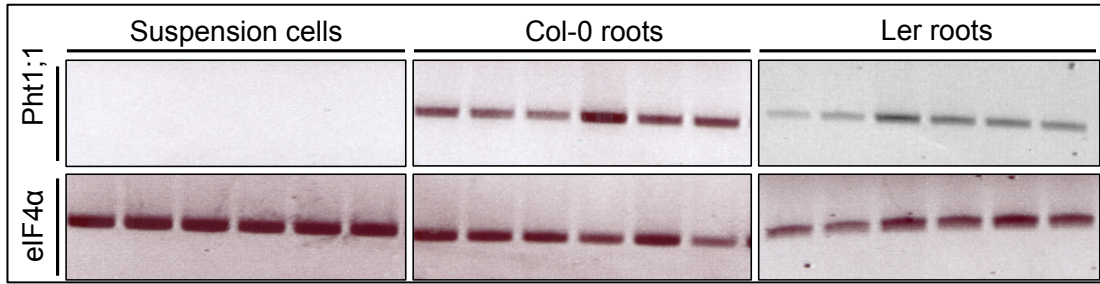


Fig. 4.1 RT-PCR with cDNA from *Arabidopsis* suspension cells, Col-0 roots and Ler roots.

RT-PCR was performed to amplify *Pht1;1* (At5g43350) and eIF4α (At3g13920). Primers designed for qRT-PCR were used in reactions. cDNA was prepared from either suspension cells, Col-0 roots or Ler roots.

To optimize the qRT-PCR amplification, the sequence of *Pht1;1* forward primer was modified to fit the Ler *Pht1;1* cDNA sequence. However, PCR reactions with the new primer pair still did not generate a strong signal with suspension cell cDNA samples. Two more primer pairs were designed using QuantPrime software (<http://www.quantprime.de/>). With the new primers, qRT-PCR analysis gave very weak signals even with cDNA samples from Pi starved suspension cells (data not shown). These results supported the view that the *Pht1;1* gene might be expressed at a very low level in this specific cell culture line, and thus could not be used to repeat previous experiments.

Fortunately, a Col-0 suspension cell culture line could be obtained. PCR reactions were performed to confirm its Col-0 genotype (Fig. 4.2). The suspension cells were sub-cultured in a continuously illuminated environment for 6 weeks before being used for any treatments. To examine the response of marker genes to Pi starvation, the suspension cells were grown in full nutrient media (with 2.5 mM Pi) for 7 days, and then transferred to Pi-free media. qRT-PCR was performed with cDNAs from suspension cell samples. As shown in Fig. 4.3, expression of *MGD3* did not dramatically respond to Pi starvation within 6 hours after transfer. In contrast, the expression of *Pht1;1* was strongly induced by Pi starvation, and the induction was constant. This indicated that the starvation treatment was effective and the suspension cells perceived the Pi starvation signal. However, the result was not consistent with previous data in our group (see Chapter 1, section 1.6). In previous study, *Pht1;1* only exhibited a transient increase during 2-4 hours after transfer of suspension cells from +Pi media to -Pi media, and its expression was subsequently

suppressed (Lai, 2006). The difference in the result suggested that the regulation of *Pht1;1* expression might be different in suspension cells under the current growth conditions in continuous light.

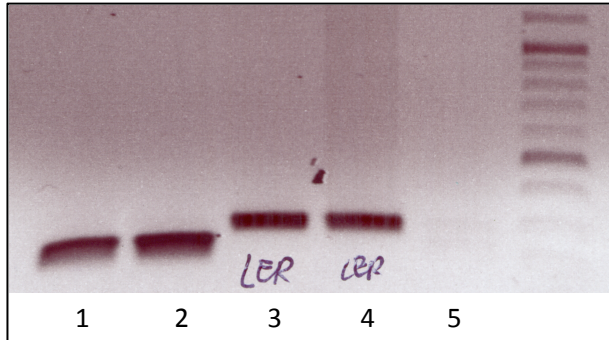


Fig.4.2 PCR reactions with genomic DNA extracted from new suspension cells (lane 1), Col-0 roots (lane 2), Ler roots (lane 3) and Ler suspension cells (lane4). As negative control (lane 5), PCR was performed without DNA template. Primers for F1;1-2 fragment from EMSA experiment was used to amplify the DNA fragment.

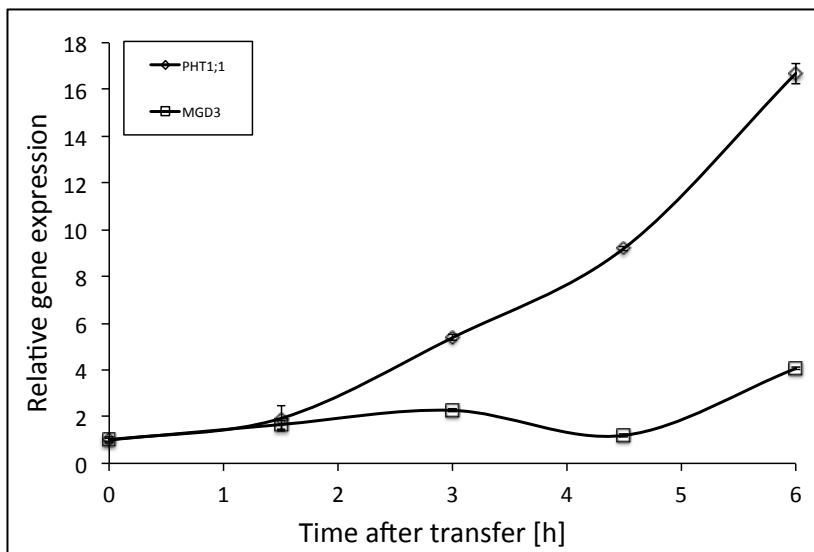


Fig. 4.3 Gene expression kinetics in *Arabidopsis* suspension cell culture after transfer from +Pi media to -Pi media. Gene expression was monitored in a time course by qRT-PCR. Error bars indicate standard error of the mean (SEM) from 3 biological repeats, and are smaller than the symbol when not visible.

Previously, the suspension cell culture was kept in a dark environment. Therefore, the cells lost their chlorophyll, which mimicked *Arabidopsis* root cells. Considering that *Pht1;1* is mainly expressed in plant roots, the previous growth condition for suspension cells might better reflect the regulation of *Pht1;1* expression in plant root

cells. To obtain a similar cell culture, suspension cells were sub-cultured in a dark room for 4 weeks to completely remove chlorophyll. To subject the suspension cells to Pi starvation treatment, half volume of the 7-day old cell culture was transferred to Pi-free media, while the other half was transferred to fresh +Pi media as control. As shown in *Fig. 4.4A*, the expression of *Pht1;1* gradually increased in 4.5 hours after the media switch, and decreased subsequently. For *MGD3*, the expression was rapidly repressed after transfer of the suspension cells to fresh +Pi media (*Fig. 4.4B*). This suggested that the suspension cells might already be slightly starved before the treatment. The rapid down-regulation of *MGD3* in Pi-free condition was unexpected. This suggested that a trace of Pi contamination might be introduced into suspension cell culture during manipulation, which further suggested that *MGD3* expression was highly sensitive to the Pi availability.

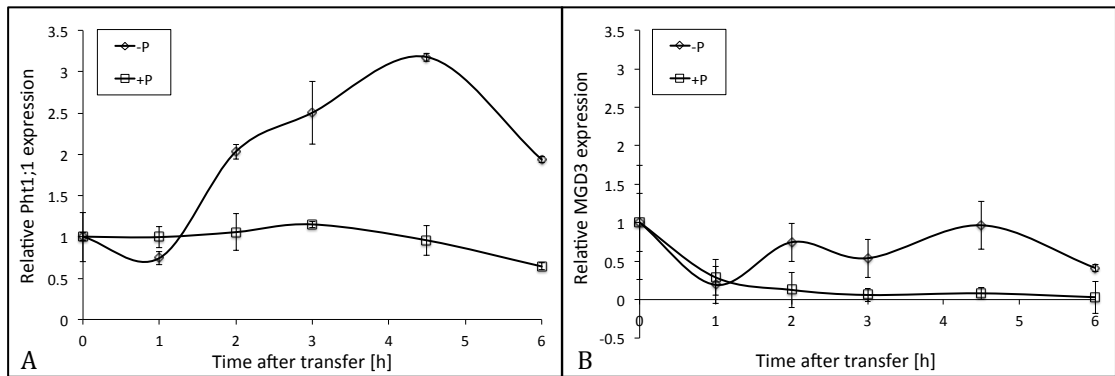


Fig. 4.4 Gene expression kinetics in 7-day old *Arabidopsis* suspension cell culture after transfer from +Pi media to -Pi media.

The suspension cells were grown in dark environment. Gene expression was monitored in a time course by qRT-PCR. Error bars indicate standard error of the mean (SEM) from 3 biological repeats, and are smaller than the symbol when not visible.

The transient peak in expression kinetics of *Pht1;1* during Pi deprivation was promising, however, the result was still different from previous data in two aspects. Firstly, the magnitude of induction was lower in my experiment. The reason could be due to the fact that the growth of suspension cells had already plateaued in the 7-day old cultures before treatment. In this stage, the growth rate of suspension cells was already very slow and some cells had begun to die, therefore, the demand for Pi was likely reduced significantly. Second, the peak of *Pht1;1* expression was delayed by ~2.5 hours, which could be related to the properties of this specific cell culture line.

To increase the magnitude of induction, we decided to use 5-day old culture in which the growth rate of suspension cells was still in exponential phase. The fast growth could increase the demand for phosphate, and thus increase the sensitivity towards the change in external Pi. To ensure the growth of suspension cells was not limited by any shortage of nutrients, the growth media for the cell cultures were refreshed with +Pi media (with 2.5 mM Pi) 16 hours before the starvation treatment. As shown in *Fig. 4.5A*, the expression of *Pht1;1* was induced and reached a transient peak in 3 hours after transfer of cells to Pi free media. The magnitude of induction was slightly higher than that in 7-day old culture (*Fig. 4.4A*). However, the induction continued after the peak, instead of being suppressed. The expression of *MGD3* showed a different pattern (*Fig. 4.5B*). The induction of *MGD3* only happened from 4.5 hours after media switch. Interestingly, the *MGD3* was still rapidly down regulated by addition of fresh +Pi media. Together with data from *Fig. 4.4B*, this reproducible result from *MGD3* expression in fresh +Pi media indicated that the suspension cells were possibly starved for Pi before subjected to Pi starvation treatment.

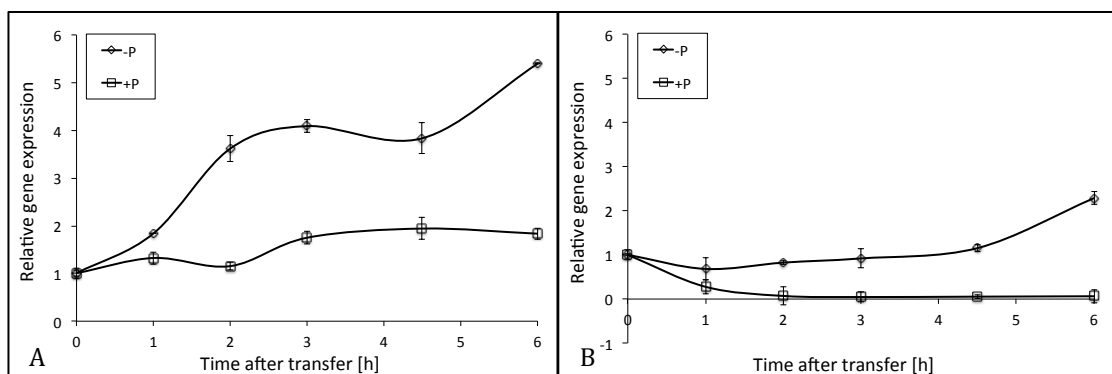


Fig. 4.5 Gene expression kinetics in 5-day old *Arabidopsis* suspension cell culture after transfer from +Pi media to -Pi media.

The suspension cells were grown in a dark environment. Gene expression was monitored in a time course by qRT-PCR. Error bars indicate standard error of the mean (SEM) from 3 biological repeats, and are smaller than the symbol when not visible.

To test the hypothesis, 5-day old suspension cell culture was prepared as usual. The growth media was refreshed by 16 hours before treatment. As shown in *Fig. 4.6*, instead of subjecting the cells to Pi starvation, phosphate, sucrose or both were added to the suspension cell culture. As negative control, samples were collected from culture without any addition. The expression of both *Pht1;1* and *MGD3* in the negative control steadily increased as time passed (*Fig. 4.6A&B*). Addition of Pi

rapidly suppressed the expression of both genes (*Fig. 4.6*). This result confirms that the suspension cells were already Pi starved before treatment. Moreover, the expression of *MGD3* began to slightly increase at 6 hour after addition of Pi compared to that at 3 hour (*Fig. 4.6B*). This result suggested that this suspension cell culture line could consume Pi in a very fast way. Addition of sucrose could force the cells to grow faster, and thus increase the demand for Pi. However, the addition of sucrose suppressed the expression of both marker genes in 3 hour. Although the expression was up regulated at 6 hour, the magnitude of induction was not as high as that of negative control (*Fig. 4.6A&B*). These results suggested that sucrose might not only affect the cell growth but also affect the Pi starvation-signalling pathway.

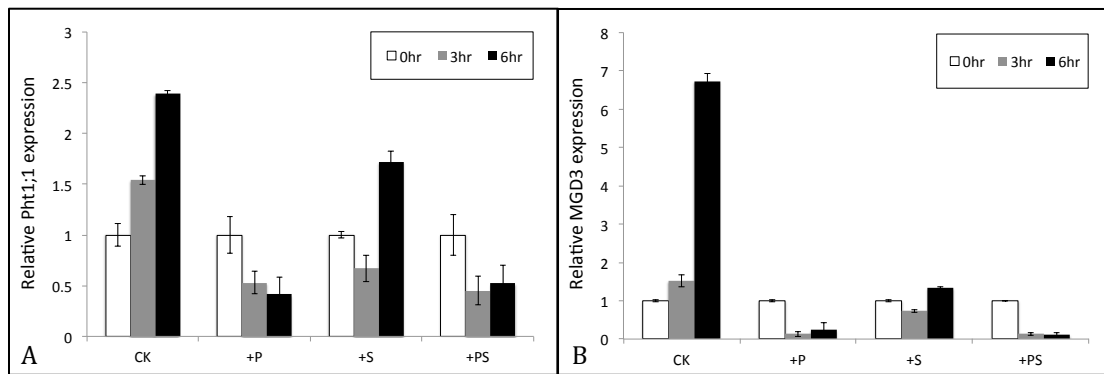


Fig. 4.6 Gene expression in 5-day old *Arabidopsis* suspension cell culture. For treatment, 1.5 mM phosphate (+P) or 3% sucrose (+S) or both (+PS) were added to suspension cell culture. Samples were collected at 0 hour, 3 hour or 6 hour after addition. Gene expression was monitored by qRT-PCR. Error bars indicate standard error of the mean (SEM) from 3 biological repeats.

To avoid any Pi starvation effects on behavior of suspension cells, 1.5 mM phosphate was always added to the 5 day old culture 3 hours before the cells were treated with Pi starvation in the following experiment. As shown in *Fig. 4.7B*, the down regulation of *MGD3* in fresh +Pi media was slower than that in previous experiment (*Fig. 4.5B*), and the expression slowly went up after 2 hours. This suggested that the addition of Pi was effective. Under current experiment condition, the expression of *Pht1;1* reached the peak in 4.5 hours after transfer of cells from +Pi media to -Pi media, and which was slightly suppressed subsequently (*Fig. 4.7A*). However, this experiment only included samples collected within 6 hours after transfer. It was hard to tell whether the expression of *Pht1;1* kept reducing or not. Therefore, a repeat experiment was performed with more samples. As shown in *Fig.*

4.8, two more samples were included in analysis. The expression of *MGD3* showed same pattern as that in Fig.4.7B. Apparently, the expression of *Pht1;1* gradually increased after transfer of suspension cells from +Pi to –Pi media (Fig. 4.7A).

Together, these data suggested that the current suspension cell culture line behaved differently compared to the previous culture line in our group during Pi deprivation (Lai, 2006). The expression of the *Pht1;1* gene did not exhibit a reproducible transient peak during early response to Pi deprivation, but was rather continuously induced by Pi starvation in current suspension cells (Fig.4.3, Fig. 4.5, Fig. 4.8).

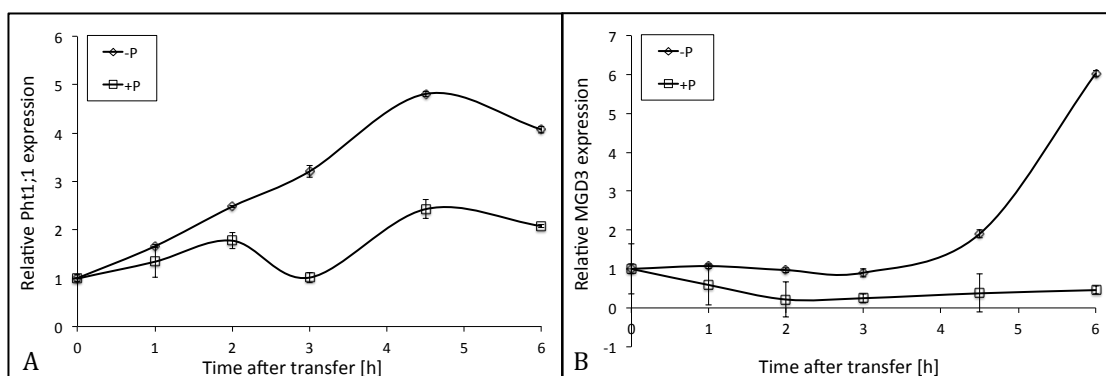


Fig. 4.7 Gene expression kinetics in 5-day old *Arabidopsis* suspension cell cultures after transfer from +Pi media to –Pi media.

The suspension cells were grown in dark environment. 1.5mM Pi was added to culture by 3 hours before Pi starvation treatment. Gene expression was monitored in a time course by qRT-PCR. Error bars indicate standard error of the mean (SEM) from 3 biological repeats, and are smaller than the symbol when not visible.

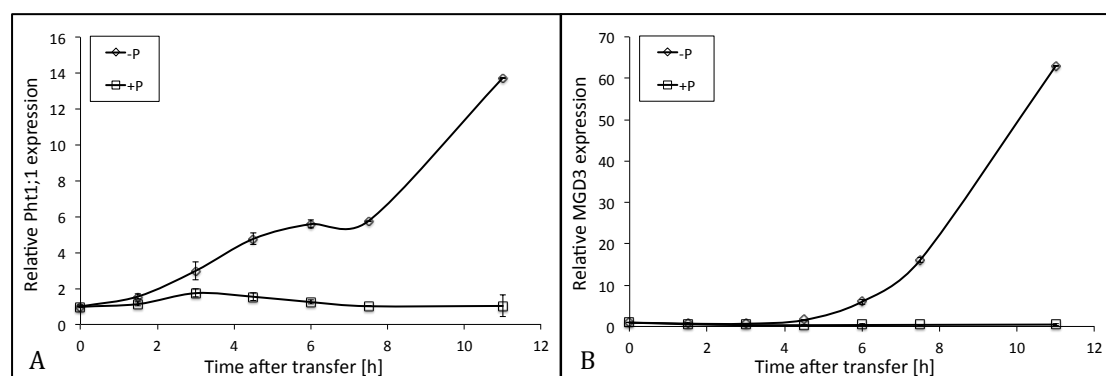


Fig. 4.8 Gene expression kinetics in 5-day old *Arabidopsis* suspension cell culture after transfer from +Pi media to –Pi media.

The suspension cells were grown in dark environment. 1.5mM Pi was added to culture by 3 hours before Pi starvation treatment. Gene expression was monitored in a time course by qRT-PCR. Error bars indicate standard error of the mean (SEM) from 3 biological repeats, and are smaller than the symbol when not visible.

4.2.1.2 *Pht1;1* & *MGD3* expression in response to inhibitor treatment

Cycloheximide (CHX) is an inhibitor of protein synthesis in eukaryotic organisms. It has been shown to bind the ribosome and inhibit eEF2-mediated translocation, and thus block the elongation phase of eukaryotic translation (Muchhal *et al.*, 1996; Schneider-Poetsch *et al.*, 2010; Bari *et al.*, 2006). Previous study in our group has shown that *Pht1;1* and *MGD3* responded to CHX differently (Lai, 2006). Here, I repeated the experiment.

The 5-day old suspension cell culture was prepared, and 1.5 mM phosphate was added to culture by 3 hours before addition of inhibitor. As shown in *Fig. 4.9*, the expression of *Pht1;1* started to increase from 1 hour after addition of 20 μ M CHX (*Fig. 4.9A*). In contrast, *MGD3* expression was first induced and then suppressed by CHX (*Fig. 4.9B*). The different expression profiles suggested that they might be regulated through different regulators. Compared to previous data, the pattern of marker gene expression kinetics was similar, but the magnitude of response was much lower in the current cell culture line.

In the next experiment, *Arabidopsis* suspension cells were treated with MG132, which is a reversible proteasome inhibitor. MG132 is usually used to inhibit the degradation of ubiquitin-conjugated proteins by the 26S complex. As shown in *Fig. 4.10*, the addition of MG132 could mimic the effect of Pi by suppressing the expression of *Pht1;1* expression (*Fig. 4.10A*). This was consistent with our previous data (Lai, 2006). Surprisingly, the expression of *MGD3* was also suppressed by addition of MG132 (*Fig. 4.10B*), which was opposite to previous data. Together, the results from CHX and MG132 treatments indicated that the current cell culture line might have different gene regulation, and thus behaved differently with the previous one in our group. Considering the big variation in different suspension cell culture lines, it was not easy to find a line that could behave exactly same as the one used previously to set up the gene regulation model in our group. Therefore, I decided to test the marker gene expression in *Arabidopsis* seedlings, which could be a more robust experimental system.

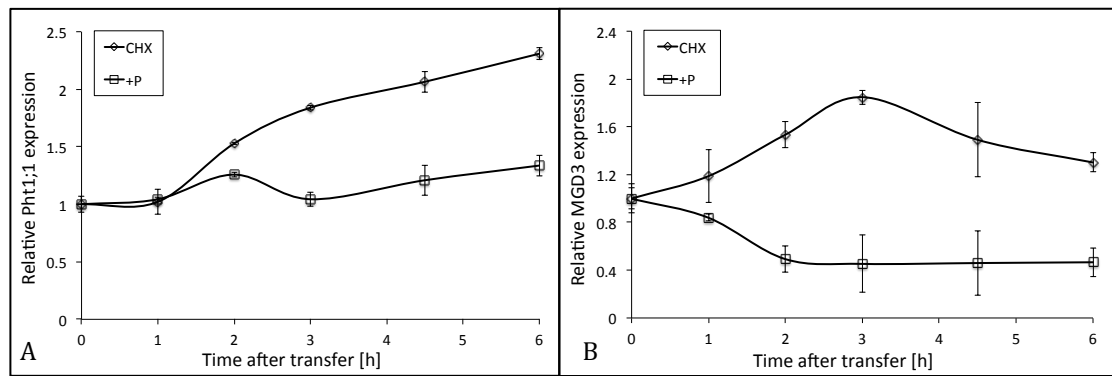


Fig. 4.9 Gene expression kinetics of phosphate starvation responsive genes in *Arabidopsis* suspension cell culture after exposure to 20 μ M CHX. The suspension cells were grown in dark environment. 1.5mM Pi was added to culture by 3 hours before treatment. Gene expression was monitored in a time course by qRT-PCR. Error bars indicate standard error of the mean (SEM) from 3 biological repeats.

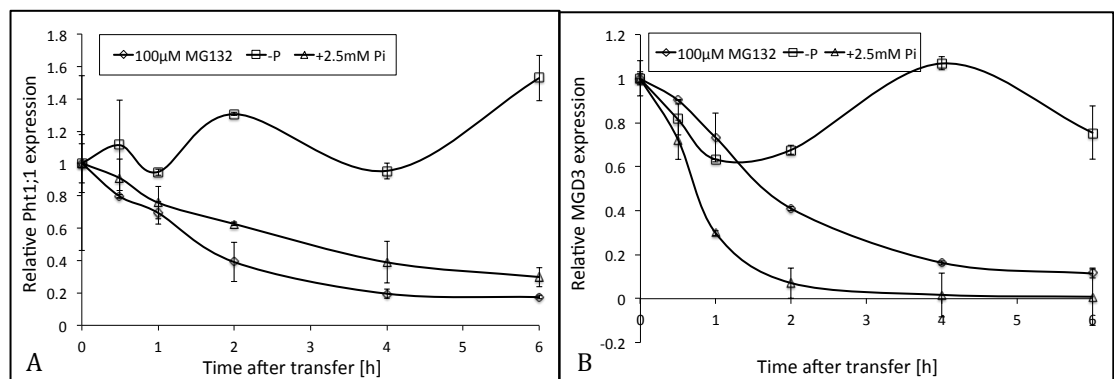


Fig. 4.10 Gene expression kinetics of phosphate starvation responsive genes in Pi-deplete *Arabidopsis* suspension cells after exposure to MG132. The suspension cells were grown in dark environment. 1.5mM Pi was added to culture by 3 hours before treatment. Gene expression was monitored in a time course by qRT-PCR. Error bars indicate standard error of the mean (SEM) from 3 biological repeats.

4.2.2 Expression kinetics of phosphate starvation responsive genes in *Arabidopsis* seedlings during Pi deprivation

To set up the experiment, the *Arabidopsis* seeds were germinated and grown in liquid half strength MS (0.5xMS) media with 1.5mM Pi and 1% sucrose. 18-DAG (days after germination) seedlings were used for Pi starvation treatment. To subject to Pi starvation, the seedlings were briefly rinsed with Pi free media, and then fresh Pi free media was added.

As shown in Fig. 4.11B, the expression of *MGD3* gently fluctuated after media switch. In contrast, the *Phl1;1* expression exhibited transient up regulation in both –Pi and +Pi media (Fig. 4.11A). The expression pattern of *Phl1;1* in response to Pi starvation was expected and similar to that in the cell culture in our previous data (Lai, 2006). However, the similar expression pattern also showed up in +Pi control samples. This result suggested that the response of *Phl1;1* in current experiment might not be only due to the Pi starvation. As high affinity phosphate transporter, *Phl1;1* has not been reported to respond to other treatments so far. Therefore, it seemed to be puzzling that *Phl1;1* showed the transient up regulation in +Pi media.

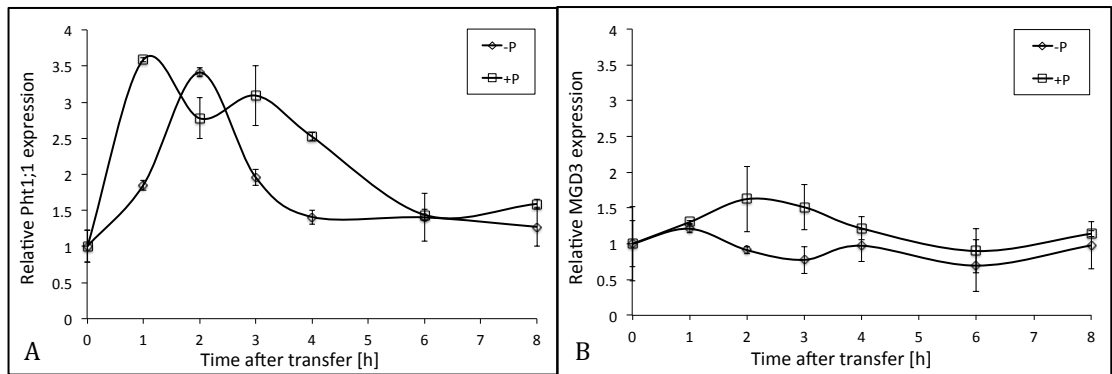


Fig. 4.11 Gene expression kinetics in 18-DAG *Arabidopsis* seedling roots after transfer from +Pi media to –Pi media.

Gene expression was monitored in a time course by qRT-PCR. Error bars indicate standard error of the mean (SEM) from 3 biological repeats.

Previous study in our group has shown that the growth history of *Arabidopsis* seedlings could affect the expression of Pi starvation responses. Particularly, a higher concentration of sugar in growth media could enhance the induction of phosphate starvation responsive genes during Pi deprivation (Lai *et al.*, 2007). Therefore, the amount of sucrose in media was modified and the growth history of *Arabidopsis* seedlings was slightly changed. To ensure the normal growth of young seedlings, the *Arabidopsis* seeds were still germinated and grew in 0.5xMS with 1% sucrose for 2 weeks. Afterwards, the media was replaced by 0.5xMS with 0.3% sucrose. Again, 18-DAG seedlings were subjected to Pi starvation. As shown in Fig.4.12A, *Phl1;1* exhibited strong transient up regulation when fresh media was added. Surprisingly, the induction still occurred irrespective of the presence of Pi. In this experiment,

another control (Fig.4.12, +P-2) was included in which the media was just removed and added back. Interestingly, even this manipulation could cause a weak transient up regulation of *Pht1;1*. The addition of fresh media, irrespective of Pi presence, seemed to only magnify the response. This result led to the suspicion that some other component(s) in the media were actually stimulating the *Pht1;1* expression.

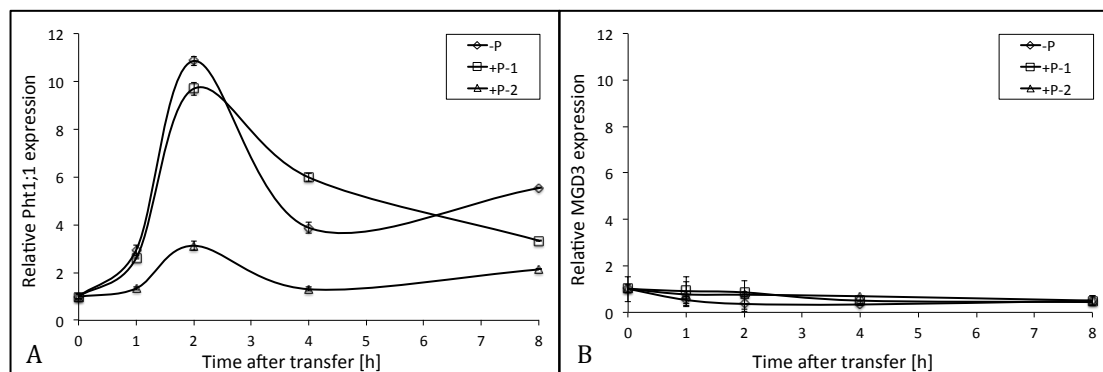


Fig. 4.12 Gene expression kinetics in 18-DAG *Arabidopsis* root after transfer from +Pi media to -Pi media. Gene expression was monitored in a time course qRT-PCR. Error bars indicate standard error of the mean (SEM) from 3 biological repeats. The seeds were germinated and grown in 0.5xMS media with 1% sucrose for 2 weeks. Afterwards, the media was replaced with 0.5xMS with 0.3% Sucrose. All media for treatment contained 0.3% sucrose. For treatment, the media was replaced with either fresh Pi free media (-P) or fresh +Pi media (+P-1). As 2nd control, the growth media was removed, and then added back (+P-2).

In the above experiments with *Arabidopsis* seedlings, a custom MS media from Duchefa Company was always used to ensure consistency between each experiment. The composition of the media was listed in Table 4.1., The commercial media supposedly strictly followed the recipe of classic MS media according to the description of the product, except that Pi was removed.

To confirm this, Inductively Coupled Plasma (ICP) analysis was performed to check the actual concentration of each element in the commercial media. As control, a user-made media was prepared strictly following the recipe of classic MS media in half strength. As shown in Table 4.2, there was still a trace of Pi in 0.5x Duchefa MS (-Pi) media, but the amount was ~70 fold lower than that in +Pi media. In Duchefa media, the concentrations of most other elements were similar to that in user-made media. However, the concentration of Sulphur (S) was ~7 fold lower in both +Pi and -Pi Duchefa media than that in user-made media. Compared to the classic 0.5xMS media,

the concentration of sulphur was the only component that significantly differed in the Duchefa media except Pi. This significant difference can be explained by the addition of 5mM MES buffer, which contains one, non bio-accessible sulphur atom to the self-made media, but not to the Duchefa custom media.

Although previous studies have indicated cross-talk between phosphate and sulfate starvation responses (Hsieh *et al.*, 2009; Gojon *et al.*, 2009; Rouached *et al.*, 2010; Rouached, 2011), it is not likely that this is the underlying cause for the observed results, because the additional sulphur (in the MES molecule) is not accessible. These results raise the possibility that shifts in external pH (which affect the efficiency of proton pumps, and hence the steady-state levels of ATP in the cytosol) affect the transcription of *Pht1;1*. To test this hypothesis, the expression of *Pht1;1* (and of other marker genes like MGD3) should be examined after changes to buffering capacity and pH of the media.

Table 4.1 Media composition of Duchefa media and classic MS media. For “0.5xDuchefa MS (+Pi)” media, the Pi was added separately.

Component	0.5xDuchefa MS (-Pi)	0.5xMS(+Pi)
<i>KNO₃</i>	9.39 mM	9.39 mM
<i>CaCl₂</i>	1.49 mM	1.49 mM
<i>NH₄NO₃</i>	10.30 mM	10.30 mM
<i>MgSO₄</i>	0.75 mM	0.75 mM
<i>KH₂PO₄</i>	0 mM	1.5mM
<i>H₃BO₃</i>	0.05 mM	0.05 mM
<i>MnSO₄·H₂O</i>	0.05 mM	0.05 mM
<i>CoCl₂·6H₂O</i>	0.055 µM	0.055 µM
<i>ZnSO₄·7H₂O</i>	14.95 µM	14.95 µM
<i>CuSO₄·5H₂O</i>	0.05 µM	0.05 µM
<i>KI</i>	2.50 µM	2.50 µM
<i>Na₂MoO₄·2H₂O</i>	0.52 µM	0.52 µM
<i>FeNaEDTA</i>	0.05 mM	0.05 mM

Table 4.2 ICP results of the commercial 0.5xMS media (Duchefa) and user-made 0.5xMS media. The concentration of each element was indicated as “mM”. STD means standard deviation.

Element	0.5xDuchefa MS (+Pi)		0.5xDuchefa MS (-Pi)		0.5xMS (+Pi)	
	Conc. (mM)	STD	Conc. (mM)	STD	Conc. (mM)	STD
Li 7	8.57E-05	0.0001	1.71E-04	0.0008	7.14E-05	0.0001
B 11	7.18E-02	0.03	9.27E-02	0.13	9.73E-02	0.24
Na 23	1.56E-01	0.06	1.78E-01	0.20	6.22E-02	0.03
Mg 25	4.46E-01	0.13	5.93E-01	0.42	6.59E-01	0.42
P 31	1.43	1.73	1.94E-02	0.51	1.64	3.27
S 34	0.605	1.54	0.772	3.99	5.41	7.73
K 39	12.2	6.41	10.2	14.51	12.5	16.90
Ca 43	1.26	2.08	1.55	2.02	1.25	2.39
Mn 55	4.65E-02	0.06	5.95E-02	0.12	5.47E-02	0.11
Fe 57	2.72E-02	0.01	4.26E-02	0.11	2.96E-02	0.10
Co 59	5.08E-05	0.000	5.08E-05	0.000	6.78E-05	0.000
Ni 60	1.67E-05	0.000	1.67E-05	0.000	3.33E-05	0.000
Cu 65	4.62E-05	0.000	7.69E-05	0.001	6.15E-05	0.000
Zn 66	1.37E-02	0.035	1.81E-02	0.043	1.64E-02	0.028
As 75	2.67E-06	0.0001	1.33E-06	0.0000	4.00E-06	0.0000
Se 82	1.01E-03	0.008	8.17E-04	0.004	6.83E-04	0.001
Rb 85	2.12E-04	0.000	1.76E-04	0.001	8.24E-05	0.000
Sr 88	2.95E-04	0.000	3.64E-04	0.002	3.98E-04	0.001
Mo 98	4.49E-04	0.000	3.88E-04	0.001	4.69E-04	0.001
Cd 114	1.75E-06	0.0000	1.75E-06	0.0001	3.51E-06	0.0000

4.3 Discussion

Transcriptional responses during Pi starvation have been studied for many years. A few classic Pi starvation responsive (PSR) genes have been identified, and have been widely used as marker genes to demonstrate the Pi starvation status in plants. In *Arabidopsis*, the most common marker genes include *Pht1;1*, *Pht1;4*, *ACP5*, *IPSI*, *At4*, *RNS1*, *MGD3* etc. These genes function in different aspects of plant responses during Pi starvation. Their expression is usually identified to be highly induced in later stage of Pi starvation. Until now, there have not been any reports about the response of these PSR genes during very early stage of Pi starvation responses.

In our group, we focus on the dissection of immediately early events in Pi starvation signalling pathways. Previous studies in our group already showed that *Pht1;1* and *MGD3* could rapidly respond to Pi availability (Lai, 2006). The study of marker gene expression kinetics under different conditions allowed us to propose a model for the regulation of *Pht1;1* gene expression in early responses to Pi starvation (see Chapter 1, section 1.6). This model was based on the results from several key experiments. Firstly, by providing Pi to Pi depleted *Arabidopsis* suspension cells, the expression of both marker genes was rapidly suppressed, which suggested that the early responses to Pi starvation were under negative control. Secondly, by subjecting *Arabidopsis* suspension cells to Pi starvation, the expression of *Pht1;1* was transiently induced followed by down regulation within 4 hours after transfer of suspension cells from +Pi to -Pi media. Meanwhile, the expression of *MGD3* did not exhibit any change. In the presence of both Pi and cycloheximide (CHX), *Pht1;1* expression was still highly induced, which supported the view that *Pht1;1* was under negative control, and possibly by a labile repressor. The result from the MG132 treatment showed that MG132 could mimic the effect of Pi in terms of suppressing *Pht1;1* expression, which suggested that the postulated labile repressor could be degraded through the proteolysis pathway.

To prove the regulatory model, EMSA was performed aiming to demonstrate the existence of a protein that could bind to the promoter of *Pht1;1* (Chapter 3). However, the result was not satisfactory. The protein-DNA complexes detected in my experiments were not what we expected, nor were they reproducible. Therefore,

the above key experiments were repeated aiming to recapitulate the data obtained previously in the lab, using the current plant materials. As previous data were mainly obtained using *Arabidopsis* suspension cell cultures, I started my experiments with cell culture systems as well.

In the first experiments, the suspension cells used in EMSA experiments were subjected to Pi starvation. However, the quantitative RT-PCR (qRT-PCR) did not manage to amplify the *Pht1;1* fragment from cDNA prepared from RNA isolated from suspension cells with a primer pair designed based on the Col-0 genome sequence. It is worthwhile to point out that this primer pair was used in previous studies in our group. This may suggest that the suspension cell culture used by former lab members was Col-0 ecotype. As mentioned earlier in Chapter 3, the suspension cells used for EMSA were genotyped to be of the Ler ecotype. The difference in genome sequence between two ecotypes could result in the poor efficiency in qRT-PCR. To optimize the qRT-PCR, the coding region of *Pht1;1* in current cell culture line was sequenced. It turned out that the forward primer had one nucleotide mismatch. However, the correction of this mismatch did not improve the efficiency of qRT-PCR amplification. We also designed two more pairs of primer in different region of *Pht1;1* with perfect match. Surprisingly, none of them managed to efficiently amplify the DNA fragment from cDNA of suspension cells. This suggested that the poor amplification might not be due to the quality of qRT-PCR primers, but due to the low expression level of *Pht1;1* in this specific cell culture line.

Fortunately, we obtained a Col-0 cell culture line with a rapid growth rate. The cell culture line was kept under both light and dark conditions. Interestingly, the response to Pi starvation was quite different in these conditions. Under constant light conditions, the expression of *Pht1;1* was strongly and constantly induced by Pi starvation (Fig. 4.3). In contrast, its expression was gradually induced, and the magnitude of induction was ~3 fold lower in dark condition than that in light condition (Fig. 4.4, Fig.4.7). This suggested that light perception might affect the response to Pi starvation at the transcriptional level in this cell culture line. A recent study has linked light responses and Pi starvation responses by function of PHR1 transcription factor (Nilsson *et al.*, 2012). The *Arabidopsis* plants lacking PHR1 were reported to be more sensitive to photochemical stress. Therefore, the *phr1* mutant

suffers severely from permanent photoinhibition compared to wild type plants, when exposed to high light during P-starvation conditions. However, the link between light signals and the Pi starvation response needs further study.

Considering that a faster growth rate might increase the sensitivity to Pi starvation (Lai *et al.*, 2007), we tried to use 5-day old cells for starvation treatment. But that did not change the expression profile of *Pht1;1* in response to Pi starvation (Fig. 4.5, Fig. 4.7 and Fig. 4.8). Besides, the expression of *Pht1;1* exhibited different responses to treatment of CHX and MG132 compared to previous data obtained in our group (Fig. 4.9 and Fig. 4.10). Together, these results indicated that the current Col-0 cell culture line behaved differently from previous cell culture line used by former lab members. As the suspension cell culture derived from specific plant tissues, it is possible that different lines behave differently and have different gene regulation. Therefore, the marker gene expression was tested in *Arabidopsis* seedlings during early Pi starvation.

In the experiments with *Arabidopsis* seedlings, the expression of *Pht1;1* exhibited a transient up regulation, but this response was observed irrespective of Pi presence (Fig. 4.11 and Fig. 4.12). The result from one experiment (Fig. 4.12), showed that the *Pht1;1* expression could even respond to the manipulation, and the fresh media seemed to only magnify the response. Therefore, we analyzed the composition of the media used in the experiment with the ICP technique. Surprisingly, the media used in these experiments had ~7 fold less sulfur than expected and found in the 'classic' MS media. It is likely that this difference is due to the buffering of all media, except for the Duchefa custom media, with MES, which contains 1 M of S per M of MES.

Furthermore, cross-talk between Pi and SO₄ starvation responses have become clear recently. The homeostasis of Pi and SO₄ in *Arabidopsis* was regulated by miR399 and miR395, respectively. Interestingly, the expression of miR395, which was known to be up regulated by SO₄ starvation, was identified to be suppressed in Pi deficient plants (Hsieh *et al.*, 2009). The suppression of miR395 could trigger the up regulation of SULTR2;1, which served to increase the translocation of SO₄ and increase the biosynthesis of sulfolipid to compensate for reduced phospholipids during Pi deprivation (Rouached, 2011).

In *Arabidopsis*, PHR1 has been proved to play an important role in regulation of Pi homeostasis. It functions through binding to the PHR1-binding sequence (P1BS) in the promoter of downstream genes. Bioinformatics analysis showed that the P1BS cis-element existed in the promoter of SULTR1;3, which encodes a transporter involved in SO₄ translocation (Rouached *et al.*, 2011). Experimental data indicated that PHR1 could positively regulate the expression of SULTR1;3, while negatively regulate the expression of SULTR2;1. Interestingly, a similar regulatory mechanism was also found in *Chlamydomonas reinhardtii* by the study of PSR1, a PHR1 orthologue. These results indicated a complex interaction in regulation of Pi and SO₄ homeostasis in plants. Further study is needed to identify the signalling networks that coordinate the response to these two elements.

In my experiments, the growth media for *Arabidopsis* seedlings used in the short-term phosphate shift experiments was unbuffered. Thus, it is likely that fresh media had a different pH than the media in which the plants had grown. Proton ATPase activity is very sensitive to external pH, and thus changes in external pH are expected to rapidly affect cytosolic steady-state ATP concentrations, because Proton ATPase are major consumers of ATP in the cytosol. It will be worthwhile to perform short-term media shift experiments to evaluate *Phl1;1* expression responses comparing buffered and non-buffered media at different pH.

5. *AtPht1;1* promoter deletion

5.1 Introduction

The regulation of gene expression at the transcriptional level is mainly controlled by the activity of its promoter, specifically by different transcription factors (TFs). TFs perform regulatory functions through binding to specific promoter sequences, which are known as *cis*-elements. Binding of TFs to *cis*-elements can result in transcription activation or suppression, depending on the property of the specific TF. Therefore, analysis of promoter sequences and identification of *cis*-elements (TF binding sites) can provide important information on understanding the regulation of gene.

In *Arabidopsis*, over 2000 TF genes have been identified in the genome. A few of them have been reported to be involved in the regulation of Pi starvation responses, including PHR1, ZAT6, WRKY6, WRKY75, bHLH32. In contrast, the only elucidated *cis*-element involved in Pi starvation responses is the P1BS motif (GnATATnC), which is bound by PHR1 (Rubio, 2001). BLAST searches showed that the P1BS motif is widely present in the promoter of many Pi starvation responsive genes, including Pht1 family genes, *IPS1/At4*, *RNS1*, *ACP5* etc. In 2001, Mukatira *et al.* reported two regions of *Pht1;4* and *TPSII* promoters that specifically bound nuclear protein factors from Pi-sufficient plants (Mukatira *et al.*, 2001), which suggested the existence of novel *cis*-element(s) involved in Pi starvation response. However, promoter deletion analysis carried out by Karthikayan *et al.* showed that deletion of the two regions responsible for binding protein factors from promoter of *Pht1;4* did not affect reporter gene expression (Karthikeyan *et al.*, 2009). Further studies are still needed to evaluate these regions.

To study a promoter, a reporter gene is often used to examine the activity and spatio-temporal regulation of a specific promoter. The common reporter genes include firefly luciferase (LUC) and *Escherichia coli* β -glucuronidase (GUS) gene. To gain further insight into the regulation of the promoter, progressive deletion analysis is a helpful approach to delineate the regulatory regions in the promoter sequence. In 2004, Schunmann *et al.* reported data from deletion analysis of the *HvPht1;1* promoter in Rice, which indicated that the promoter element responsible for trichoblast-specific expression was located between -574bp to -856bp upstream of

the translation start site (Schunmann, 2004). Their data also confirmed the function of P1BS-like motifs in regulating the inducibility of *HvPht1;1* expression under Pi starvation (Schunmann, 2004). Deletion analysis of the *MtPT1* promoter indicated that the sequence between -551bp to -975bp upstream of the translation start site could determine root specificity of gene expression, while the sequence between -342bp and -551bp was possibly required for induction by Pi (Xiao *et al.*, 2006). In *Arabidopsis*, deletion analysis was performed with *Pht1;4* promoter by Karthikeyan *et al.* They showed that a 164bp fragment upstream of the translational start site appeared to be sufficient for the basal expression of *Pht1;4* in roots and leaves. Their data also indicated the importance of 5'UTR intron in enhancement of *Pht1;4* expression (Karthikeyan *et al.*, 2009).

In my experiment, a labile repressor was proposed to bind to the promoter of *AtPht1;1* and suppress its expression under Pi sufficient conditions. To facilitate the study of such a proposed repressor, it became important to locate the position of the repressor-binding region. Therefore, promoter deletion analysis was designed in parallel with the EMSA experiment. In parallel, the deletion analysis could also dissect the role of different regions on the promoter in controlling *Pht1;1* expression during Pi deprivation. The data from analysis are described and discussed in this chapter.

5.2 Results

5.2.1 Construction of a promoter deletion series for *AtPht1;1*

In order to determine regulatory regions in the promoter sequence, a promoter deletion series for *AtPht1;1* was designed (Fig. 5.1A). The DNA sequence of each truncated promoter was placed upstream of the *uidA* reporter gene to generate the expression cassette (Fig. 5.1B). In my experiment, the full-length promoter covered the DNA sequence from 1898 nucleotides immediately upstream of the translational start site of the *AtPht1;1* gene and 18 nucleotides downstream. This full-length promoter contained an intron of 227 bp. Several reports have shown that introns played important roles in regulating gene expression (Karthikeyan *et al.*, 2009; Curie *et al.*, 1992; Rose and Beliakoff, 2000; Rose, 2004). To test the effect of intron on *AtPht1;1* expression pattern, two additional constructs (*Pht1;1-FLΔI* and *Pht1;1-*

Δ1ΔI) were designed without intron (Fig. 5.1A). The promoter-reporter constructs were transformed into *Arabidopsis* through Agrobacterium-mediated transformation. For each construct, ~12 individual lines were obtained, and 2 of them with strongest GUS expression were chosen for analysis. The homozygotes were selected and used for further experiments.

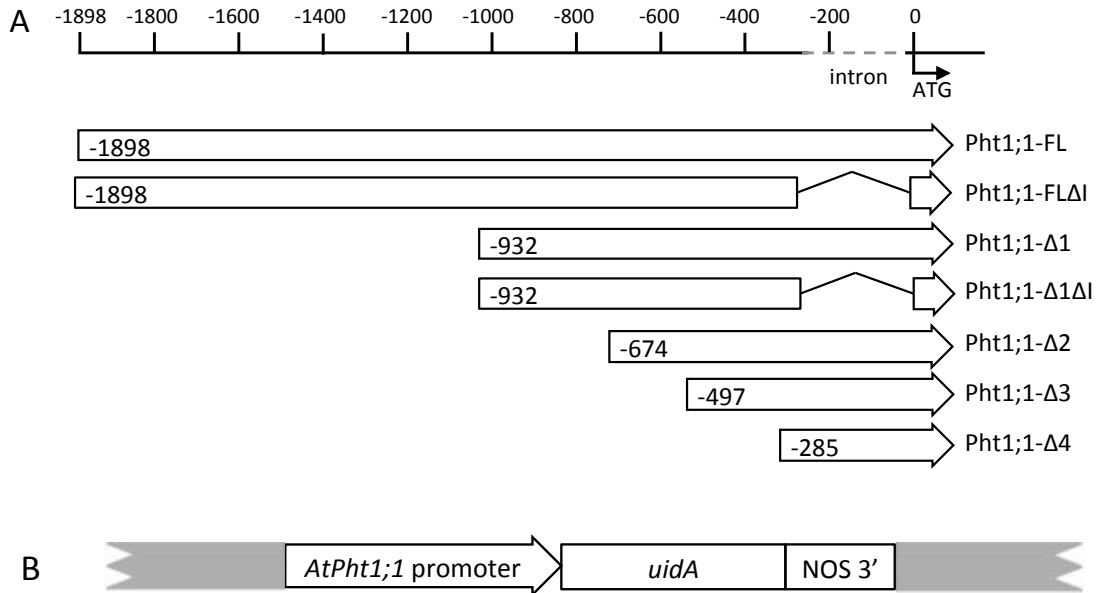


Fig. 5.1 Schematic structure of the *AtPht1;1* promoter deletion constructs
A, The *AtPht1;1* full-length promoter and truncated derivatives. The positions and approximate lengths (in nucleotides) of each derivative are indicated by the scale bar. The translation start site was indicated as 0. The negative number in the box indicated the length of the promoter.
B, Structure of the *AtPht1;1* promoter::*uidA* gene expression cassette.

5.2.2 Histochemical staining analysis of *uidA* expression driven by full-length *Pht1;1* promoter in *Arabidopsis* roots

The seedlings carrying full-length promoter construct were firstly used for histochemical staining analysis. Surface sterilized seeds were germinated in half-strength MS (0.5xMS) medium (Murashige and Skoog, 1962). 5-day old seedlings were transferred to liquid 0.5xMS media with Pi (1.5 mM) or without Pi for another 6 days before histochemical analysis. The media was refreshed every 2 days to ensure the seedlings were not starved by shortage of essential nutrients. Following the GUS staining, the seedling root was immersed in Ponceau red for 3 min before

photography, which stained the tissue without *uidA* expression pink. In my experiment, I only analyzed the *uidA* expression in seedling roots.

The full-length promoter exhibited very strong activity. The seedling root started to show weak blue staining in 10 min after being immersed in staining solution. For detailed *uidA* expression analysis, the seedlings stained for 1 hour was used. As shown in Fig.5.2A, strong *uidA* expression was observed in seedling roots. Close-up views showed that *uidA* expression was weak in the root tip area of both primary root and lateral root, and no expression was observed in the root meristem zone (Fig. 5.2A, b&c). Under Pi starvation, the *uidA* expression was induced, judging by the dark blue color after staining (Fig. 5.2B), which suggested the full-length promoter (*Pht1;1-FL*) contained *cis*-elements responsible for inducibility of *Pht1;1* expression. Interestingly, under Pi starvation the GUS activity expanded towards the root tip of both primary and lateral roots compared to the roots grown in Pi sufficient conditions (Fig.5.2B, b&c). Moreover, the blue staining appeared at the tip of the lateral root tip (Fig.5.2Bb, indicated by arrowhead). To confirm the expression pattern in the lateral root tip, seedlings carrying a *Pht1;1::GFP* fusion protein driven by *Pht1;1* native promoter was analyzed. Consistent with GUS activity, the GFP signal was also detected in the tip of the lateral root under Pi starvation (Fig. 5.3, indicated by arrowhead). Together, these data suggested that the GUS activity pattern driven by full-length promoter could reflect the *Pht1;1* expression pattern in seedling root.

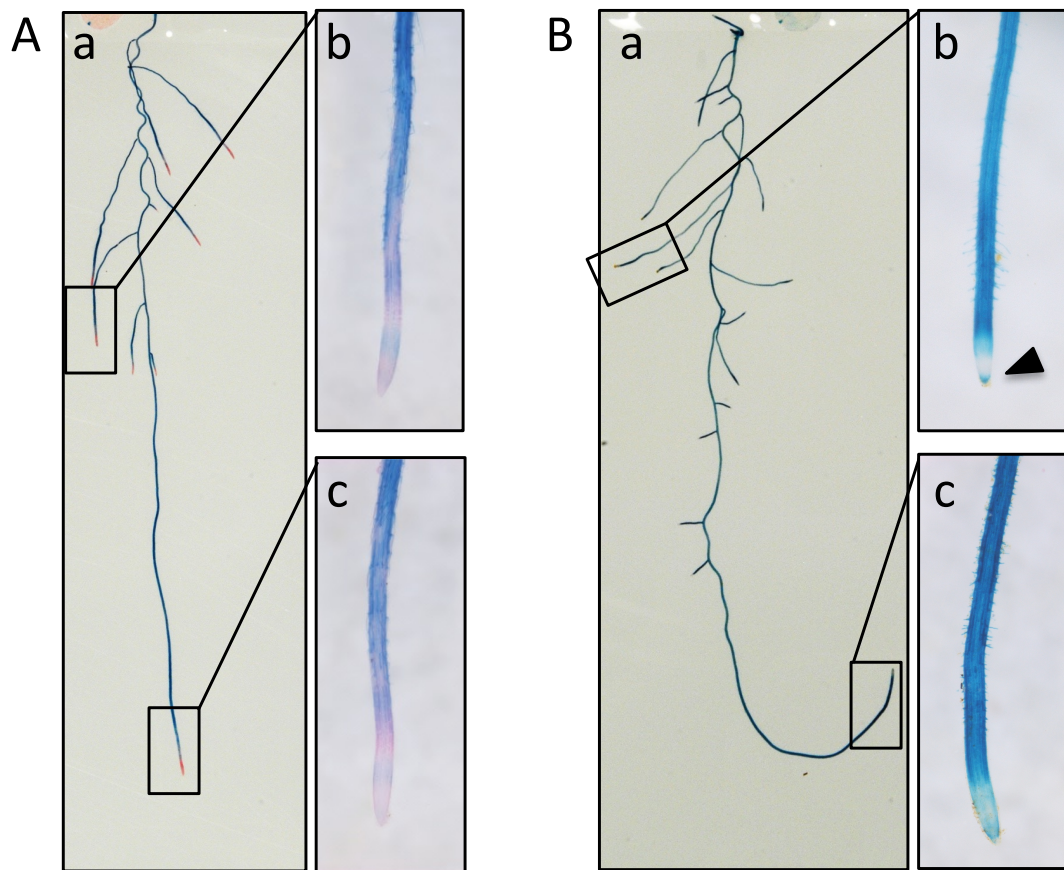


Fig. 5.2 Histochemical localization of GUS activity driven by full-length *Pht1;1* promoter in *Arabidopsis* root.

5-day old seedlings of transgenic lines carrying *Pht1;1-FL::uidA* expression cassette were treated for 6 more days in Pi sufficient (A) or deficient (B) media and used for histochemical analysis of GUS expression. The seedlings were processed simultaneously following histochemical staining protocol. The seedlings were kept in X-gluc solution for 1 hour.

a: overview of whole root; b: close-up view of frontier of lateral root; c: close-up view of frontier of primary root.

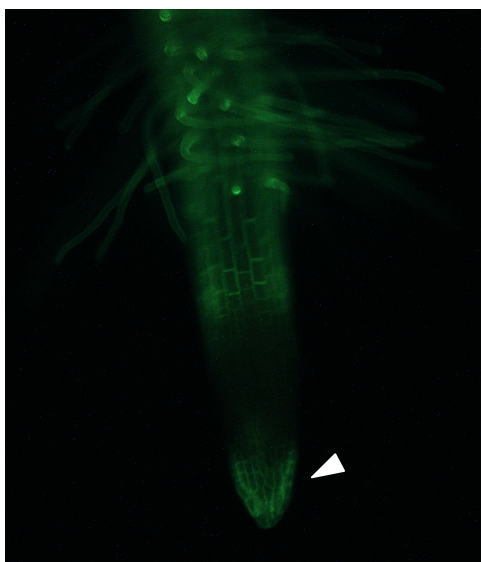


Fig. 5.3 Pht1;1::GFP fusion protein localization driven by Pht1;1 native promoter in *Arabidopsis* lateral root tip under Pi starvation.

5.2.3 Deletion of fragments affected expression of reporter gene in *Arabidopsis* roots under both Pi sufficient and Pi deficient condition.

The seedlings carrying different truncated promoter-reporter constructs were used to examine the effect of deletion on the expression pattern of the reporter gene. 5-day old seedlings were prepared and treated as described above. The seedlings after Pi starvation treatment were used for histochemical staining. During staining, the truncated promoters showed much weaker activity than that of the full-length promoter. It took over 2 hours before the blue color started to appear for all truncated promoter constructs. Preliminary experiment showed that overnight staining was necessary for seedlings carrying truncated promoter constructs (data not shown). Therefore, the overnight stained seedlings were used for analysis.

As shown in *Fig. 5.4A*, the pattern of GUS activity was significantly altered by deletion of the first fragment (from -1898 to -932). In Pi sufficient conditions, the GUS activity was mainly confined to the region close to the root tip in both primary and lateral roots (*Fig. 5.4A, f~j*). In the mature zone next to the primary root tip, weak blue staining was observed, but the staining was not uniform (*Fig. 5.4A, f & h*). In the mature primary root (where lateral roots were forming), there was no GUS activity detectable (*Fig. 5.4A, f & g*). This suggested that important *cis*-element(s)

existed in the sequence from -1898 to -932 that control the *Pht1;1* expression pattern in roots. Deletion of a second fragment (from -932 to -674) did not further change GUS activity (*Fig.5.4A, k~o*). Interestingly, deletion of a third fragment (from -674 to -497) slightly expanded GUS activity (*Fig. 5.4A, d,k&i*), which suggested that the fragment might contain *cis*-element(s) with minor roles in controlling the *Pht1;1* expression pattern. Further deletion to position -285 completely abolished GUS activity in both root and shoot (data not shown).

In response to Pi starvation, GUS activity was increased when driven by the full-length promoter (*Fig.5.2, Fig.5.4B, a~e*). For truncated promoter constructs, the GUS staining was confined to the newly generated root hair zone in both primary and lateral roots under Pi starvation (*Fig.5.4B, f~t*). Pi starvation did not increase the level of GUS activity for any of the truncated promoter constructs (*Fig.5.4B, f~t*). These data suggested that the *cis*-element(s) responsible for Pi starvation responses might be located mainly in the sequences from -1898 to -932.

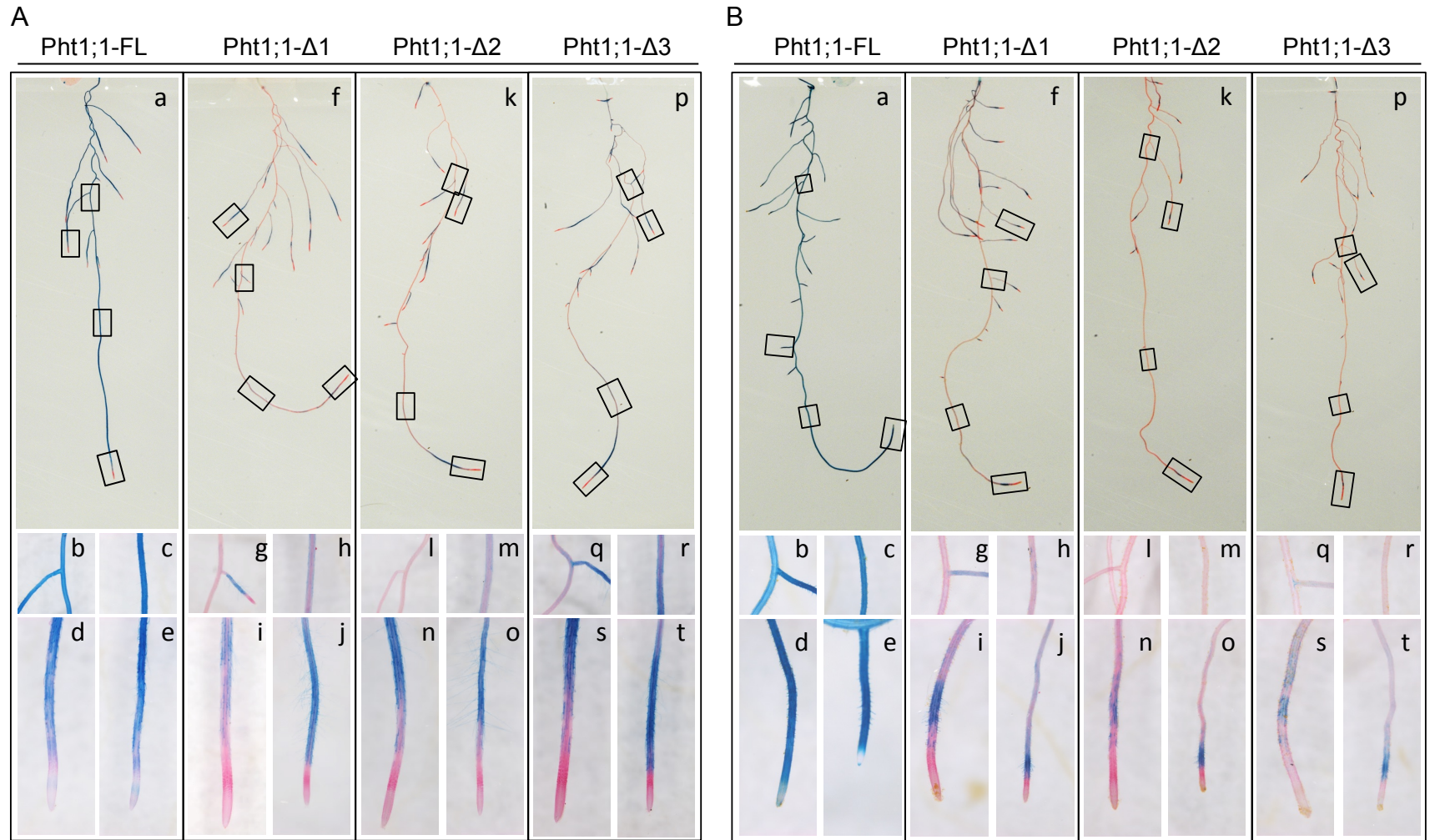


Fig. 5.4 Histochemical localization of GUS activity driven by full-length and truncated *Pht1;1* promoter in *Arabidopsis* root. 5-day old seedlings of transgenic lines carrying various expression cassettes were treated for 6 more days in Pi sufficient (A) or deficient (B) media and used for histochemical analysis of GUS expression. b,g,l,q: junction between primary and lateral root; c,h,m,r: mature zone of primary root; d,i,n,s: primary root tip; e,j,o,t: lateral root tip.

5.2.4 The intron in the 5'UTR regulates the spatio-temporal expression of *Pht1;1* gene expression

To test the effect of intron on the expression of *Pht1;1*, the 227bp intron was removed from *Pht1;1-FL* and *Pht1;1-ΔI* to generate two more constructs, namely *Pht1;1-FLΔI* and *Pht1;1-ΔIΔI*. 5-day seedlings carrying these constructs were prepared and treated as described above. The seedlings were used for histochemical staining after Pi starvation treatment.

As shown in *Fig. 5.5A*, removal of intron resulted in reduced GUS staining in the young part of both primary and lateral roots in seedlings carrying the *Pht1;1-FLΔI* construct (*Fig.5.5A, a,c&e*). As the root grew older, GUS staining became stronger. Interestingly, deletion of intron did not affect the increase of GUS activity under Pi starvation. As shown in *Fig. 5.5B*, Pi starvation not only expanded the GUS activity, but also increased the intensity of GUS staining (*Fig.5.5B*). These data suggested that the intron might participate in regulation of spatio-temporal expression of *Pht1;1* gene. Furthermore, this regulation needed the existence of sequence from -1898 to -932, as deletion of both intron and this sequence abolished the expression of *uidA* expression in both and shoot (data not shown).

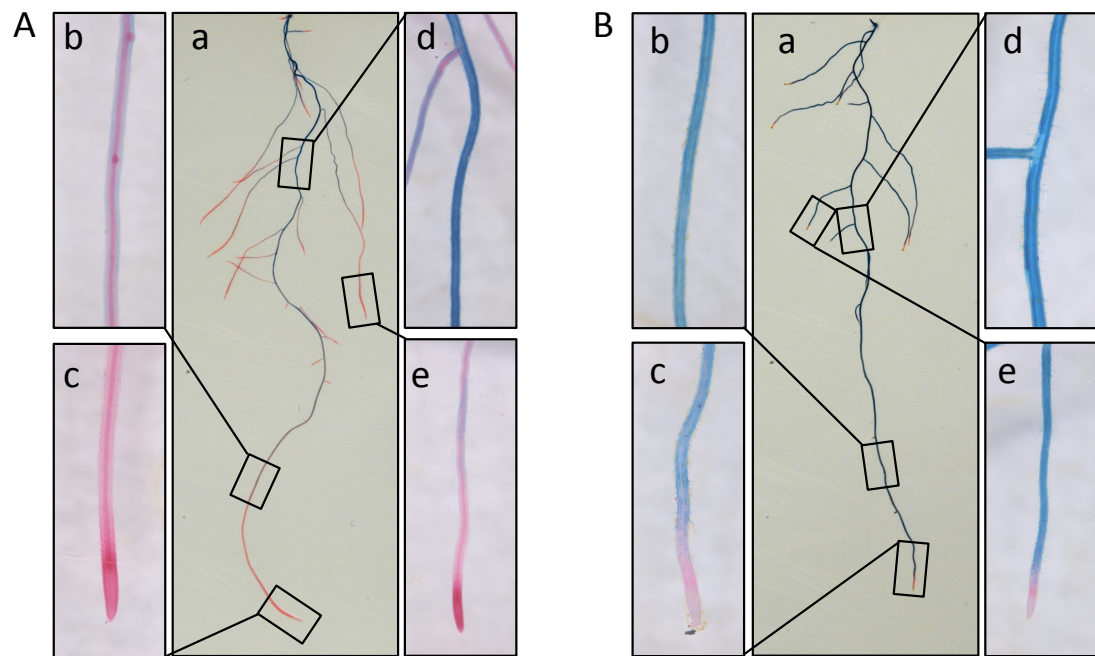


Fig. 5.5 Histochemical localization of GUS activity driven by full-length *Pht1;1* promoter without intron (*Pht1;1-FLΔI*) in *Arabidopsis* roots.

5-day old seedlings of transgenic lines carrying *Pht1;1-FLΔI::uidA* expression cassette were treated for 6 more days in Pi sufficient (A) or deficient (B) media and used for histochemical analysis of GUS expression.

a: overview of whole root; b: close-up view of older mature zone of primary root; c: close-up view of primary root; d: close-up view of junction of primary and lateral root area; e: close-up view of lateral root.

5.3 Discussion

Previous studies have proved the function of *Pht1;1* as a high affinity Pi transporter (Muchhal *et al.*, 1996), and examined its inducibility following the removal of Pi (Muchhal *et al.*, 1996; Bari *et al.*, 2006). The spatio-temporal expression has also been examined by fusing the long promoter of *Pht1;1* to the *uidA* reporter gene (Mudge *et al.*, 2003; Koyama *et al.*, 2005). However, detailed analysis is still missing on the regulatory role of different regions in the promoter. Furthermore, the data from our group allowed us to propose that a labile repressor protein might exist to regulate the expression of *Pht1;1* in early responses to Pi starvation. Identification of the repressor-binding region could help to isolate the repressor protein. Therefore, we designed the promoter deletion

analysis to dissect the possible role of specific regions of the promoter in controlling the expression of *Pht1;1* during Pi deprivation. In this study, we generated the transgenic *Arabidopsis* plants expressing *uidA* reporter gene driven by progressively deleted *Pht1;1* promoter. Histochemical staining analysis of GUS activity was carried out to analyze the *uidA* expression.

In the design of the deletion series, the full-length promoter was designated as 1898 bp sequence upstream of the translational start site of *Pht1;1*. The strong GUS activity driven by this promoter was localized in both primary and lateral roots. Interestingly, no expression was detected in the meristem zone under Pi sufficient condition. This is in agreement with an earlier report published by Koyama et al (Koyama *et al.*, 2005). In their study, a 3891 bp DNA sequence upstream of translational start site was used as the full promoter of *Pht1;1* to drive *uidA* reporter gene. Their histochemical analysis showed same result as in my study. Together, these data suggested that 1898 bp promoter sequence is sufficient to reflect the *Pht1;1* expression pattern in roots.

In response to Pi starvation, GUS activity was induced when driven by the full-length promoter. However, deletion of the fragment from -1898 to -932 abolished induction, which indicates that cis-element(s) responsible for the inducibility of *Pht1;1* in low Pi are located in this region. This result provided a possible explanation for the failure of the EMSA assays aimed to isolate the labile repressor-binding region (see details in Chapter 3). In the EMSA experiment, the probes were designed from promoter sequence up to -1056 bp from transcription start site, which is based on the information from similar analysis of *Pht1;4* regulation (Mukatira *et al.*, 2001). However, the promoter deletion analysis indicates that the key region for the regulation of *Pht1;1* inducibility locates between -1898 to -932 bp. It is possible that the probes in EMSA did not cover the major binding regions for *cis*-elements. To evaluate the role of this region (from -1898 to -932 bp), detailed deletion analysis is still needed. The EMSA experiment could be repeated based on the results of the promoter deletion analysis.

Interestingly, when driven by the full promoter, the GUS staining appeared in the frontier of lateral root tip under Pi starvation. This expression pattern was confirmed by

the Pi starved seedlings carrying a *Pht1;1::GFP* fusion protein driven by native *Pht1;1* promoter. A few studies have suggested that the root tip area could serve as the local sensing site for Pi availability (Linkohr *et al.*, 2002; Svistoonoff *et al.*, 2007; Chiou and Lin, 2011). As a high affinity Pi transporter, the expression of *Pht1;1* in the lateral root apex may suggest its involvement in the Pi sensing.

Earlier studies have demonstrated the role of introns in regulating gene expression (Curie *et al.*, 1992; Rose and Beliakoff, 2000; Rose, 2004; Karthikeyan *et al.*, 2009). Particularly, the 5'UTR intron could enhance the expression of *Pht1;4* in *Arabidopsis* root. The expression of *Pht1;4* in root apex also requires the existence of intron in the promoter (Karthikeyan *et al.*, 2009). Likewise, our study showed that the intron also played a regulatory role in controlling the expression pattern of *Pht1;1* in *Arabidopsis* root. Under Pi sufficient condition, removal of intron from full-length promoter caused loss of GUS activity in young part of both primary and lateral roots. In contrast, the induction of GUS activity was not affected for the full-length promoter without intron. This indicates the intron plays a role in controlling spatio-temporal expression of *Pht1;1* in roots. Interestingly, removal of intron from *Pht1;1-ΔI* construct completely abolished the *uidA* expression, suggesting the intron and the sequence from -1898 to -932 are both required to ensure the *Pht1;1* expression in root.

In my project, a labile repressor was proposed to control the *Pht1;1* expression. One aim of promoter deletion analysis is to locate the repressor-binding region. Ideally, deletion of repressor binding region would change the expression kinetic of *uidA* in early response to Pi starvation. However, as discussed in Chapter 4, the results from experiments with *Arabidopsis* plants were not ideal due to problems with the media, which means that the identification of the best conditions for experiments with *uidA* reporter lines still needs more work. Therefore, I paused further experiments with the reporter lines and dedicated more time to improve the experimental condition. New expression kinetic studies of GUS activity in early response to Pi starvation will be performed once the experimental conditions are optimized.

6 Zat18 is a new regulator in phosphate starvation response

6.1 Introduction

Transcription factors are generally divided into two categories: transcription activators and transcription repressors. In plants, transcription activators usually contain domains rich in the acidic amino acids glutamine or proline, such as DREBs, ARFs, TOC1 *etc* (Mitsuda and Ohme-Takagi, 2009). In contrast, transcription repressors were not elucidated until the identification of the ethylene-responsive factor 3 (NtERF3) as the first repressor of transcription in tobacco (Ohta *et al.*, 2001). Subsequent analysis revealed the conservation of a motif $^L_FDLN^L_F(x)P$ in the C-terminus region between NtERF3 and its homologs in other plant species including AtERF3 and AtERF4 in *Arabidopsis*, OsERF3 in rice (Ohta *et al.*, 2001). The motif is also found in the C-terminus region of six other ERF proteins in *Arabidopsis*, AtERF7, AtERF8, AtERF9, AtERF10, AtERF11 and AtERF12 (Ohta *et al.*, 2001). This six amino acid motif was, therefore, named as ERF-associated amphiphilic repression (EAR) motif. In 2003, Keiichiro *et al.* showed that fusion of EAR motif domain to a transcriptional activator could convert it into a dominant repressor, which indicating that the EAR motif functioned as a strong repression domain (Hiratsu *et al.*, 2003). Therefore, transcription factors containing EAR motifs are usually assumed to act as transcription repressors.

A database search revealed the presence of the EAR motif in the C-terminal regions of several C2H2-type zinc finger proteins (Ohta *et al.*, 2001). Zinc finger proteins play important roles in many cellular processes, including transcriptional regulation, RNA binding, and protein-protein interactions (Ciftci-Yilmaz and Mittler, 2008). Among the different types of zinc finger protein, C2H2-type zinc finger proteins are the best studied. The first C2H2 zinc finger motif was identified in the *Xenopus* oocyte transcription factor TFIIA (Miller *et al.*, 1985). Since then, many C2H2 zinc finger proteins have been identified. An *in silico* analysis suggested that, ~0.7% of all genes encode C2H2 type zinc finger proteins in *Arabidopsis* (Englbrecht *et al.*, 2004). Recent studies have

shown the involvement of C2H2 zinc finger proteins in plant responses to environmental stresses. Constitutive expression of *Zat12* increased plant tolerance to high light, osmotic and oxidative stresses (Davletova *et al.*, 2005). In contrast, *Zat10* has more complicated regulatory roles. Transgenic plants that overexpress *Zat10* were found to be more tolerant to drought, osmotic, salinity and heat stresses. Interestingly, *Zat10*-knockout and RNAi plants exhibited similar tolerance to those stresses. These data suggested that *Zat10* possibly played a dual role in controlling plant response to abiotic stresses (Mittler *et al.*, 2006). *Zat6* has been recently identified to be involved in regulation of phosphate homeostasis and root development (Devaiah *et al.*, 2007b). *Zat6* was induced to varying levels in different part of plants during Pi starvation. Overexpression of *Zat6* resulted in retarded seedling growth as a result of decreased Pi acquisition. In older plants, the overexpression of *Zat6* increased the root-to-shoot mass ratio by reducing the primary root growth while increasing the lateral growth. As a result, Pi uptake and accumulation was increased. Moreover, enhanced expression of *Zat6* repressed several phosphate starvation responsive genes during Pi deprivation, such as *At4* and *Pht1;1* (Devaiah *et al.*, 2007b). It is possible that the EAR domain of *Zat6* is involved in transcriptional repression during phosphate starvation and development of primary root growth.

As a plant specific repression domain, the EAR motif is currently the only conserved repression motif identified in a large group of transcription repressor encoding genes. In Chapter 1, a labile repressor was proposed to control the expression of *Pht1;1* during early Pi deprivation. It is possible that the labile repressor would contain an EAR motif. Therefore, it would be interesting to isolate transcription factors with EAR motifs and examine their stability during immediate-early Pi starvation. The TFs would have a great chance to be the labile repressor if they both contain EAR motif and respond rapidly to Pi starvation.

6.2 Results

6.2.1 Identification of Zat18 as a transcriptional regulator, possibly a repressor

A BLAST search was performed against the *Arabidopsis* protein database, aiming to isolate all proteins with an EAR motif. The search resulted in identification of 148 protein sequences encoded by 115 unique genes (*Table 6.1*). Among them, 36 genes encoded transcription factors belonging to different families (*Table 6.1*). Afterwards, we examined the expression of these transcription factor encoding genes in the microarray data published by Misson *et al.* (Misson *et al.*, 2005). Interestingly, only At3g53600 was responsive to the Pi starvation treatment.

Previous studies indicated that At3g53600 encoded a C2H2 type zinc finger protein, namely Zat18 (Ciftci-Yilmaz *et al.*, 2007; Englbrecht *et al.*, 2004). As shown in *Fig. 6.1*, Zat18 comprised 175 amino acids. The sequence contains two C2H2 zinc finger domains, both of which contained an invariant QALGGH motif. The C-terminus of the protein, carries an EAR motif (LDLNLxP), suggesting it could act as a transcription repressor. In my project, a labile repressor was proposed to control the *Phl1;1* expression in early response to Pi starvation. As a potential transcription repressor, Zat18 could be a good candidate as a labile repressor.

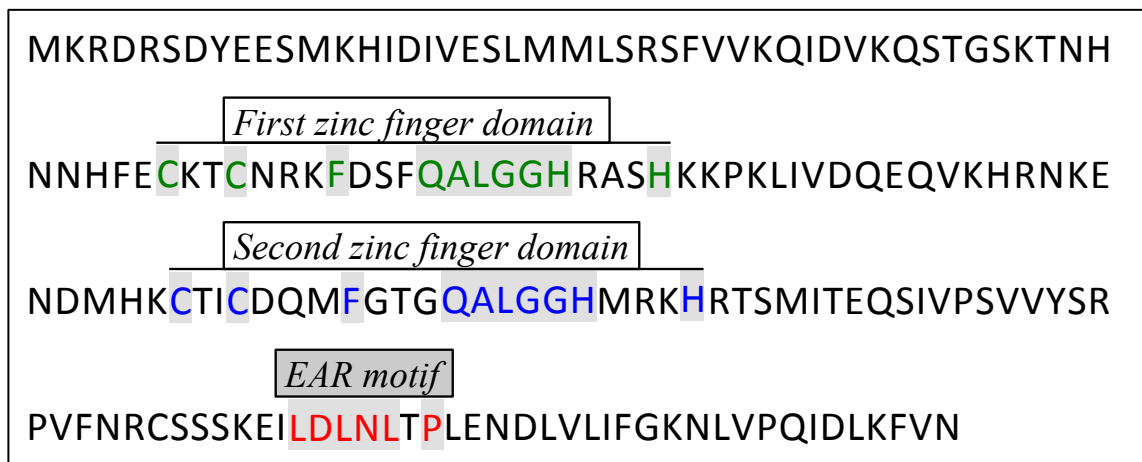


Fig. 6.1 Amino acid sequence of Zat18 (At3g53600). Two zinc finger domains and a C-terminus EAR motif domain was indicated.

Table 6.1 The list of genes encoding proteins containing EAR motif

Gene ID	TF family	Annotation
At1g04210	---	Leucine-rich repeat protein kinase family protein
At1g28370	ERF	ATERF11, ERF11, ERF domain protein 11
At1g53170	ERF	ATERF-8, ATERF8, ERF8, ethylene response factor 8
At5g06500	M-type	AGL96, AGAMOUS-like 96
At4g35280	C2H2	C2H2-like zinc finger protein
At1g13530	---	Protein of unknown function (DUF1262)
At5g01290	---	mRNA capping enzyme family protein
At5g12400	---	DNA binding; zinc ion binding; DNA binding
At1g78580	---	ATTPS1, TPS1, TPS1, trehalose-6-phosphate synthase
At2g38170	---	ATCAX1, CAX1, RCI4, cation exchanger 1
At1g07390	---	AtRLP1, RLP1, receptor like protein 1
At5g07790	---	unknown protein
At5g63200	---	tetratricopeptide repeat (TPR)-containing protein
		Ankyrin repeat family protein / BTB/POZ domain-containing protein
At4g26120	---	protein
At3g58030	---	RING/U-box superfamily protein
At1g27730	C2H2	STZ, ZAT10, salt tolerance zinc finger
At2g15260	---	RING/U-box superfamily protein
At5g04340	C2H2	C2H2, CZF2, ZAT6, zinc finger of <i>Arabidopsis thaliana</i> 6
At4g21550	B3	VAL3, VP1/ABI3-like 3
At4g02460	---	PMS1, DNA mismatch repair protein, putative
At3g25882	---	NIMIN-2, NIM1-interacting 2
At4g17850	---	unknown protein
At4g35700	C2H2	zinc finger (C2H2 type) family protein
At4g35610	C2H2	zinc finger (C2H2 type) family protein
At1g28390	---	Protein kinase superfamily protein
At1g50640	ERF	ATERF3, ERF3, ethylene responsive element binding factor 3
At1g53420	---	Leucine-rich repeat transmembrane protein kinase
At2g33480	NAC	ANAC041, NAC041, NAC domain containing protein 41
At5g43170	C2H2	AZF3, ZF3, zinc-finger protein 3
At5g28540	---	BIP1, heat shock protein 70 (Hsp 70) family protein
		ATERF-4, ATERF4, ERF4, RAP2.5, ethylene responsive element binding factor 4
At3g15210	ERF	
At3g10010	---	DML2, demeter-like 2
At3g44530	---	HIRA, homolog of histone chaperone HIRA
At5g48655	---	RING/U-box superfamily protein
At1g12850	---	Phosphoglycerate mutase family protein
At2g42030	---	RING/U-box superfamily protein

At3g20310	ERF	ATERF-7, ATERF7, ERF7, ethylene response factor 7
At2g43980	---	AtITPK4, ITPK4, inositol 1,3,4-trisphosphate 5/6-kinase 4
		ATKS, ATKS1, GA2, KS, KS1, Terpenoid cyclases/Protein
At1g79460	---	prenyltransferases superfamily protein
At3g59430	---	unknown protein
At1g75770	---	unknown protein
At3g61810	---	Glycosyl hydrolase family 17 protein
At4g30940	---	BTB/POZ domain with WD40/YVTN repeat-like protein
At1g03800	ERF	ATERF10, ERF10, ERF domain protein 10
At5g19270	---	unknown protein
At4g36050	---	endonuclease/exonuclease/phosphatase family protein
At3g09100	---	mRNA capping enzyme family protein
At5g44210	ERF	ATERF-9, ATERF9, ERF9, erf domain protein 9
At2g37430	C2H2	C2H2 and C2HC zinc fingers superfamily protein
At3g53600	C2H2	C2H2-type zinc finger family protein
At4g16610	C2H2	C2H2-like zinc finger protein
At2g28710	C2H2	C2H2-type zinc finger family protein
At5g01840	---	ATOFP1, OFP1, ovate family protein 1
At4g38960	DBB	B-box type zinc finger family protein
		systemic acquired resistance (SAR) regulator protein NIMIN-
At4g01895	---	1-related
At5g61300	---	unknown protein
At5g61380	TOC1	regulator protein
At3g08840	---	D-alanine--D-alanine ligase family
At5g67450	C2H2	AZF1, ZF1, zinc-finger protein 1
At5g07700	MYB	AtMYB76, MYB76, myb domain protein 76
At1g01900	---	ATSBT1.1, SBT1.1, subtilase family protein
At3g48060	---	BAH domain ; TFIIS helical bundle-like domain
At2g16090	---	ARI2, ATARI2, RING/U-box superfamily protein
At5g06290	---	2-Cys Prx B, 2CPB, 2-cysteine peroxiredoxin B
At4g10520	---	Subtilase family protein
At3g53840	---	Protein kinase superfamily protein
At5g44530	---	Subtilase family protein
At3g14067	---	Subtilase family protein
At3g12780	---	PGK1, phosphoglycerate kinase 1
At3g10470	C2H2	C2H2-type zinc finger family protein
At3g49930	C2H2	C2H2 and C2HC zinc fingers superfamily protein
At3g19580	C2H2	AZF2, ZF2, zinc-finger protein 2
At5g49350	---	Glycine-rich protein family
		Double Clp-N motif-containing P-loop nucleoside
At2g40130	---	triphosphate hydrolases superfamily protein

At3g14172	---	unknown protein
At4g34370	---	ARI1, ATARI1, RING/U-box superfamily protein
At2g39850	---	Subtilisin-like serine endopeptidase family protein
At5g58410	---	HEAT/U-box domain-containing protein
At1g79570	---	Protein kinase superfamily protein with octicosapeptide/Phox/Bem1p domain
At1g26610	C2H2	C2H2-like zinc finger protein
At5g28830	---	calcium-binding EF hand family protein
At1g78020	---	Protein of unknown function (DUF581)
At3g54090	---	FLN1, fructokinase-like 1
At3g45530	---	Cysteine/Histidine-rich C1 domain family protein
At2g28200	C2H2	C2H2-type zinc finger family protein
At1g74940	---	Protein of unknown function (DUF581)
At2g17180	C2H2	C2H2-like zinc finger protein
At1g76580	SBP	Squamosa promoter-binding protein-like (SBP domain) transcription factor family protein
At5g52790	---	CBS domain-containing protein with a domain of unknown function (DUF21)
At2g11810	---	ATMGD3, MGD3, MGDC, monogalactosyldiacylglycerol synthase type C
At3g11630	---	Thioredoxin superfamily protein
At1g07200	---	Double Clp-N motif-containing P-loop nucleoside triphosphate hydrolases superfamily protein
At2g45120	C2H2	C2H2-like zinc finger protein
At5g11940	---	Subtilase family protein
At1g74830	---	Protein of unknown function, DUF593
At5g04390	C2H2	C2H2-type zinc finger family protein
AtMg00760	---	ORF109B, hypothetical protein
At1g32970	---	Subtilisin-like serine endopeptidase family protein
At5g18640	---	alpha/beta-Hydrolases superfamily protein
At5g67360	---	ARA12, Subtilase family protein
At5g52530	---	dentin sialophosphoprotein-related
At1g56190	---	Phosphoglycerate kinase family protein
At1g02030	C2H2	C2H2-like zinc finger protein
At1g79550	---	PGK, phosphoglycerate kinase
At2g29970	---	Double Clp-N motif-containing P-loop nucleoside triphosphate hydrolases superfamily protein
At1g69200	---	FLN2, fructokinase-like 2
At3g48050	---	BAH domain ;TFIIS helical bundle-like domain
At4g21323	---	Subtilase family protein
At4g10530	---	Subtilase family protein

At5g03510	C2H2	C2H2-type zinc finger family protein
At4g21326	---	ATSBT3.12, SBT3.12, subtilase 3.12
At3g60580	C2H2	C2H2-like zinc finger protein
At5g43610	---	ATSUC6, SUC6, sucrose-proton symporter 6
At5g18630	---	alpha/beta-Hydrolases superfamily protein
At2g24240	---	BTB/POZ domain with WD40/YVTN repeat-like protein

6.2.2 Low Pi induces *Zat18* expression and increases ZAT18 accumulation in *Arabidopsis* roots

To test whether *Zat18* would behave as a labile repressor, we prepared a recombinant construct by fusing the coding region of *Zat18* to the N-terminus of VENUS (a yellow fluorescent protein). The construct was driven by the native *Zat18* promoter (Fig. 6.2A). Transgenic plants carrying the construct were generated through agrobacterium-mediated transformation. To examine the accumulation of the *Zat18*::VENUS fusion protein, the transgenic seeds were germinated and grown on half strength MS (0.5xMS) media for 5 days. The seedlings were transferred to liquid 0.5xMS for another 4 days. The root of seedlings was examined under a fluorescence microscope. As shown in Fig. 6.2Ba, a weak VENUS expression was detected in the root hair cells. DAPI staining result confirmed its nuclear localization (Fig. 6.2Bb), which was consistent with the predicted function of ZAT18 as a transcription factor.

In our hypothesis, a labile repressor could exist in a stable steady-state under sufficient Pi conditions. During Pi starvation, the repressor would be rapidly degraded to allow the up-regulation of *Phl1;1* and other primary response genes. Therefore, the seedlings grown in liquid media were transferred to Pi-free media for 4 hours. The expression was checked every hour. However, there was not any visible change during 4 hours starvation (data not shown). This suggested that the fusion protein might not be degraded during early Pi starvation.

To further test the inducibility of *Zat18*, the seedlings were kept in Pi free media for another 4 days. Interestingly, the expression of *Zat18* was visibly induced in root hair cells (Fig. 6.2Bd). This was consistent with the data from the microarray analysis

performed by Misson *et al.* (Misson *et al.*, 2005). In their result, the expression of *Zat18* was induced by ~6 fold in the roots during a 3-day Pi starvation. We also performed qPCR to confirm the expression pattern of *Zat18* at the transcriptional level under our experimental conditions. 14-day old wild type *Arabidopsis* seedlings grown in liquid media were transferred to Pi free media for 7 days. The media were refreshed twice during starvation treatment to ensure that no other nutrients became limiting for plant growth. As shown in *Fig. 6.3*, the expression of *MGD3* was dramatically induced, indicating the plants were deeply starved by shortage of Pi. The expression of *Zat18* was also induced by over 5-fold. Together, the results indicated increased expression and enhanced accumulation of *Zat18* at transcriptional and translational levels during Pi starvation.

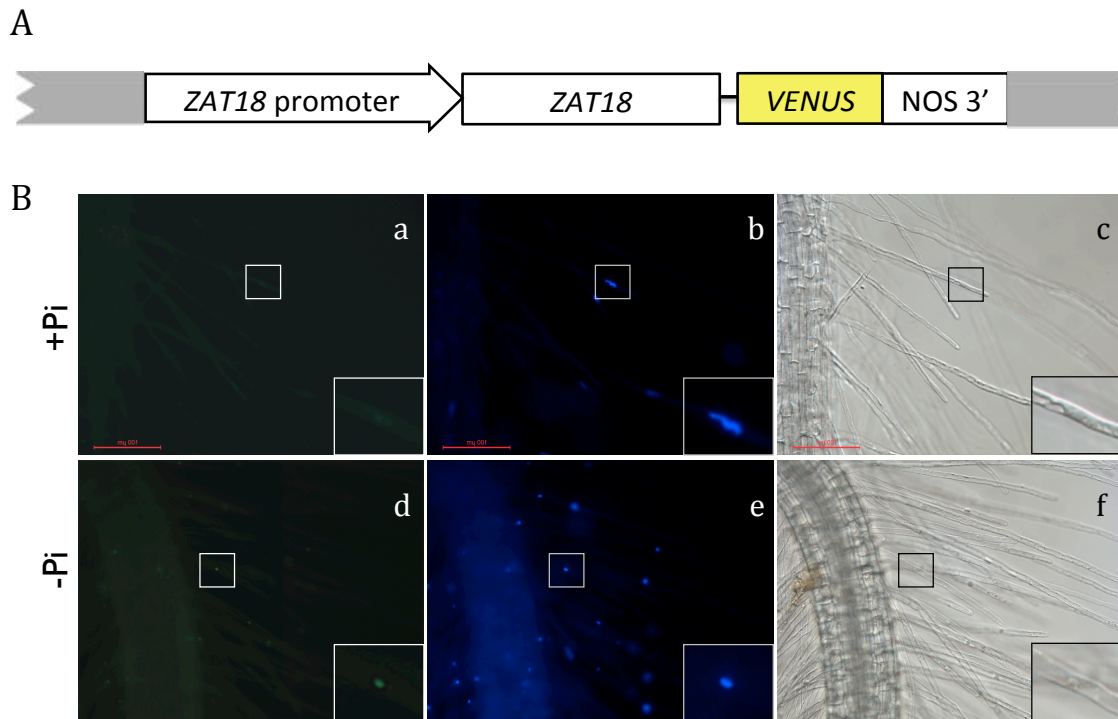


Fig. 6.2 Localization of VENUS tagged *Zat18* in *Arabidopsis* root hair cells. A: Schematic structure of the *Zat18* promoter::*Zat18*::*VENUS* gene expression cassette. B: Localization of *Zat18*::*VENUS* fusion protein in *Arabidopsis* root hair cells. a, b & c, root hair cells grown in Pi sufficient media. d, e & f, root hair cells grown in Pi free media. c & f, image was taken in bright field. a & d, image was taken in dark field through green channel (488 nm, GFP). b & e, image was taken in dark field through UV channel (350 nm DAPI). The box in each image showed the close-up view of the indicated spot.

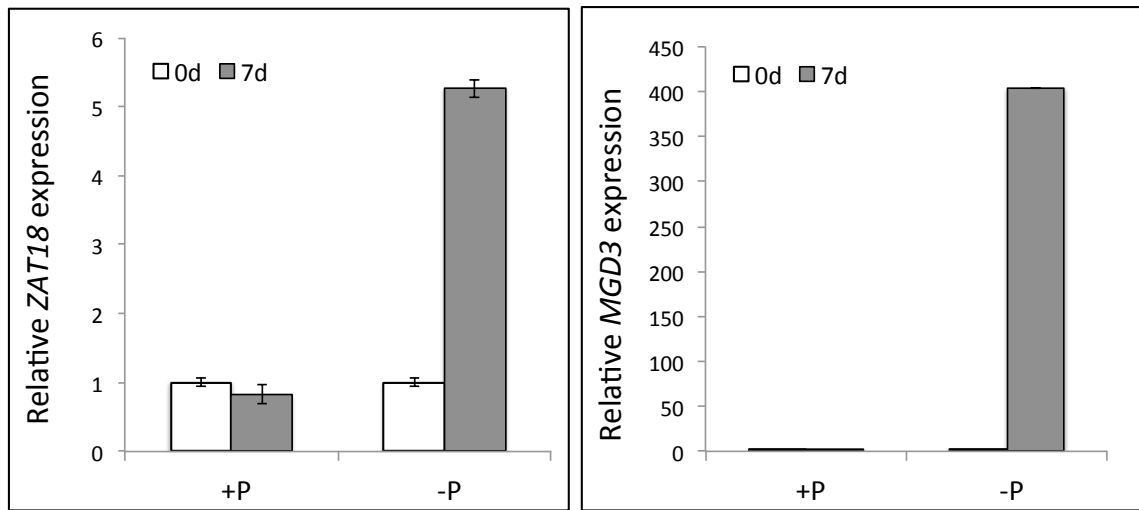


Fig. 6.3 Gene expression in *Arabidopsis* seedling roots under +Pi and –Pi conditions
14-day-old *Arabidopsis* seedlings grown in liquid ½ MS media were transferred to +Pi or –Pi media for 7 days. Gene expression was monitored by qRT-PCR from root samples. Error bars indicate standard error of the mean (SEM) from 3 biological repeats.

6.3. Discussion

A new C2H2 zinc finger protein, Zat18 was identified, which responds to Pi starvation. The amino acid sequence of Zat18 contains a conserved EAR-motif near its C-terminus, suggesting it could behave as a transcription repressor. Initially, we thought that Zat18 could be a candidate for the labile repressor in our proposed regulatory model. To test the possibility, a fusion protein was generated by construction of the coding region of Zat18 to upstream of VENUS. According to our model, the labile repressor should be relatively stable in order to accumulate to a certain level in plant cells and inhibit *Phl1;1* expression under Pi sufficient conditions. During early Pi starvation, the labile repressor would be easily degraded to allow the up regulation of *Phl1;1*. Therefore, we examined the expression kinetics of the fusion protein after transfer of transgenic seedlings from Pi sufficient media to Pi free media. However, no visible changes were observed in the first 4 hours after the media switch (data not shown). This suggested that Zat18 stayed stable

during immediate-early Pi starvation, and thus would not be the labile repressor in our model.

As indicated by a previous microarray result, Zat18 was induced during a 3-day Pi starvation. Therefore, we tested the inducibility of Zat18 during long Pi starvation treatments. Our results showed that the Zat18 accumulated to significantly higher levels after 4-day starvation treatments as indicated by the intensity of Zat18::VENUS fusion protein fluorescence. We also performed qPCR to show that Zat18 was up-regulated by over 5-fold at the transcriptional level during 7-day starvation. Together, these data indicated Zat18 responds to Pi starvation at later stages, which suggested that it might participate in the regulation of the late starvation responses in *Arabidopsis*. As a potential transcription repressor, it would interesting to further characterize Zat18 and elucidate its role in Pi starvation responses in plants.

Recently, Kagale *et al.* reported a genome-wide analysis of EAR-motif containing transcription factors in *Arabidopsis* (Kagale *et al.*, 2010). In their study, a literature survey was initially performed which identified 49 known EAR-motif containing proteins. Sequence comparison allowed them to identify two variants of EAR-motif, namely DLNxxP and LxLxL. Afterwards, a sophisticated BLAST method was employed to isolate bona fide EAR-motif containing TFs using the two variants of the EAR-motif as seed sequence. The search isolated a total of 219 TF-encoding genes, which was more than what we found in our BLAST search. The reason could be that we used original EAR-motif ($^{L/F}DLN^{L/F}(x)P$) as seed sequence for BLAST search, whereas they employed two other variants. The different BLAST method could also lead to different results. Published data suggested that approximately 40% of 219 proteins function as negative regulators of gene expression (Kagale *et al.*, 2010), while the rest still need to be verified by experiments. So far, a few more Pi-related microarray datasets have been publicly available; therefore, it would be interesting to check the expression of these 219 genes in those datasets and find out if there would be any more EAR-motif containing TFs that respond to Pi signals.

7. Transcriptomic analysis of gene expression in Col-0 wild type roots under different Pi conditions

7.1 Introduction

Microarray analysis is a powerful method to analyze changes of gene expression at the transcriptome level during biological processes, *e.g.* during development or environmental stress. The use of the technique has opened new possibilities to investigate sensing, signalling, and regulatory pathways. In previous studies, microarray analyses have been performed to examine global changes in gene expression in response to changes of Pi availability (Hammond, 2003; Wu *et al.*, 2003; Misson *et al.*, 2005; Muller *et al.*, 2006; Morcuende *et al.*, 2007; Thibaud *et al.*, 2010; Lin *et al.*, 2011; Woo *et al.*, 2012).

Due to technical limitations, these previous studies only employed microarrays covering part of the *Arabidopsis* genome. In the study by Wu *et al.*, a self-made microarray was used to examine the changes of gene expression in *Arabidopsis* roots and shoots following removal of Pi from growth media for up to 3 days (Wu *et al.*, 2003). The microarray included 6172 genes that covered less than one third of the *Arabidopsis* genome. Their data showed that ~29% of the genes in the array exhibited altered expression at the RNA level in response to Pi starvation. Classification of differentially expressed genes indicated that they belonged to a wide range of functional categories. Another study conducted by Hammond *et al.* indicated that many differentially expressed genes within 4 hours after removal of Pi were actually non-specific to Pi, and many commonly shock-inducible genes were up-regulated during the early response to Pi. In contrast, the responsive genes involved in later stages of starvation were more specific to Pi (Hammond *et al.*, 2003).

The first microarray analysis covering the majority of the *Arabidopsis* genome was performed by Misson *et al.* in 2005 (Misson *et al.*, 2005). The advent of the Affymatrix 22K ATH1 GeneChip allowed the examination of 22,810 *Arabidopsis* probe sets per array. The analysis included *Arabidopsis* root and shoot samples separately, which had

been exposed to short, medium and long-term Pi starvation. Their data led to the identification of 612 and 254 Pi-responsive genes, which were induced or suppressed, respectively. The regulated genes were involved in a wide range of functional groups related to metabolism, ion transport, signal transduction, transcriptional regulation, and growth and development. Another study conducted by Morcuende *et al.* used *Arabidopsis* young seedlings for microarray experiments (Morcuende *et al.*, 2007). Over 1000 genes were identified with >2 fold altered expression during Pi deprivation. Their study also included seedling samples recovered from Pi starvation. Interestingly, the data indicated that >90% of genes with strong induction (>5 fold) during Pi deprivation were strongly reversed in 3 hours after Pi re-supply. This group of genes was suggested to be specifically responsive to Pi availability. Comparison between these two datasets suggested that only 38% of genes with >2 fold changes in the dataset from Misson *et al.* were present as regulated genes in the data published by Morcuende *et al.*. The variability could be attributed to differences in plant growth conditions and the materials included in the analysis. For example, roots and shoots were analysed separately in the study of Misson *et al.*, while the whole seedlings were used by Morcuende *et al.*.

Recently, Lin *et al.* reported the microarray analysis of early transcriptional responses to Pi deficiency in the *Arabidopsis* root (Lin *et al.*, 2011). The young seedlings were exposed to a short Pi starvation for 1 hr, 6 hr or 24 hr. The roots from each time point were collected for further experiment. Their analysis revealed a total of 797 genes with changed expression of over 2-fold for at least one time point. Subsequent co-expression based clustering analysis predicted three major clusters of Pi responsive genes. These clusters were enriched in genes putatively functioning in transcriptional regulation, root hair formation, and developmental adaptations. The validation of microarray data by qRT-PCR demonstrated that a few responsive genes were robustly induced within 1 hr after the change in the Pi regime. Further study of these genes could be helpful in dissecting the early Pi starvation signalling pathway.

Re-supply of Pi to Pi-starved plants is another approach to study the plant response to Pi signals. In 2012, Woo *et al.* used micro- and tiling-array platforms to examine gene

expression of *Arabidopsis* roots and shoots during the Pi starvation and recovery process (Woo *et al.*, 2012). From ATH1 microarray data, a total of 1257 genes were identified as regulated during either starvation or recovery in roots, while 182 genes were regulated in shoots. Taking advantage of the tiling-array, 5044 genes that were not present on ATH1 microarray, were also analysed. The result showed that 477 of tiling-array-specific genes were differentially expressed, including *IPSI*, *GDPD3* (a membrane-remodeling factor) and *CPL3* (a MYB TF), *etc* (Woo *et al.*, 2012).

Although many microarray analyses have been applied to study transcriptomic changes in response to Pi availability, the results from these studies shared relatively little overlap. Based on literature and database searches, Woo *et al.* identified a total of 84 genes that have been variously described in the literature and annotated by TAIR as being Pi-responsive. However, only 40% of these genes were detected by their own study (Woo *et al.*, 2012). Comparison across previous studies showed that 14%, 33%, 3% and 8% of these 84 genes were identified as regulated genes in the studies by Misson *et al.* (2005), Morcuende *et al.* (2006), Muller *et al.* (2007), and Nilsson *et al.* (2010), respectively. The lack of overlapping results suggested that the data from transcriptional analysis is likely strongly dependent on the experimental approaches.

In my project, a microarray analysis was designed to study transcriptome changes in *Arabidopsis* roots during Pi starvation and the rapid recovery process. Compared to the study by Woo *et al.*, we are more interested in gene expression within 4 hours after re-supply of Pi to starved plants rather than 3 days in their study. The results from microarray analysis was described and discussed in this chapter.

7.2 Results

7.2.1 Experimental design

As discussed above, microarray analysis is likely sensitive to experimental conditions. To facilitate our study on early Pi starvation signalling pathway, we designed a microarray experiment to examine gene expression in *Arabidopsis* roots under our experimental conditions. Briefly, the young seedlings would receive long-term Pi starvation treatment, so that the Pi starvation responsive (PSR) genes would be highly induced. Afterwards, a Pi would be provided to the seedlings for a short recovery time course. Genes that are highly regulated during starvation while rapidly reversed after recovery would be particularly interesting for further studies.

In the preliminary experiment, we grew seedlings in liquid ½ strength MS media as described in Chapter 4. Briefly, the seedlings were germinated and grown in full nutrient media for 16 days before subjected to Pi starvation. To determine the starvation period, the samples were harvested in either 3 days or 7 days after transfer of seedlings to Pi deficient media. The expression of marker genes was examined by qRT-PCR to validate the plant response to starvation. As shown in *Fig. 7.1*, the expression of *MGD3* and *At4* was induced at 3-day after transfer. The induction became much stronger at 7-day. Therefore, we decided to use 7-day starved seedlings for the recovery treatment.

To generate the samples for microarray analysis, 16-day old *Arabidopsis* seedlings were transferred to Pi deficient (P^{starv}) or Pi sufficient (P^{mock}) media for 7 days to measure the transcriptional response to Pi starvation. Seedlings grown in Pi deficient media were re-supplied with 1.5 mM Pi for a recovery treatment of 2 hours (P^{rec2}) or 4 hours (P^{rec4}). Roots were harvested from various plant samples from 3 replicate experiments. RNA was extracted from these samples (P^{mock} , P^{starv} , P^{rec2} , P^{rec4}) for microarray analysis.

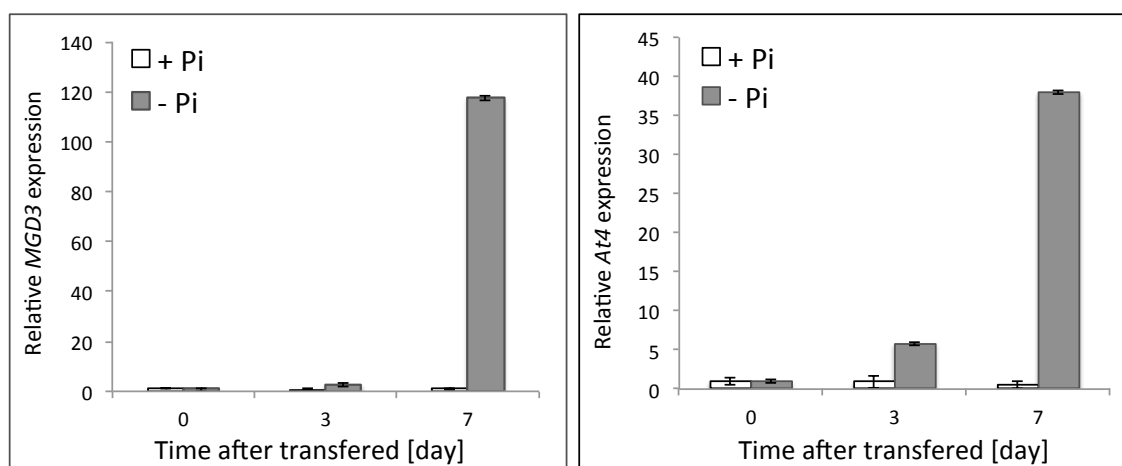


Fig. 7.1 Gene expression in *Arabidopsis* seedling roots during Pi starvation. *Arabidopsis* seedlings grown in liquid half strength MS media for 16 days were transferred to +Pi/-Pi media for another 3 days or 7 days for treatment. Gene expression was monitored by qRT-PCR. Error bars indicate standard error of the mean (SEM) from 3 biological repeats.

7.2.2 Overview of regulated gene expression in *Arabidopsis* seedling roots identified by microarray analysis

To assess the regulation of genes in response to Pi starvation and recovery, transcriptomic analysis was performed with Nimblegen 12x135K microarray system. On each microarray, there are ~13500 probe-sets that cover 37118 RNA transcripts from the *Arabidopsis* genome based on the annotation of TAIR9.0. During the experiment, all steps strictly followed the instructions of the Nimblegen microarray user guide. The raw data were analyzed by R software, and the Limma package was used for statistical analysis. To isolate the differentially expressed genes, the criteria of ≥ 2 -fold change and Bonferroni-corrected *p*-value < 0.05 was applied for each comparison.

After 7-day Pi starvation, a total of 478 transcripts exhibited regulated expression, representing 446 unique genes (Table 7.1). As shown in Table 7.1, 258 genes were induced by Pi^{starv} , while 188 genes were suppressed compared to Pi^{mock} . This was consistent with previous studies that more genes were up-regulated rather than down-regulated during Pi starvation (Misson *et al.*, 2005). After re-supply of Pi, 120 genes

were down regulated in 2 hours compared to P_i^{starv} , while 133 genes were up regulated. The number increased to 197 and 222, respectively, after 4 hours recovery.

Table 7.1 Number of regulated genes in various comparisons identified by microarray analysis. ↑ indicated up-regulation and ↓ indicated down-regulation.

		$P_i^{\text{starv}}/P_i^{\text{mock}}$	$P_i^{\text{rec2}}/P_i^{\text{starv}}$	$P_i^{\text{rec4}}/P_i^{\text{starv}}$
Regulated Transcripts	↑	279	151	254
	↓	199	132	212
	Total	478	283	466
Regulated Genes	↑	258	133	222
	↓	188	120	197
	Total	446	253	419

7.2.3 Expression profiles of Pi starvation responsive (PSR) genes during Pi recovery

A total of 258 and 188 genes were induced or suppressed after 7-day Pi starvation treatment, respectively. For these Pi starvation responsive (PSR) genes, the expression of many, but not all, of them was reversed during rapid Pi recovery. As shown in *Fig. 7.2A*, a total of 149 Pi-starvation-induced genes exhibited down regulation during 2 or 4 hour Pi recovery (P_i^{rec}) compared to P_i^{starv} . Among Pi recovered genes, 145 of them kept reduced expression level at 4 hours, and 107 of them started to show down regulation within 2 hours. In contrast, only ~43% of Pi starvation suppressed genes were reversed by Pi recovery (*Fig. 7.2B*).

In our study, we were particularly interested in isolation of rapidly responsive genes. Therefore, the 107 induced genes and 60 repressed genes that showed reversible expression patterns during Pi recovery were considered as the candidates for rapid responsive genes. A list of selected genes were shown in Table 7.2 and Table 7.3. In the list, a few classic PSR marker genes appeared, including IPS1, MGD3 SQD2, Pht1;4, Pht1;8, Pht1;9, SPX3 *etc.*.

To gain further insight into our list of rapid responsive genes, we performed GO annotation and enrichment analysis using DAVID, a bioinformatics tool for functional annotation and enrichment analysis (<http://david.abcc.ncifcrf.gov/home.jsp>). To distinguish between Pi starvation induced and suppressed genes, we uploaded the lists of

expression data of up- or down-regulated genes separately. As we expected, the highest ranked term, in the group of Pi-starvation-induced genes, was “cellular response to phosphate starvation” with a Bonferroni adjusted $p\text{-value}=4.8\times 10^{-16}$. Additional terms identified as significant include: glycolipid biosynthetic process, anion transport. However, there was not a significantly enriched term in the group of Pi-starvation-suppressed genes according to the Bonferroni adjusted $p\text{-value}$. This indicated that the induced genes identified in our result would be more specific to Pi starvation.

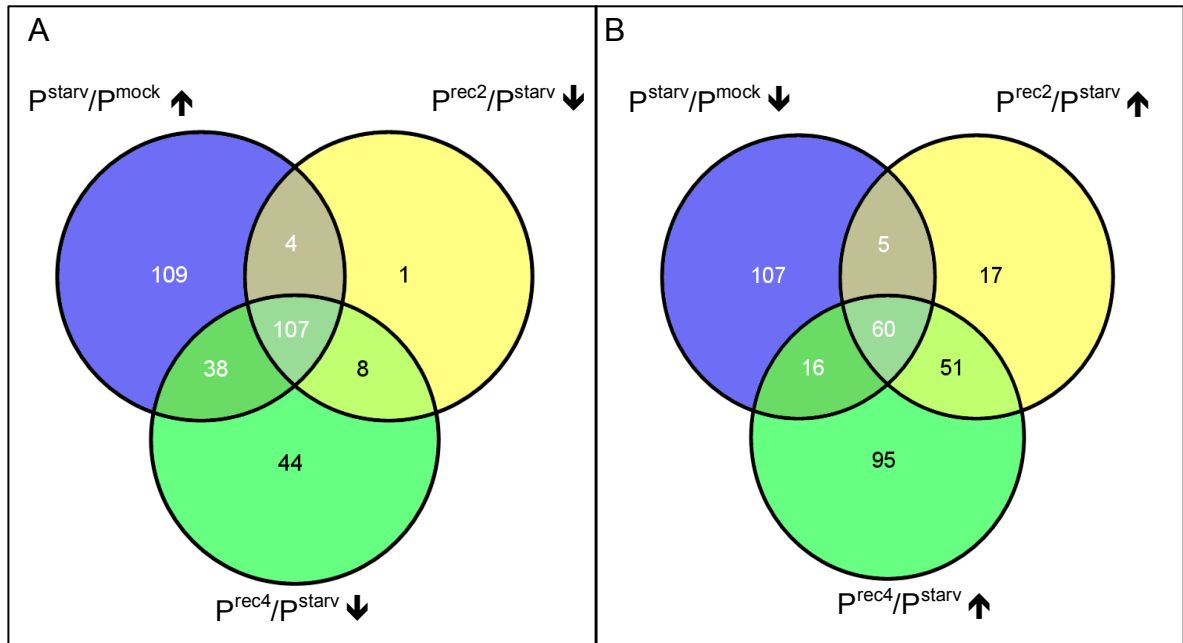


Fig. 7.2 Venn diagram illustrates common and unique differential gene expression in different comparisons.
 \uparrow indicated up-regulation and \downarrow indicated down-regulation

Table 7.2 The list of selected Pi starvation induced genes from microarray data.

Gene ID	Fold Change (Log2)			Annotation
	P^{starv}/P^{mock}	P^{rec2}/P^{starv}	P^{rec4}/P^{starv}	
AT5G20790	6.892	-3.885	-4.811	unknown protein
AT3G09922	5.716	-1.588	-2.035	ATIPS1
AT1G73010	5.07	-2.827	-3.615	ATPS2, PS2, phosphate starvation-induced gene 2
AT5G20410	4.841	-2.711	-3.206	ATMGD2, MGD2, monogalactosyldiacylglycerol synthase 2
AT2G11810	4.64	-3.5475	-3.8375	ATMGD3, MGD3, MGDC, monogalactosyldiacylglycerol synthase type C
AT3G03530	4.565	-3.272	-3.698	NPC4, non-specific phospholipase C4
AT2G45130	4.376	-3.951	-4.425	ATSPX3, SPX3, SPX domain gene 3
AT1G20860	3.762	-3.267	-3.632	PHT1;8, phosphate transporter 1;8
AT3G05630	3.725	-2.24	-2.429	PDLZ2, PLDP2, PLDZETA2, phospholipase D P2
AT5G20150	3.385	-1.701	-2.301	ATSPX1, SPX1, SPX domain gene 1
AT2G38940	3.369	-1.732	-2.356	ATPT2, PHT1;4, phosphate transporter 1;4
AT1G76430	2.967	-2.212	-2.202	PHT1;9, phosphate transporter 1;9
AT4G31240	2.953	-1.915	-2.13	protein kinase C-like zinc finger protein PHO1;H1, EXS (ERD1/XPR1/SYG1) family
AT1G68740	2.706	-1.001	-2.122	protein
AT3G02040	2.697	-1.576	-1.781	SRG3, senescence-related gene 3
AT5G01220	2.693	-2.051	-2.311	SQD2, sulfoquinovosyldiacylglycerol 2
AT5G02200	2.613	-1.465	-1.591	FHL, far-red-elongated hypocotyl1-like
AT1G67600	2.607	-1.468	-1.274	Acid phosphatase/vanadium-dependent haloperoxidase-related protein
AT1G23140	2.438	-1.894	-1.927	Calcium-dependent lipid-binding (CaLB domain) family protein
AT4G13700	2.174	-2.024	-2.051	ATPAP23, PAP23, purple acid phosphatase 23
AT1G22150	2.124	-1.718	-2.318	SULTR1;3, sulfate transporter 1;3
AT3G17790	2.109	-1.54	-1.619	ATACP5, ATPAP17, PAP17, purple acid phosphatase 17
AT4G33770	2.063	-1.101	-1.373	Inositol 1,3,4-trisphosphate 5/6-kinase family protein
AT5G62162	2.049	-1.658	-2.172	MIR399C, MIR399C; miRNA
AT4G12090	2.029	-1.594	-1.669	Cornichon family protein
AT3G47420	1.991	-1.109	-1.723	ATPS3, PS3, phosphate starvation-induced gene 3
AT2G16430	1.874	-1.291	-1.541	ATPAP10, PAP10, purple acid phosphatase 10
AT1G56360	1.846	-1.746	-1.481	ATPAP6, PAP6, purple acid phosphatase 6
AT4G33030	1.816	-1.301	-1.24	SQD1, sulfoquinovosyldiacylglycerol 1

AT4G24890	1.813	-1.198	-1.177	ATPAP24, PAP24, purple acid phosphatase 24
AT2G32830	1.764	-1.865	-1.955	PHT1;5, PHT5, phosphate transporter 1;5
AT1G13750	1.719	-1.4	-1.671	Purple acid phosphatases superfamily protein
AT2G26660	1.705	-1.239	-1.276	ATSPX2, SPX2, SPX domain gene 2
AT1G22220	1.537	-1.504	-1.356	F-box family protein
AT3G52190	1.377	-1.308	-1.435	PHF1, phosphate transporter traffic facilitator1
AT1G45249	1.132	-1.134	-1.164	ABF2, AREB1, ATAREB1, abscisic acid responsive elements-binding factor 2

Table 7.3 The list of selected Pi starvation repressed genes from microarray data.

Gene ID	Folc Change (Log2)			Annotation
	P^{starv}/P^{mock}	P^{rec2}/P^{starv}	P^{rec4}/P^{starv}	
AT3G05950	-5.475	2.177	2.19	RmLC-like cupins superfamily protein
AT3G49620	-4.049	2.235	2.615	DIN11, 2-oxoglutarate (2OG) and Fe(II)-dependent oxygenase superfamily protein
AT5G43580	-3.029	3.552	3.869	Serine protease inhibitor, potato inhibitor I-type family protein
AT5G03860	-2.616	1.747	1.897	MLS, malate synthase
AT3G26220	-2.612	2.781	2.38	CYP71B3, cytochrome P450, family 71, subfamily B, polypeptide 3
AT4G30270	-2.28	1.796	1.631	MER1-5, MER15B, SEN4, XTH24, xyloglucan endotransglucosylase/hydrolase 24
AT4G24350	-2.227	1.8465	1.654	Phosphorylase superfamily protein
AT1G15330	-2.185	1.61	1.687	Cystathionine beta-synthase (CBS) protein
AT1G10070	-2.0995	2.606	2.738	ATBCAT-2, BCAT-2, branched-chain amino acid transaminase 2
AT2G22980	-1.9905	1.7305	2.1415	SCPL13, serine carboxypeptidase-like 13
AT4G21120	-1.799	1.65	1.92	AAT1, CAT1, amino acid transporter 1
AT1G21400	-1.789	2.279	2.273	Thiamin diphosphate-binding fold (THDP-binding) superfamily protein
AT3G15500	-1.771	2.276	2.341	ANAC055, ATNAC3, NAC055, NAC3, NAC domain containing protein 3
AT1G77210	-1.744	2.116	2.331	AtSTP14, STP14, sugar transporter 14
AT1G68010	-1.589	1.241	1.466	ATHPR1, HPR, hydroxypyruvate reductase
AT1G71030	-1.534	1.693	1.894	ATMYBL2, MYBL2, MYB-like 2
AT4G36000	-1.478	1.107	1.123	Pathogenesis-related thaumatin superfamily protein
AT3G10450	-1.46	1.393	1.446	SCPL7, serine carboxypeptidase-like 7
AT1G70810	-1.446	1.668	1.534	Calcium-dependent lipid-binding family protein
AT2G24130	-1.431	1.282	1.17	Leucine-rich receptor-like protein kinase family protein

			AGT, AGT1, SGAT, alanine:glyoxylate
AT2G13360	-1.403	1.226	1.342 aminotransferase
AT3G63110	-1.402	1.041	1.292 ATIPT3, IPT3, isopentenyltransferase 3
AT2G22990	-1.3888	1.372	1.5568 SCPL8, SNG1, sinapoylglucose 1
AT2G41210	-1.364	1.09	1.352 PIP5K5, phosphatidylinositol- 4-phosphate 5-kinase 5
AT2G47400	-1.356	1.606	1.891 CP12, CP12-1, CP12 domain-containing protein 1
AT3G09390	-1.345	1.784	2.093 ATMT-1, ATMT-K, MT2A, metallothionein 2A
AT3G44300	-1.341	1.489	1.415 AtNIT2, NIT2, nitrilase 2
AT5G63600	-1.303	1.493	1.448 ATFLS5, FLS5, flavonol synthase 5
AT2G23030	-1.281	2.738	3.375 SNRK2-9, SNRK2.9, SNF1-related protein kinase 2.9
AT5G67520	-1.208	1.118	1.293 APK4, adenosine-5'-phosphosulfate (APS) kinase 4
AT1G69490	-1.187	1.295	1.291 ANAC029, ATNAP, NAP, NAC-like, activated by AP3/PI
AT5G13080	-1.174	1.869	1.527 ATWRKY75, WRKY75, WRKY DNA-binding protein 75
AT5G16810	-1.031	1.127	1.199 Protein kinase superfamily protein

7.2.4 Comparison across different microarray datasets

As we discussed, the differentially expressed genes identified from various microarray analyses shared relatively low similarity, likely due to the variation of experimental conditions. However, those genes that were commonly identified in the different experiments were likely to constitute the core set of responsive genes specific for P-signalling. Here, we compared our result with two published microarray data in order to identify the commonly shared genes, and to refine our list of Pi responsive marker genes. These two microarray experiments, performed by Misson *et al.* in 2005 (Misson *et al.*, 2005) and Woo *et al.* in 2012 (Woo *et al.*, 2012), employed a comparable experimental design to ours. Both of the designs include long term Pi starvation, and in the experiment by Woo *et al.*, a Pi recovery treatment was included.

To increase the accuracy of the comparison, the original datasets from the above two publication were downloaded from public microarray database for our analysis. As both published datasets were obtained from the Affymatrix microarray platform, their probe identifiers were converted into AGI identifiers to match the format of our dataset. Preliminary comparison indicated that a total of 23539 unique genes from the *Arabidopsis* genome were shared in the 3 independent datasets. Therefore, we only analysed the expression of these genes for comparison. To get the regulated genes, we re-analysed datasets from those two experiments using the same method as used for the analysis of our dataset, and set the same criteria for the selection of differentially expressed genes (fold change ≥ 2 and Bonferroni-corrected *p-value* < 0.05).

The re-calculation resulted in a total of 353, 286, and 615 regulated genes during Pi starvation in our dataset, and the datasets from Misson *et al.* and Woo *et al.*, respectively (Table 7.4). For the Pi recovery, there were 336 and 894 genes showing altered expression in our dataset and the one from Woo *et al.*, respectively (Table 7.4). Regarding the Pi recovery time, Woo *et al.* examined gene expression at 3-days after re-addition of Pi, while we checked gene expression within 4 hours after Pi addition. Although the time point was quite different between the two experiment designs, it was still interesting to identify the overlapping genes, which could help to distinguish rapid-

and slow- response genes.

Table 7.4 Number of regulated genes in different microarray datasets after re-calculation. ↑ indicated up-regulation and ↓ indicated down-regulation.

	P_i^{starv}/P_i^{mock}			P_i^{rec}/P_i^{starv}	
	Xin et al	Misson et al	Woo et al	Xin et al	Woo et al
↑	209	213	299	178	461
↓	144	73	316	158	433
Total	353	286	615	336	894

As shown in *Fig 7.3A*, three microarray datasets shared 77 commonly induced genes during Pi starvation, which accounted for 37%, 36% and 26% of the total of induced genes in the dataset of ours, Misson *et al.* and Woo *et al.*, respectively. These genes could be reasonably considered as the core set of Pi starvation specific inducible genes. Interestingly, only one gene suppressed by Pi starvation was shared by the three datasets (*Fig. 7.3B*), which supported our view that the repressed genes were less specific to Pi starvation.

During Pi recovery, a total of 336 genes and 894 genes were regulated in our dataset and the dataset from Woo *et al.*. As Woo *et al.* examined gene expression 3 days after recovery, it was not unexpected that more genes exhibited regulated expression in their study. As shown in *Fig. 7.3C & D*, 91 genes were suppressed by re-supply of Pi in both experiments, while 58 induced genes were shared in both datasets after Pi recovery, indicating these genes rapidly responded to Pi supply, and the reduced expression remained for up to 3 days. However, the overlapping genes in this comparison did not necessarily mean they were regulated during Pi starvation. Therefore, further comparison was needed to isolate the robust Pi specific responsive genes.

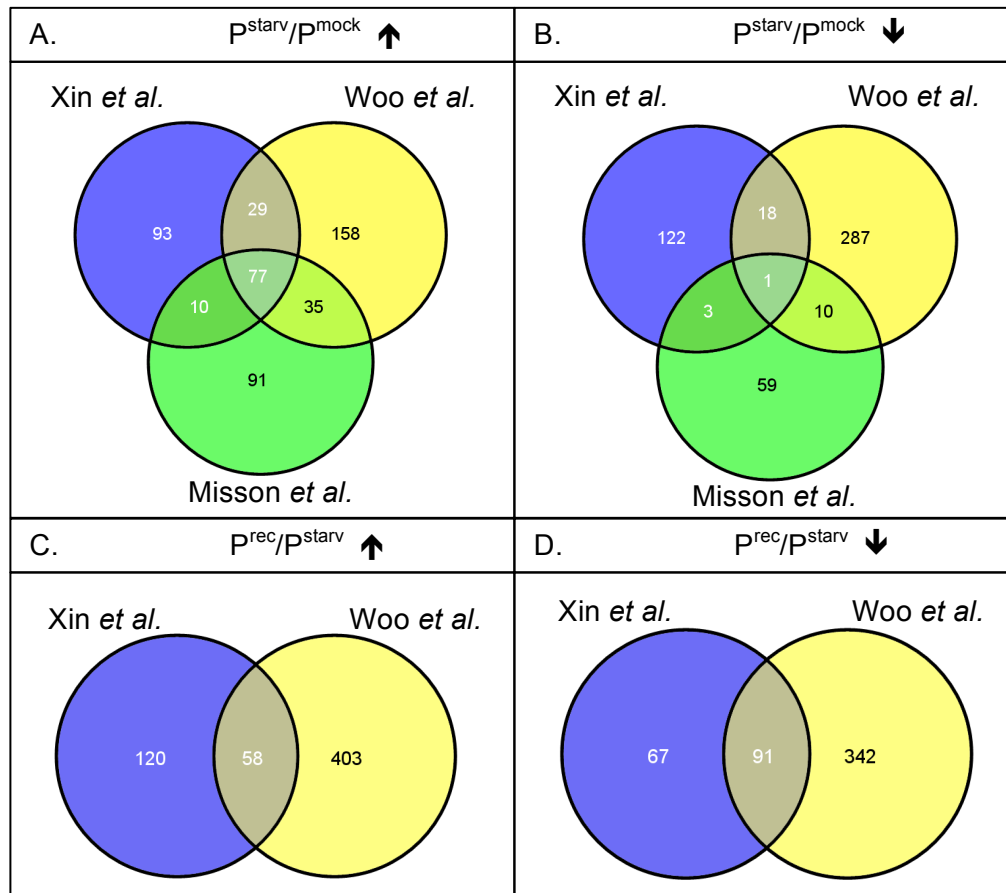


Fig. 7.3 Venn diagram illustrates common and unique differential gene expression in different comparisons.

A. Number of genes induced (\uparrow) by Pi starvation in datasets as indicated in the figure; B. Number of genes suppressed (\downarrow) by Pi starvation in three datasets as indicated in the figure; C. Number of genes induced (\uparrow) during Pi recovery in two datasets as indicated in the figure; D. Number of genes suppressed (\downarrow) during Pi recovery in two datasets as indicated in the figure.

7.2.5 A robust list of rapid Pi responsive marker genes

To further refine the list of rapid response genes, we compared the regulated genes during both Pi starvation and Pi recovery between our dataset and the one from Woo *et al.*. As shown in Fig. 7.4A, 79 genes appeared in both datasets that showed up regulation by Pi starvation and down regulation after Pi recovery, while only 14 commonly shared genes exhibited opposite expression pattern (Fig. 7.4B). Considering that the Pi

starvation suppressed genes were less specific to Pi signal (Fig. 7.3B), we only included the 79 genes for further analysis.

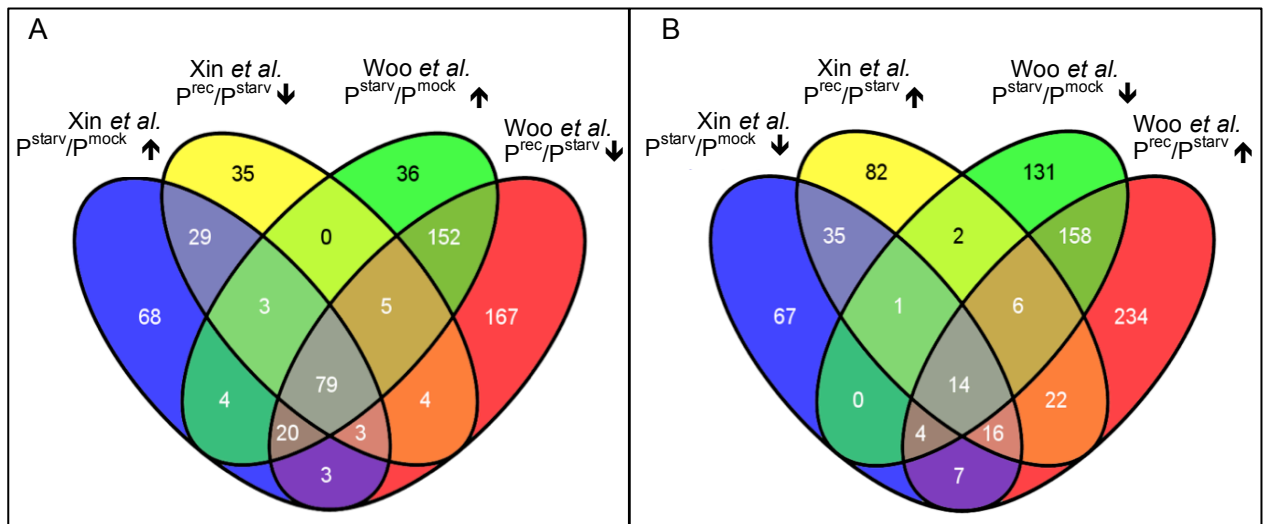


Fig. 7.4 Venn diagram illustrates common and unique differential gene expression in different comparisons.

A. Number of genes induced (↑) by Pi starvation and repressed in Pi recovery (↓) in datasets as indicated in the figure; B. Number of genes suppressed (↓) by Pi starvation and induced (↑) in Pi recovery in datasets as indicated in the figure;

To finalize the list of rapid response marker genes, the 79 commonly shared reversible genes (Fig. 7.4A) were compared to the 77 Pi-starvation-induced genes shared by 3 independent experiments (Fig. 7.3A). The comparison led to the isolation of 63 overlapping genes, which means they were robustly induced during Pi starvation while suppressed by Pi recovery within 4 hours and the suppression remained up to 3 days. Therefore, these 63 genes were considered as robust rapid Pi response marker genes (Table 7.5). Among them, 58 genes showed down regulation 2 hours after Pi recovery.

These rapid response genes were analysed by DAVID for GO term enrichment analysis. The highest ranked GO molecular function term was “phosphatase activity” with Bonferroni corrected $p\text{-value}=1.0\times 10^{-6}$. A total of 11 genes were clustered under this term, including 6 purple acid phosphatase encoding genes: *PAP1*, *PAP6*, *PAP10*, *PAP17*, *PAP23* and *PAP24*. The second major cluster of genes encoded proteins with transporter

activity. As we expected, the Pi transporter encoding genes appeared in this cluster, including *Pht1;4*, *Pht1;5*, *Pht1;8* and *Pht1;9*. Surprisingly, one of the sulphate transporter, *SULTR1;3*, showed a similar expression behaviour as the Pi transporters during Pi starvation and recovery. This suggested possible cross-talk between phosphate signalling and sulphate signalling.

Another interesting cluster of genes encoded proteins containing the SPX domain, including *SPX1*, *SPX2*, *SPX3* and *PHO1;H1*. Previous studies showed that *PHO1;H1* belongs to the *PHO1* gene family, and plays a role in loading Pi into the xylem. Loss of function mutations in *PHO1;H1* resulted in Pi deficiency in shoots, indicating a function in maintaining Pi homeostasis in *planta*. The SPX gene family was suggested to be involved in signalling pathways controlled by *PHR1* and *SIZ1*. The rapid response of *SPX1-3* in our study suggested they might play a role in early signal transduction.

Table 7.5 The list of robust rapid Pi responsive marker genes.

AGI identifier	Fold Change (Log2)			Bonferroni corrected <i>p</i> -value			Annotation
	$\frac{P^{starv}}{P^{mock}}$	$\frac{P^{rec2}}{P^{starv}}$	$\frac{P^{rec4}}{P^{starv}}$	$\frac{P^{starv}}{P^{mock}}$	$\frac{P^{rec2}}{P^{starv}}$	$\frac{P^{rec4}}{P^{starv}}$	
AT1G05000	2.0815	-1.803	-1.9805	6.2E-03	2.0E-02	6.5E-03	Phosphotyrosine protein phosphatases superfamily protein
AT1G08310	3.186	-1.84	-2.204	0.0E+00	1.0E-04	7.0E-06	alpha/beta-Hydrolases superfamily protein
AT1G13750	1.719	-1.4	-1.671	1.0E-06	1.8E-05	1.0E-06	Purple acid phosphatases superfamily protein
AT1G17710	4.3115	-3.501	-3.942	5.0E-07	3.9E-05	3.5E-06	Pyridoxal phosphate phosphatase-related protein
AT1G17830	1.272	-1.409	-1.559	5.8E-03	5.3E-03	1.1E-03	Protein of unknown function (DUF789)
AT1G19200	2.962	-2.111	-2.186	5.0E-06	4.6E-04	1.5E-04	Protein of unknown function (DUF581)
AT1G20860	3.762	-3.267	-3.632	0.0E+00	0.0E+00	0.0E+00	PHT1;8, phosphate transporter 1;8
AT1G22150	2.124	-1.718	-2.318	3.6E-05	6.6E-04	1.5E-05	SULTR1;3, sulphate transporter 1;3
AT1G56360	1.846	-1.746	-1.481	6.2E-03	1.7E-02	2.6E-02	ATPAP6, PAP6, purple acid phosphatase 6
AT1G67600	2.607	-1.468	-1.274	8.8E-05	2.2E-02	2.8E-02	Acid phosphatase/vanadium-dependent haloperoxidase-related protein
AT1G68740	2.706	-1.001	-2.122	1.0E-06	2.0E-02	1.2E-05	PHO1;H1, EXS (ERD1/XPR1/SYG1) family protein
AT1G70900	1.462	-1.215	-1.279	1.4E-03	1.1E-02	4.0E-03	unknown protein

AT1G71130	1.486	-1.054	-1.221	3.4E-05	2.1E-03	2.5E-04	Integrase-type DNA-binding superfamily protein
AT1G73010	5.07	-2.827	-3.615	0.0E+00	6.1E-04	2.5E-05	ATPS2, PS2, phosphate starvation- induced gene 2
AT1G73220	3.571	-2.547	-4.2	1.1E-05	7.5E-04	2.0E-06	1-Oct, AtOCT1, organic cation/carnitine transporter1
AT1G76430	2.967	-2.212	-2.202	0.0E+00	1.1E-05	5.0E-06	PHT1;9, phosphate transporter 1;9
AT2G04460	5.268	-3.491	-4.464	0.0E+00	1.0E-06	0.0E+00	transposable element gene ATMGD3, MGD3, MGDC, monogalactosyldiacylglycerol
AT2G11810	4.64	3.5475	-3.8375	3.0E-06	1.6E-04	2.9E-05	synthase type C ATPAP10, PAP10, purple acid
AT2G16430	1.874	-1.291	-1.541	2.1E-04	1.0E-02	1.3E-03	phosphatase 10
AT2G26660	1.705	-1.239	-1.276	3.7E-04	1.0E-02	4.2E-03	ATSPX2, SPX2, SPX domain gene 2
AT2G30540	4.057	-2.1	-2.5	3.3E-05	2.0E-02	3.1E-03	Thioredoxin superfamily protein PHT1;5, PHT5, phosphate
AT2G32830	1.764	-1.865	-1.955	3.4E-03	4.4E-03	1.4E-03	transporter 1;5 ATPT2, PHT1;4, phosphate
AT2G38940	3.369	-1.732	-2.356	0.0E+00	1.0E-04	2.0E-06	transporter 1;4 alpha/beta-Hydrolases superfamily
AT2G42690	2.138	-1.137	-1.749	0.0E+00	2.0E-06	0.0E+00	protein
AT2G45130	4.376	-3.951	-4.425	0.0E+00	0.0E+00	0.0E+00	ATSPX3, SPX3, SPX domain gene 3
AT3G02040	2.697	-1.576	-1.781	0.0E+00	2.7E-04	3.5E-05	SRG3, senescence-related gene 3 VTC4, Inositol monophosphatase
AT3G02870	1.737	-1.263	-1.724	0.0E+00	6.7E-07	0.0E+00	family protein NPC4, non-specific phospholipase
AT3G03530	4.565	-3.272	-3.698	6.5E-05	3.2E-03	5.1E-04	C4 ankyrin repeat family protein / regulator of chromosome condensation (RCC1) family
AT3G03790	1.267	-1.348	-1.409	1.5E-05	2.0E-05	5.0E-06	protein PDLZ2, PLDP2, PLDZETA2,
AT3G05630	3.725	-2.24	-2.429	0.0E+00	2.3E-05	4.0E-06	phospholipase D P2 ATACP5, ATPAP17, PAP17, purple
AT3G17790	2.109	-1.54	-1.619	2.0E-06	1.9E-04	5.0E-05	acid phosphatase 17 alpha/beta-Hydrolases superfamily
AT3G19970	1.683	-1.364	-1.65	4.0E-06	1.0E-04	6.0E-06	protein
AT3G43110	1.915	-1.521	-1.864	2.3E-04	3.9E-03	3.0E-04	unknown protein alpha/beta-Hydrolases superfamily
AT3G44510	1.924	-1.466	-1.632	9.9E-05	2.7E-03	4.8E-04	protein ATPS3, PS3, phosphate starvation-
AT3G47420	1.991	-1.109	-1.723	0.0E+00	3.4E-04	1.0E-06	induced gene 3 PHF1, phosphate transporter
AT3G52190	1.377	-1.308	-1.435	0.0E+00	1.0E-06	0.0E+00	traffic facilitator1 UGP3, UDP-glucose
AT3G56040	2.152	-1.79	-1.908	1.0E-06	1.7E-05	4.0E-06	pyrophosphorylase 3
AT3G61410	1.47	-1.337	-1.487	3.2E-05	2.0E-04	3.0E-05	unknown protein
AT4G00500	1.049	-1.029	-1.021	3.6E-05	1.0E-04	4.9E-05	alpha/beta-Hydrolases superfamily

							protein
AT4G01470	1.91	-1.215	-1.389	6.6E-04	3.5E-02	8.2E-03	ATTIP1.3, GAMMA-TIP3, TIP1;3, tonoplast intrinsic protein 1;3
AT4G13700	2.174	-2.024	-2.051	0.0E+00	1.0E-06	1.0E-06	ATPAP23, PAP23, purple acid phosphatase 23
AT4G14070	1.19	-1.203	-1.098	2.2E-04	4.5E-04	4.7E-04	AAE15, acyl-activating enzyme 15
AT4G17615	1.027	-1.039	-1.365	8.5E-03	1.4E-02	8.6E-04	ATCBL1, CBL1, SCABP5, calcineurin B-like protein 1
AT4G23000	2.783	-2.071	-2.124	0.0E+00	1.0E-06	0.0E+00	Calcineurin-like metallo-phosphoesterase superfamily protein
AT4G24890	1.368	-1.318	-1.326	3.7E-05	1.3E-04	5.3E-05	ATPAP24, PAP24, purple acid phosphatase 24
AT4G25160	2.953	-1.915	-2.13	6.0E-05	6.3E-03	1.3E-03	U-box domain-containing protein kinase family protein
AT4G31240	1.816	-1.301	-1.24	2.0E-06	1.9E-04	1.4E-04	protein kinase C-like zinc finger protein
AT4G33030	2.063	-1.101	-1.373	0.0E+00	1.0E-04	5.0E-06	SQD1, sulfoquinovosyldiacylglycerol 1
AT5G01220	2.693	-2.051	-2.311	0.0E+00	1.0E-06	0.0E+00	SQD2, sulfoquinovosyldiacylglycerol 2
AT5G02200	2.613	-1.465	-1.591	1.2E-05	6.4E-03	1.7E-03	FHL, far-red-elongated hypocotyl1-like
AT5G09570	3.257	-1.706	-1.801	2.0E-06	3.2E-03	9.5E-04	Cox19-like CHCH family protein
AT5G13820	1.563	-1.045	-1.202	1.1E-05	1.5E-03	1.8E-04	ATBP-1, ATBP1, ATTBP1, HPPBF-1, TBP1, telomeric DNA binding protein 1
AT5G17340	5.313	-4.864	-4.806	0.0E+00	1.0E-06	0.0E+00	Putative membrane lipoprotein
AT5G20150	3.385	-1.701	-2.301	2.0E-06	5.0E-03	1.6E-04	ATSPX1, SPX1, SPX domain gene 1
AT5G20410	4.841	-2.711	-3.206	2.0E-06	2.5E-03	2.5E-04	ATMGD2, MGD2, monogalactosyldiacylglycerol synthase 2
AT5G20790	6.892	-3.885	-4.811	1.0E-06	1.1E-03	6.3E-05	unknown protein
AT5G63130	3.13	-2.532	-2.355	2.0E-06	6.3E-05	4.8E-05	Octicosapeptide/Phox/Bem1p family protein
AT5G67080	3.456	-2.432	-2.87	1.4E-05	1.2E-03	1.1E-04	MAPKKK19, mitogen-activated protein kinase kinase kinase 19
AT3G04530	1.134	-0.998	-1.06	4.8E-03	2.1E-02	7.4E-03	ATPPCK2, PEPCK2, PPK2, phosphoenolpyruvate carboxylase kinase 2
AT3G09560	1.062	-0.916	-1.097	6.5E-05	6.1E-04	4.6E-05	ATPAH1, PAH1, Lipin family protein
AT4G03960	2.289	-1.171	-1.383	6.4E-04	9.8E-02	2.7E-02	Phosphotyrosine protein phosphatases superfamily protein
AT4G21470	1.806	-1	-1.072	0.0E+00	4.9E-04	1.2E-04	Calcium-dependent lipid-binding (CaLB domain) family protein
AT5G51050	1.223	-0.884	-1.074	2.0E-06	2.0E-04	1.2E-05	ATFMN/FHY, FMN/FHY, riboflavin kinase/FMN hydrolase

7.3 Discussion

Microarray analyses have been applied to examine the transcriptomic changes in many biological processes. The global view of gene expression helps scientists to understand more complicated gene networks in plants. This high-throughput technique has been employed to assess gene expression responses during Pi starvation in a few studies (Hammond *et al.*, 2003; Wu *et al.*, 2003; Misson *et al.*, 2005; Muller *et al.*, 2006; Morcuende *et al.*, 2007; Lin *et al.*, 2011; Woo *et al.*, 2012; Thibaud *et al.*, 2010). Their results led to the identification of many Pi starvation responsive genes, which help to define the Pi signalling pathway. Particularly in the study by Bari *et al.*, the microarray analysis was applied to examine the transcriptomic differences between the *pho2* mutant and wild type plants (Bari *et al.* 2006). Their results showed that the expression of a few Pi-starvation-responsive genes changed in +Pi grown *pho2* plants compared to wild type plants, indicating that part of the Pi-starvation signalling network remains activated in the *pho2* mutant under Pi-replete condition. Further studies revealed the signalling network involving *PHO2*, miR399 and *PHR1*. Therefore, the *pho2* microarray dataset became even more interesting as it could help to distinguish between the genes affected by the *PHO2* signalling pathway and other Pi-signalling pathways.

Intriguingly, comparison across the datasets from different experiments revealed surprisingly limited agreement. The difference could mainly be attributed to differences in the experimental approaches used in each study. For example, Misson *et al.* examined gene expression changes in both roots and shoots during short (3~12 hr), medium (1~2 day) and long-term Pi starvation (Misson *et al.*, 2005), while Muller *et al.* only focused on shoots during 7-day Pi starvation (Muller *et al.*, 2006). The growth of plants was also different between these experiments. Misson *et al.* grew seedlings in liquid media, while Muller *et al.* grew seedlings in soil and transferred plants to rockwool cubes for Pi starvation treatment. Due to these differences, it is not surprising that the datasets generated in each study share only little similarity. Therefore, to facilitate our research work, we performed our own microarray analysis to examine the gene expression

response to Pi starvation and recovery under our experimental conditions, and generate a robust list of rapid responsive marker genes.

In our experimental design, we focused on the evaluation of gene expression responses in *Arabidopsis* roots during Pi starvation, and more importantly, during the rapid Pi recovery process within 4 hours. Our data showed that a total of 446 genes were regulated by 7-day Pi starvation with fold change ≥ 2 and p-value < 0.05 . During Pi recovery, 253 genes exhibited up- or down-regulation in 2 hours compared to their expression under Pi starvation. This number increased to 419 in 4 hours. Among 446 Pi starvation responsive genes, the expression of 221 genes was reversed during Pi recovery, indicating that they respond more specifically to the Pi signal.

As discussed above, the regulated genes identified from microarray analysis could be largely affected by the experimental conditions. However, the commonly shared genes in different experiments are likely to constitute the core response to Pi signalling. Therefore, we compared our dataset with two other datasets from different research groups in order to generate a robust list of rapid response marker genes. These two datasets were included in our comparison because of their similar experimental design as ours. Our comparison analysis showed that 77 induced genes commonly appeared in all three datasets during long-term Pi starvation, indicating they were Pi starvation-inducible irrespective of the environmental effect. In contrast, only 1 overlapping gene is repressed in all three experiments. Together, these data indicates that the Pi starvation inducible genes are more specific to Pi signal.

For Pi recovery, we compared our dataset with the one from Woo *et al.*. In this comparison, we divided the regulated genes into 2 categories: Pi starvation induced and Pi starvation repressed genes. Our comparison identified 79 shared Pi starvation-induced genes, which showed a rapid suppression during Pi recovery. Only 14 genes were shared with the opposite expression pattern during Pi starvation and recovery. This supported our view that Pi starvation-inducible genes were more specific to Pi signal. Therefore, we only consider these 79 genes as the candidates of rapid response marker genes. After comparison with the 77 robust Pi starvation inducible genes, 63 out of 79 reversible

genes left, which consist of our robust marker genes with rapid response to Pi signal. GO enrichment analysis indicates the existence of several over-represented gene families, including acid phosphatase family, ion transporter family and SPX domain family. Further studies on these marker genes could help to dissect the early events in Pi sensing and define the early Pi signalling pathway.

8. Summary and Discussion

Phosphate starvation responses have been studied for many years. However, the early Pi starvation signalling pathway has not yet been elucidated. Previous studies in our group allowed us to propose the existence of a labile repressor that controlled *Pht1;1* expression during immediate-early Pi starvation (*Fig. 1.3, Fig1.4 & Fig.1.5*). Our evidence indicated that stability of the repressor was dependent on Pi availability. During Pi starvation, it rapidly became susceptible to protein degradation by proteasome-dependent pathways. Rapid turnover of the repressor and its function in controlling downstream gene expression suggested that it would be an important component of early Pi starvation signalling pathway(s).

In this project, we initially focused on the isolation of the labile repressor by applying two strategies. First, we tried to locate the putative labile repressor binding region in the *Pht1;1* promoter, which could then serve as a probe in Yeast-One-Hybrid assays, for example, to isolate the cognate transcription factor. Initially, EMSA was performed using DNA fragments from different regions of the *Pht1;1* promoter as probes, together with protein extracts from *Arabidopsis* suspension cells or young seedling roots. Only a weak binding activity was observed between the *Pht1;1* promoter and unknown protein(s) (*Fig. 3.9, Fig. 3.10 & Fig. 3.11*). As the observed protein-DNA binding activity is labile and appears to be transient, it is hard to conclude whether the observed binding results from the activity of the proposed labile repressor. Overall, our results indicated that the observed protein-DNA binding activity is too weak to be reproducibly detected by the EMSA technique. Although EMSA is highly sensitive, it also has limitations, such as the dissociation of protein-DNA complexes during electrophoresis. Meanwhile, the binding site detected by EMSA may not play the expected function in plants. For example, Mukatira *et al.* identified two regions in the promoter of *Pht1;4*, which could be bound by unknown protein(s) under Pi sufficient conditions. The binding activity disappeared in Pi deficient condition, which suggested that the *Pht1;4* was under negative regulation during Pi starvation (Mukatira *et al.*, 2001). However, promoter deletion analysis from Karthikeyan *et al.* showed that deletion of the two negative

factor-binding regions did not affect the expression of *Pht1;4* under both high and low Pi conditions (Karthikeyan *et al.*, 2009). Therefore, caution must be taken in this type of analysis. To isolate the labile repressor binding site, alternative techniques should be tested in future work, such as *in vivo* foot-printing assays, which would not only detect binding activity under *in vivo* conditions, but also directly determine the protein-binding site. Once the binding region is determined, its role in regulation of *Pht1;1* expression must be confirmed, such as by promoter deletion analysis, before use as probe in Yeast-One-Hybrid experiments.

In a second approach, we identified ZAT18 as a candidate for the proposed labile repressor based on two features. First, ZAT18 has an EAR motif in its protein sequence, which is a strong repression domain in many plant species. Second, the expression of ZAT18 is induced by Pi starvation treatment according to an analysis by microarray (Misson *et al.*, 2005). However, our results indicated that it was relatively stable at the protein level during early Pi starvation (*Fig. 6.2*), which suggests it would not be the labile repressor involved in immediate-early Pi starvation responses. Even though, it is still possible that ZAT18 plays a role in Pi starvation responses, as it is induced at both the translational and transcriptional level during long-term Pi starvation treatments (*Fig. 6.2 & Fig. 6.3*). As ZAT18 possesses an EAR motif, it is likely that it plays a function as a transcription repressor. Previous studies have shown that a few members of ZAT TF family with EAR domain act as transcription repressor in plant response to abiotic stresses, such as ZAT10 (Ohta *et al.*, 2001; Mittler *et al.*, 2006), ZAT11 (Ohta *et al.*, 2001), and ZAT12 (Vogel *et al.*, 2005; Davletova *et al.*, 2005). In plant signalling pathways, it is not unusual that several repressor proteins work together to control target gene expression. For example, *FLOWERING LOCUS C (FLC)* is major transcription repressor in floral signalling pathway in *Arabidopsis* (Michaels and Amasino, 1999; Sheldon *et al.*, 1999). The expression of FLC could delay the flowering by suppression of three flowering genes, *SUPPRESSOR OF OVEREXPRESSON OF CONSTANS 1 (SOC1)*, *FLOWERING LOCUS D (FD)* and *FLOWERING LOCUS T (FT)* (Searle *et al.*, 2006; Helliwell *et al.*, 2006). Notably, the expression of *FLC* is negatively regulated by *FLOWERING LOCUS D (FLD)* and vernalization (He *et al.*, 2003). Moreover, a

previous study has shown that ZAT6 played a role in plant responses to Pi starvation by controlling root development (Devaiah *et al.*, 2007b). Overexpression of *Zat6* led to repression of several Pi starvation responsive genes, such as *At4* and *Phl1;1*. As a close family member, it is possible that ZAT18 would be involved in late stage of Pi response. Further characterization is needed to reveal the function of ZAT18 in plant responses to Pi starvation.

To consolidate the hypothesis of a labile repressor, we repeated a few key experiments, whose results were previously used to set up the regulatory model. Our experiments with *Arabidopsis* suspension cells suggested that the gene regulatory network might vary in different cell culture lines. As the previous cell culture line used in the experiments in the lab died, we tried to test the responses of several new cell culture lines during early Pi starvation. However, none of them behaved as the previous one, based on analysis of the expression kinetics of marker genes during early Pi starvation (*Fig. 4.3, Fig.4.4 & Fig. 4.8*). This indicated large variations in gene regulation between cell culture lines. A recent study has also shown that DNA mutation rates are strongly elevated during clonal regeneration (Jiang *et al.*, 2011). The mutation frequencies increased in proportion to the duration during which cells are maintained in tissue culture. Moreover, epigenetic modification, especially DNA methylation, is also frequently induced during plant cell cultures of many plant species (Wang and Wang, 2012; Miguel and Marum, 2011; Berdasco *et al.*, 2008; Tanurdzic *et al.*, 2008; Guo *et al.*, 2007). It is likely that the suspension cell culture we used was susceptible to such mutations and epigenetic modifications, and that genetic alterations gradually accumulated during sub-culture cycles, which could result in changes of gene regulatory networks.

We also examined *Phl1;1* expression kinetics in *Arabidopsis* young seedlings during early Pi starvation. To avoid the drawbacks of transferring seedlings grown in agar-based media (e.g. physical injuries), we grew the seedlings in a hydroponic system that allowed rapid media switching. To apply the treatment, growth media were refreshed with either Pi-free media for starvation treatments, or full-nutrient media as a control. Surprisingly, *Phl1;1* exhibited a transient up regulation irrespective of Pi presence (*Fig.*

4.11 and Fig. 4.12). According to our previous data (Fig. 1.5), it was expected that *Pht1;1* would be transiently induced after the seedlings were subjected to Pi starvation treatments. However, a similar response appeared in the control experiment, which suggested that *Pht1;1* was not specifically responding to Pi starvation under our experimental conditions.

As a high affinity Pi transporter, *Pht1;1* has only been reported to respond to Pi-related stresses (Muchhal *et al.*, 1996; Mudge *et al.*, 2003; Koyama *et al.*, 2005; Bari *et al.*, 2006). However, our results suggested that the expression of *Pht1;1* was also affected by other factors hidden in our experimental condition. To identify the potential factors, we first examined the composition of media used in our experiments by ICP analysis. In the experiment with *Arabidopsis* seedlings, we used the customized commercial medium mixture (MS basal salt without Pi) from Duchefa Company to ensure the consistence between individual experiments. In general, the media for plant pre-growth and Pi starvation were identical except the different Pi concentration. However, the media used for these experiments was not buffered with MES, thus fresh media is likely to have a different pH than spent growth media. Changes to external pH are likely to have a significant effect on proton ATPase activity, which are likely to affect cellular metabolism and ion transport. It remains to be investigated whether this can explain the transient variations in *Pht1;1* expression that were observed in the experiments.

In my study, I investigated the regulatory roles of different regions of *Pht1;1* promoter. The result indicated that the promoter sequence from -1898 to -932 upstream of the translation start site may contain important *cis*-element(s) in charge of inducibility of *Pht1;1* during Pi starvation (Fig. 5.4). Detailed deletion analysis in this region is needed to identify the regulatory motifs in future work. Interestingly, we also found that the intron in the 5'UTR region regulated *Pht1;1* expression in the young parts of roots in high Pi conditions. Deletion of the intron results in loss of *Pht1;1* expression at the boundary between primary and lateral roots under Pi sufficient conditions (Fig. 5.5). The functioning of introns in regulating gene expression has previously been identified (Callis *et al.*, 1987; Vasil *et al.*, 1989; Maas *et al.*, 1991). While intron could have both

positive and negative roles in regulation of gene expression, most of introns are reported to be generally required for abundant expression in plants (Callis *et al.*, 1987; Rose, 2002). Early studies demonstrated that the intron-containing gene could have more than 10-fold higher expression than the identical construct without intron (Maas *et al.*, 1991; Zhang *et al.*, 1994). The increase in expression caused by intron has been termed as Intron-Mediated Enhancement (IME) (Mascarenhas *et al.*, 1990). In 2009, Karthikeyan *et al.* reported the 5'UTR intron of *Pht1;4* could enhance its expression by 2.5 fold in *Arabidopsis*. Removal of the intron from the promoter could completely suppress the expression of *Pht1;4* in the root tip, which is similar to what we observed with the regulation of *Pht1;1*. These data suggested a role of this intron in controlling organ-specific expression. Similar intron-mediated regulation has been reported in earlier work. For example, *cis*-elements located in second intron of *AGAMOUS* gene were necessary for its normal expression in the centre of flowers during floral development (Lohmann *et al.*, 2001). To identify the *cis*-element(s) in controlling the spatial-temporal expression of *Pht1;1*, further investigation is still needed with more detailed deletion analysis.

To dissect the early Pi signalling pathways, robust marker genes are necessary to reveal the gene regulation networks. Therefore, we designed a microarray assay to gain insight into gene expression at the transcriptomic level during Pi starvation and rapid recovery. Our analysis demonstrates that more genes are induced rather than repressed during Pi starvation, which is consistent with previous observations (Misson *et al.*, 2005; Thibaud *et al.*, 2010; Lin *et al.*, 2011; Woo *et al.*, 2012). Interestingly, our comparison across different datasets strongly indicates that Pi starvation-induced genes are more specific to Pi signals than Pi starvation repressed genes (*Fig. 7.3*). A total of 77 genes appear in all datasets we compared, and thus considered as the core set of marker genes in late stage of Pi starvation responses. Another interesting observation is that the expression of most Pi starvation responsive genes is reversed by Pi recovery within 4 hours (*Fig. 7.2*). A literature search indicates that only one published microarray analysis included the Pi recovery treatment (Woo *et al.*, 2012). Through comparison with their data, 79 overlapping genes are isolated. Among them, 63 genes show up as the Pi specific responsive genes. Therefore, these genes are considered as robust rapid responsive

marker genes to Pi signals (*Table. 7.5*). Among these marker genes, several gene families are over-represented, including members of the acid phosphatase family, ion transporter family and SPX domain family. In this gene list, a few classic Pi responsive genes are present, such as *Pht1;4*, *Pht1;8*, *Pht1;9*, *MGD3*, *SQD1*, *SQD2*, *SPX3*. However, we also notice that several classic marker genes are lost, such as *IPS1*, *At4*, *RNS1*, which suggest that their response to Pi signal are not as specific as previous studies suggested. In the future work, the expression of a selection of these marker genes should be tested by other techniques, such as qPCR or Northern blot, to confirm their response to Pi signal. We expect that more regulatory components will be identified by further studies of these Pi responsive marker genes, and the early Pi signalling pathway will be clearer in the near future.

9. References

- Adams, M.A., Bell, T.L. and Pate, J.S.** (2002) Phosphorus sources and availability modify growth and distribution of root clusters and nodules of native Australian legumes. *Plant Cell Environ*, **25**, 837–850
- Aung, K., Lin, S.-I., Wu, C.-C., Huang, Y.-T., Su, C.-L. and Chiou, T.-J.** (2006) *pho2*, a phosphate overaccumulator, is caused by a nonsense mutation in a microRNA399 target gene. *Plant Physiol*, **141**, 1000–1011.
- Awai, K., Maréchal, E., Block, M.A., Brun, D., Masuda, T., Shimada, H., Takamiya, K., Ohta, H. and Joyard, J.** (2001) Two types of MGDG synthase genes, found widely in both 16:3 and 18:3 plants, differentially mediate galactolipid syntheses in photosynthetic and nonphotosynthetic tissues in *Arabidopsis thaliana*. *Proc. Natl. Acad. Sci. U.S.A.*, **98**, 10960–10965.
- Bari, R., Datt Pant, B., Stitt, M. and Scheible, W.-R.** (2006) *PHO2*, microRNA399, and *PHR1* define a phosphate-signaling pathway in plants. *Plant Physiol.*, **141**, 988–999.
- Bates, T.R. and Lynch, J.P.** (1996) Stimulation of root hair elongation in *Arabidopsis thaliana* by low phosphorus availability. *Plant Cell Environ.* **19**, 529–538.
- Berdasco, M., Alcázar, R., García-Ortiz, M.V., Ballestar E., Fernández A.F., Roldán-Arjona T., Tiburcio A.F., Altabella T., Buisine N., Quesneville H., Baudry A., Lepiniec L., Alaminos M., Rodríguez R., Lloyd A., Colot V., Bender J., Canal M.J., Esteller M., Fraga M.F.** (2008) Promoter DNA Hypermethylation and Gene Repression in Undifferentiated *Arabidopsis* Cells. *PLoS ONE*, **3**, e3306.
- Bieleski, R.L.** (1973) Phosphate pools, phosphate transport, and phosphate availability. *Annu. Rev. Plant Physiol.*, **24**, 225–252.
- Bolan, N.S.** (1991) A critical review on the role of mycorrhizal fungi in the uptake of phosphorus by plants. *Plant Soil*, **134**, 189–207.
- Bonser, A.M., Lynch, J. and Snapp, S.** (1996) Effect of phosphorus deficiency on growth angle of basal roots in *Phaseolus vulgaris*. *New Phytol.*, **132**, 281–288.
- Burleigh, S.H. and Harrison, M.J.** (1997) A novel gene whose expression in *Medicago truncatula* roots is suppressed in response to colonization by vesicular-arbuscular mycorrhizal (VAM) fungi and to phosphate nutrition. *Plant Mol. Biol.*, **34**, 199–208.
- Burleigh, S.H. and Harrison, M.J.** (1998) The down-regulation of Mt4-like genes by phosphate fertilization occurs systemically and involves phosphate translocation to the shoots. *Plant Physiol.*, **119**, 241–248.

- Burleigh, S.M. and Harrison, M.J.** (1998) Characterization of the Mt4 gene from *Medicago truncatula*. *Gene*, **216**, 47–53.
- Callis, J., Fromm, M. and Walbot, V.** (1987) Introns increase gene expression in cultured maize cells. *Genes & Dev.*, **1**, 1183–1200.
- Chen, Y.-F., Li, L.-Q., Xu, Q., Kong, Y.-H., Wang, H. and Wu, W.-H.** (2009) The WRKY6 transcription factor modulates PHOSPHATE1 expression in response to low Pi stress in Arabidopsis. *The Plant Cell*, **21**, 3554–3566.
- Chen, Z.-H., Nimmo, G.A., Jenkins, G.I. and Nimmo, H.G.** (2007) BHLH32 modulates several biochemical and morphological processes that respond to Pi starvation in Arabidopsis. *Biochem. J.*, **405**, 191–198.
- Chiou, T.-J. and Lin, S.-I.** (2011) Signaling network in sensing phosphate availability in plants. *Annu. Rev. Plant Biol.*, **62**, 185–206.
- Ciftci-Yilmaz, S. and Mittler, R.** (2008) The zinc finger network of plants. *Cell. Mol. Life Sci.*, **65**, 1150–1160.
- Ciftci-Yilmaz, S., Morsy, M.R., Song, L., Coutu A., Krizek B.A., Lewis M.W., Warren D., Cushman J., Connolly E.L., Mittler R.** (2007) The EAR-motif of the Cys2/His2-type Zinc Finger Protein Zat7 Plays a Key Role in the Defense Response of Arabidopsis to Salinity Stress. *Journal of Biological Chemistry*, **282**, 9260–9268.
- Curie, C., Liboz, T., Montané, M.H., Rouan, D., Axelos, M. and Lescure, B.** (1992) The activation process of Arabidopsis thaliana A1 gene encoding the translation elongation factor EF-1 alpha is conserved among angiosperms. *Plant Mol. Biol.*, **18**, 1083–1089.
- Daram, P., Brunner, S., Persson, B.L., Amrhein, N. and Bucher, M.** (1998) Functional analysis and cell-specific expression of a phosphate transporter from tomato. *Planta*, **206**, 225–233.
- Daram, P., Brunner, S., Rausch, C., Steiner, C., Amrhein, N. and Bucher, M.** (1999) Pht2;1 encodes a low-affinity phosphate transporter from Arabidopsis. *The Plant Cell*, **11**, 2153–2166.
- Davletova, S., Schlauch, K., Coutu, J. and Mittler, R.** (2005) The zinc-finger protein Zat12 plays a central role in reactive oxygen and abiotic stress signaling in Arabidopsis. *Plant Physiol.*, **139**, 847–856.
- del Pozo, J.C., Allona, I., Rubio, V., Leyva, A., la Pena, de, A., Aragoncillo, C. and Paz-Ares, J.** (1999) A type 5 acid phosphatase gene from Arabidopsis thaliana is induced by phosphate starvation and by some other types of phosphate mobilising/oxidative stress conditions. *Plant J*, **19**, 579–589.

- Delhaize, E. and Randall, P.J.** (1995) Characterization of a Phosphate-Accumulator Mutant of *Arabidopsis thaliana*. *Plant Physiol.*, **107**, 207–213.
- Devaiah, B.N., Karthikeyan, A.S. and Raghothama, K.G.** (2007a) WRKY75 transcription factor is a modulator of phosphate acquisition and root development in *Arabidopsis*. *Plant Physiol.*, **143**, 1789–1801.
- Devaiah, B.N., Nagarajan, V.K. and Raghothama, K.G.** (2007b) Phosphate homeostasis and root development in *Arabidopsis* are synchronized by the zinc finger transcription factor ZAT6. *Plant Physiol.*, **145**, 147–159.
- Dong, B., Rengel, Z. and Delhaize, E.** (1998) Uptake and translocation of phosphate by pho2 mutant and wild-type seedlings of *Arabidopsis thaliana*. *Planta*, **205**, 251–256.
- Duan, K., Yi, K., Dang, L., Huang, H., Wu, W. and Wu, P.** (2008) Characterization of a sub-family of *Arabidopsis* genes with the SPX domain reveals their diverse functions in plant tolerance to phosphorus starvation. *Plant J*, **54**, 965–975.
- Englbrecht, C.C., Schoof, H. and Böhm, S.** (2004) Conservation, diversification and expansion of C2H2 zinc finger proteins in the *Arabidopsis thaliana* genome. *BMC Genomics*, **5**, 39.
- Essigmann, B., Güler, S., Narang, R.A., Linke, D. and Benning, C.** (1998) Phosphate availability affects the thylakoid lipid composition and the expression of SQD1, a gene required for sulfolipid biosynthesis in *Arabidopsis thaliana*. *Proc. Natl. Acad. Sci. U.S.A.*, **95**, 1950–1955.
- Franco-Zorrilla, J.M.** (2004) The transcriptional control of plant responses to phosphate limitation. *Journal of Experimental Botany*, **55**, 285–293.
- Franco-Zorrilla, J.M., Valli, A., Todesco, M., et al.** (2007) Target mimicry provides a new mechanism for regulation of microRNA activity. *Nat Genet*, **39**, 1033–1037.
- Fujii, H., Chiou, T., Lin, S., Aung, K. and Zhu, J.** (2005) A miRNA involved in phosphate-starvation response in *Arabidopsis*. *Current Biology*, **15**, 2038–2043.
- Gazzarrini, S. and McCourt, P.** (2003) Cross-talk in Plant Hormone Signalling: What *Arabidopsis* Mutants Are Telling Us. *Annals of Botany*.
- Gilroy, S. and Jones, D.L.** (2000) Through form to function: root hair development and nutrient uptake. *Trends in Plant Science*, **5**, 56–60.
- Gojon, A., Nacry, P. and Davidian, J.-C.** (2009) Root uptake regulation: a central process for NPS homeostasis in plants. *Curr. Opin. Plant Biol.*, **12**, 328–338.
- Guo, B., Jin, Y., Wussler, C., Blancaflor, E.B., Motes, C.M. and Versaw, W.K.**

- (2008) Functional analysis of the Arabidopsis PHT4 family of intracellular phosphate transporters. *New Phytologist*, **177**, 889–898.
- Guo, W.L., Wu, R., Zhang, Y.F., Liu, X.M., Wang, H.Y., Gong, L., Zhang, Z.H. and Liu, B.** (2007) Tissue culture-induced locus-specific alteration in DNA methylation and its correlation with genetic variation in *Codonopsis lanceolata* Benth. et Hook. f. *Plant Cell Rep*, **26**, 1297–1307.
- Hamburger, D.** (2002) Identification and Characterization of the Arabidopsis PHO1 Gene Involved in Phosphate Loading to the Xylem. *The Plant Cell*, **14**, 889–902.
- Hammond J. P., Bennett M. J., Bowen H. C., Broadley M.R., Eastwood D. C., May S. T., Rahn C., Swarup R., Woolaway K. E., and White P. J.** (2003) Changes in Gene Expression in Arabidopsis Shoots during Phosphate Starvation and the Potential for Developing Smart Plants. *Plant Physiol.*, **132**, 578–596.
- Haran, S., Logendra, S., Seskar, M., Bratanova, M. and Raskin, I.** (2000) Characterization of Arabidopsis acid phosphatase promoter and regulation of acid phosphatase expression. *Plant Physiol.*, **124**, 615–626.
- He, Y., Michaels, S.D. and Amasino, R.M.** (2003) Regulation of flowering time by histone acetylation in Arabidopsis. *Science*, **302**, 1751–1754.
- Helliwell, C.A., Wood, C.C., Robertson, M., James Peacock, W. and Dennis, E.S.** (2006) The Arabidopsis FLC protein interacts directly in vivo with SOC1 and FT chromatin and is part of a high-molecular-weight protein complex. *Plant J*, **46**, 183–192.
- Hiratsu, K., Matsui, K., Koyama, T. and Ohme-Takagi, M.** (2003) Dominant repression of target genes by chimeric repressors that include the EAR motif, a repression domain, in Arabidopsis. *Plant J*, **34**, 733–739.
- Hsieh, L.C., Lin, S.-I., Shih, A.C.C., Chen, J.W., Lin, W.-Y., Tseng, C.Y., Li, W.H. and Chiou, T.-J.** (2009) Uncovering Small RNA-Mediated Responses to Phosphate Deficiency in Arabidopsis by Deep Sequencing. *Plant Physiol.*, **151**, 2120–2132.
- Hudson, J.M., Crowe, M. and Fried, M.G.** (1993) Effects of anions on the binding of the cAMP receptor protein to the lactose promoter. *Eur. J. Biochem.*, **212**, 539–548.
- Jiang, C., Mithani, A., Gan, X., Belfield, E.J., Klingler, J.P., Zhu, J.-K., Ragoussis, J., Mott, R. and Harberd, N.P.** (2011) Regenerant Arabidopsis Lineages Display a Distinct Genome-Wide Spectrum of Mutations Conferring Variant Phenotypes. *Current Biology*, **21**, 1385–1390.
- Johnson, J.F., Vance, C.P. and Allan, D.L.** (1996) Phosphorus deficiency in *Lupinus albus*. Altered lateral root development and enhanced expression of

- phosphoenolpyruvate carboxylase. *Plant Physiol.*, **112**, 31–41.
- Kagale, S., Links, M.G. and Rozwadowski, K.** (2010) Genome-Wide Analysis of Ethylene-Responsive Element Binding Factor-Associated Amphiphilic Repression Motif-Containing Transcriptional Regulators in Arabidopsis. *Plant Physiol.*, **152**, 1109–1134.
- Kai, M., Masuda, Y., Kikuchi, Y., Osaki, M. and Tadano, T.** (1997) Isolation and characterization of a cDNA from *Catharanthus roseus* which is highly homologous with phosphate transporter. *Soil Science and Plant Nutrition*, **43**, 227–235.
- Karthikeyan, A.S., Ballachanda, D.N. and Raghothama, K.G.** (2009) Promoter deletion analysis elucidates the role of cis elements and 5'UTR intron in spatiotemporal regulation of AtPht1;4 expression in Arabidopsis. *Physiol Plantarum*, **136**, 10–18.
- Keerthisinghe, G., Hocking, P.J., Ryan, P.R. and Delhaize, E.** (1998) Effect of phosphorus supply on the formation and function of proteoid roots of white lupin (*Lupinus albus* L.). *Plant Cell Environ*, **21**, 467–478.
- Kobayashi, K., Awai, K., Takamiya, K.-I. and Ohta, H.** (2004) Arabidopsis type B monogalactosyldiacylglycerol synthase genes are expressed during pollen tube growth and induced by phosphate starvation. *Plant Physiol.*, **134**, 640–648.
- Koyama, T., Ono, T., Shimizu, M., et al.** (2005) Promoter of Arabidopsis thaliana phosphate transporter gene drives root-specific expression of transgene in rice. *J. Biosci. Bioeng.*, **99**, 38–42.
- Lai, F., Thacker, J., Li, Y. and Doerner, P.** (2007) Cell division activity determines the magnitude of phosphate starvation responses in Arabidopsis. *Plant J*, **50**, 545–556.
- Leggewie, G., Willmitzer, L. and Riesmeier, J.W.** (1997) Two cDNAs from potato are able to complement a phosphate uptake-deficient yeast mutant: identification of phosphate transporters from higher plants. *The Plant Cell*, **9**, 381–392.
- Lenburg, M.E. and O'Shea, E.K.** (1996) Signaling phosphate starvation. *Trends Biochem. Sci.*, **21**, 383–387.
- Lin, W.-D., Liao, Y.-Y., Yang, T.J.W., Pan, C.-Y., Buckhout, T.J. and Schmidt, W.** (2011) Coexpression-based clustering of Arabidopsis root genes predicts functional modules in early phosphate deficiency signaling. *Plant Physiol.*, **155**, 1383–1402.
- Linkohr, B.I., Williamson, L.C., Fitter, A.H. and Leyser, H.M.O.** (2002) Nitrate and phosphate availability and distribution have different effects on root system architecture of Arabidopsis. *Plant J*, **29**, 751–760.

- Liu, C., Muchhal, U.S. and Raghothama, K.G.** (1997) Differential expression of TPS11, a phosphate starvation-induced gene in tomato. *Plant Mol. Biol.*, **33**, 867–874.
- Liu, H., Trieu, A.T. and Blaylock, L.A.** (1998) Cloning and characterization of two phosphate transporters from *Medicago truncatula* roots: regulation in response to phosphate and to colonization by arbuscular mycorrhizal (AM) fungi. *Mol Plant Microbe Interact.* **11**, 14–22.
- Liu, T.-Y., Huang, T.-K., Tseng, C.-Y., Lai, Y.-S., Lin, S.-I., Lin, W.-Y., Chen, J.-W. and Chiou, T.-J.** (2012) PHO2-Dependent Degradation of PHO1 Modulates Phosphate Homeostasis in Arabidopsis. *The Plant Cell*.
- Lohmann, J.U., Hong, R.L., Hobe, M., Busch, M.A., Parcy, F., Simon, R. and Weigel, D.** (2001) A molecular link between stem cell regulation and floral patterning in Arabidopsis. *Cell*, **105**, 793–803.
- Louis, I., Racette, S. and Torrey, J.G.** (1990) Occurrence of cluster roots on *Myrica cerifera* L. (Myricaceae) in water culture in relation to phosphorus nutrition. *New Phytologist*, **115**, 311–317.
- Lynch, J.** (1995) Root Architecture and Plant Productivity. *Plant Physiol.*, **109**, 7–13.
- Lynch, J.P., Ho, M.D. and phosphorus, L.** (2005) Rhizoeconomics: Carbon costs of phosphorus acquisition. *Plant Soil*, **269**, 45–56.
- Maas, C., Laufs, J., Grant, S., Korfhage, C. and Werr, W.** (1991) The combination of a novel stimulatory element in the first exon of the maize Shrunken-1 gene with the following intron 1 enhances reporter gene expression up to 1000-fold. *Plant Mol. Biol.*, **16**, 199–207.
- Martín, A.C., del Pozo, J.C., Iglesias, J., Rubio, V., Solano, R., La Peña, de, A., Leyva, A. and Paz-Ares, J.** (2000) Influence of cytokinins on the expression of phosphate starvation responsive genes in Arabidopsis. *Plant J*, **24**, 559–567.
- Marschner, H.** (1995) Mineral Nutrition of Higher Plants, 2nd edn. London: Academic Press.
- Mascarenhas, D., Mettler, I.J., Pierce, D.A. and Lowe, H.W.** (1990) Intron-mediated enhancement of heterologous gene expression in maize. *Plant Mol. Biol.*, **15**, 913–920.
- Michaels, S.D. and Amasino, R.M.** (1999) FLOWERING LOCUS C encodes a novel MADS domain protein that acts as a repressor of flowering. *The Plant Cell*, **11**, 949–956.

- Miguel, C. and Marum, L.** (2011) An epigenetic view of plant cells cultured in vitro: somaclonal variation and beyond. *Journal of Experimental Botany*, **62**, 3713–3725.
- Miller, J., McLachlan, A.D. and Klug, A.** (1985) Repetitive zinc-binding domains in the protein transcription factor IIIA from *Xenopus* oocytes. *EMBO J.*, **4**, 1609–1614.
- Misson, J., Raghothama, K. and Jain, A.** (2005) A genome-wide transcriptional analysis using *Arabidopsis thaliana* Affymetrix gene chips determined plant responses to phosphate deprivation. *Proc. Natl. Acad. Sci. U.S.A.*, **102**, 11934–11939.
- Misson, J., Thibaud, M.-C., Bechtold, N., Raghothama, K. and Nussaume, L.** (2004) Transcriptional regulation and functional properties of *Arabidopsis* Pht1;4, a high affinity transporter contributing greatly to phosphate uptake in phosphate deprived plants. *Plant Mol. Biol.*, **55**, 727–741.
- Mitsuda, N. and Ohme-Takagi, M.** (2009) Functional Analysis of Transcription Factors in *Arabidopsis*. *Plant and Cell Physiology*, **50**, 1232–1248.
- Mitsukawa, N., Okumura, S., Shirano, Y., Sato, S., Kato, T., Harashima, S. and Shibata, D.** (1997) Overexpression of an *Arabidopsis thaliana* high-affinity phosphate transporter gene in tobacco cultured cells enhances cell growth under phosphate-limited conditions. *Proc. Natl. Acad. Sci. U.S.A.*, **94**, 7098–7102.
- Mittler, R., Kim, Y., Song, L., Coutu, J., Coutu, A., Ciftci-Yilmaz, S., Lee, H., Stevenson, B. and Zhu, J.-K.** (2006) Gain- and loss-of-function mutations in *Zat10* enhance the tolerance of plants to abiotic stress. *FEBS letters*, **580**, 6537–6542.
- Miura, K., Rus, A., Sharkhuu, A., Yokoi S., Kathikeyan A.S., Raghothama K.G., Baek D., Koo Y.D., Jin J.B., Bressan R.A., Yun D.J., Hasegawa P.M.** (2005) The *Arabidopsis* SUMO E3 ligase SIZ1 controls phosphate deficiency responses. *Proc. Natl. Acad. Sci. U.S.A.*, **102**, 7760–7765.
- Morcuende, R., Bari, R., Gibon, Y., et al.** (2007) Genome-wide reprogramming of metabolism and regulatory networks of *Arabidopsis* in response to phosphorus. *Plant Cell Environ.*, **30**, 85–112.
- Muchhal, U.S., Pardo, J.M. and Raghothama, K.G.** (1996) Phosphate transporters from the higher plant *Arabidopsis thaliana*. *Proc. Natl. Acad. Sci. U.S.A.*, **93**, 10519–10523.
- Mudge, S.R., Rae, A.L., Diatloff, E. and Smith, F.W.** (2003) Expression analysis suggests novel roles for members of the Pht1 family of phosphate transporters in *Arabidopsis*. *Plant J.*, **31**, 341–353.
- Mudge, S.R., Smith, F.W. and Richardson, A.E.** (2003) Root-specific and phosphate-regulated expression of phytase under the control of a phosphate transporter

- promoter enables Arabidopsis to grow on phytate as a sole P source. *Plant Science*, **165**, 871–878.
- Mukatira, U.T., Liu, C., Varadarajan, D.K. and Raghothama, K.G.** (2001) Negative Regulation of Phosphate Starvation-Induced Genes. *Plant Physiol.*, **127**, 1854–1862.
- Muller, R., Morant, M., Jarmer, H., Nilsson, L. and Nielsen, T.H.** (2006) Genome-Wide Analysis of the Arabidopsis Leaf Transcriptome Reveals Interaction of Phosphate and Sugar Metabolism. *Plant Physiol.*, **143**, 156–171.
- Murashige, T. and Skoog, F.** (1962) A Revised Medium for Rapid Growth and Bio Assays with Tobacco Tissue Cultures. *Physiol Plant*, **15**, 473–497.
- Nilsson, L., Lundmark, M., Jensen, P.E. and Nielsen, T.H.** (2012) The Arabidopsis transcription factor PHR1 is essential for adaptation to high light and retaining functional photosynthesis during phosphate starvation. *Physiol Plantarum*, **144**, 35–47.
- Nilsson, L., Müller, R. and Nielsen, T.H.** (2007) Increased expression of the MYB-related transcription factor, PHR1, leads to enhanced phosphate uptake in Arabidopsis thaliana. *Plant Cell Environ*, **30**, 1499–1512.
- Ohta, M., Matsui, K., Hiratsu, K., Shinshi, H. and Ohme-Takagi, M.** (2001) Repression domains of class II ERF transcriptional repressors share an essential motif for active repression. *The Plant Cell*, **13**, 1959–1968.
- Ohta, M., Takagi, M.O. and Shinshi, H.** (2001) Three ethylene-responsive transcription factors in tobacco with distinct transactivation functions. *Plant J*, **22**, 29–38.
- Poirier, Y. and Bucher, M.** (2002) Phosphate Transport and Homeostasis in Arabidopsis. *The Arabidopsis Book*, **1**, 1.
- Poirier, Y., Thoma, S., Somerville, C. and Schiefelbein, J.** (1991) Mutant of Arabidopsis deficient in xylem loading of phosphate. *Plant Physiol.*, **97**, 1087–1093.
- Raghothama, K.G.** (1999) PHOSPHATE ACQUISITION. *Annu. Rev. Plant Physiol. Plant Mol. Biol.*, **50**, 665–693.
- Rausch, C., Zimmermann, P., Amrhein, N. and Bucher, M.** (2004) Expression analysis suggests novel roles for the plastidic phosphate transporter Pht2;1 in auto- and heterotrophic tissues in potato and Arabidopsis. *Plant J*, **39**, 13–28.
- Richardson, A.E.** (1994) Soil microorganisms and phosphorus availability. In Soil biota management in sustainable farming systems (Prankhurst, B.D.C.E., Gupta, V.V.S.R. and Grace, P.R., eds). Melbourne: CSIRO, pp. 50–62.

- Rose, A.B.** (2002) Requirements for intron-mediated enhancement of gene expression in Arabidopsis. *RNA*, **8**, 1444–1453.
- Rose, A.B.** (2004) The effect of intron location on intron-mediated enhancement of gene expression in Arabidopsis. *Plant J*, **40**, 744–751.
- Rose, A.B. and Beliakoff, J.A.** (2000) Intron-mediated enhancement of gene expression independent of unique intron sequences and splicing. *Plant Physiol.*, **122**, 535–542.
- Roth, C., Menzel, G., Petétot, J.M.-C., Rochat-Hacker, S. and Poirier, Y.** (2004) Characterization of a protein of the plastid inner envelope having homology to animal inorganic phosphate, chloride and organic-anion transporters. *Planta*, **218**, 406–416.
- Rouached, H.** (2011) Multilevel coordination of phosphate and sulfate homeostasis in plants. *Plant Signal Behav*, **6**, 952–955.
- Rouached, H., Secco, D. and Arpat, B.A.** (2010) Regulation of ion homeostasis in plants: Current approaches and future challenges. *Plant Signal Behav*, **5**.
- Rouached, H., Secco, D., Arpat, B. and Poirier, Y.** (2011) The transcription factor PHR1 plays a key role in the regulation of sulfate shoot-to-root flux upon phosphate starvation in Arabidopsis. *BMC Plant Biol.*, **11**, 19.
- Rubio, V.** (2001) A conserved MYB transcription factor involved in phosphate starvation signaling both in vascular plants and in unicellular algae. *Genes & Development*, **15**, 2122–2133.
- Schneider-Poetsch, T., Ju, J., Eyler, D.E., Dang, Y., Bhat, S., Merrick, W.C., Green, R., Shen, B. and Liu, J.O.** (2010) Inhibition of eukaryotic translation elongation by cycloheximide and lactimidomycin. *Nat Chem Biol*, **6**, 209–217.
- Schunmann, P.H.** (2004) Promoter Analysis of the Barley Pht1;1 Phosphate Transporter Gene Identifies Regions Controlling Root Expression and Responsiveness to Phosphate Deprivation. *Plant Physiol.*, **136**, 4205–4214.
- Searle, I., He, Y., Turck, F., Vincent, C., Fornara, F., Kröber, S., Amasino, R.A. and Coupland, G.** (2006) The transcription factor FLC confers a flowering response to vernalization by repressing meristem competence and systemic signaling in Arabidopsis. *Genes & Development*, **20**, 898–912.
- Sheldon, C.C., Burn, J.E., Perez, P.P., Metzger, J., Edwards, J.A., Peacock, W.J. and Dennis, E.S.** (1999) The FLF MADS box gene: a repressor of flowering in Arabidopsis regulated by vernalization and methylation. *The Plant Cell*, **11**, 445–458.

- Shin, H., Shin, H.-S., Chen, R. and Harrison, M.J.** (2006) Loss of At4function impacts phosphate distribution between the roots and the shoots during phosphate starvation. *Plant J*, **45**, 712–726.
- Shin, H., Shin, H.-S., Dewbre, G.R. and Harrison, M.J.** (2004) Phosphate transport in Arabidopsis: Pht1;1 and Pht1;4 play a major role in phosphate acquisition from both low- and high-phosphate environments. *Plant J*, **39**, 629–642.
- Skene, K.R.** (2000) Pattern Formation in Cluster Roots: Some Developmental and Evolutionary Considerations. *Annals of Botany*, **85**, 901–908
- Smith, S.E., Read, D.J.** (1997) Mycorrhizal Symbiosis. Academic Press, Cambridge
- Smyth, G.K.** (2005) limma: Linear Models for Microarray Data. Statistics for Biology and Health, pp. 397–420.
- Svistoonoff, S., Creff, A., Reymond, M., Sigoillot-Claude, C., Ricaud, L., Blanchet, A., Nussaume, L. and Desnos, T.** (2007) Root tip contact with low-phosphate media reprograms plant root architecture. *Nat Genet*, **39**, 792–796.
- Tadano, T., Ozawa, K., Sakai, H., Osaki, M. and Matsui, H.** (1993) Secretion of acid phosphatase by the roots of crop plants under phosphorus-deficient conditions and some properties of the enzyme secreted by lupin roots. *Plant Soil*, **155-156**, 95–98.
- Tanurdzic, M., Vaughn, M.W., Jiang, H., Lee, T.-J., Slotkin, R.K., Sosinski, B., Thompson, W.F., Doerge, R.W. and Martienssen, R.A.** (2008) Epigenomic Consequences of Immortalized Plant Cell Suspension Culture. *Plos Biol*, **6**, e302.
- Thibaud, M.-C., Arrighi, J.-F., Bayle, V., Chiarenza, S., Creff, A., Bustos, R., Paz-Ares, J., Poirier, Y. and Nussaume, L.** (2010) Dissection of local and systemic transcriptional responses to phosphate starvation in Arabidopsis. *Plant J*, **64**, 775–789.
- Vasil, V., Clancy, M., Ferl, R.J., Vasil, I.K. and Hannah, L.C.** (1989) Increased gene expression by the first intron of maize shrunken-1 locus in grass species. *Plant Physiol.*, **91**, 1575–1579.
- Versaw, W.K.** (2002) A Chloroplast Phosphate Transporter, PHT2;1, Influences Allocation of Phosphate within the Plant and Phosphate-Starvation Responses. *The Plant Cell*, **14**, 1751–1766.
- Vogel, J.T., Zarka, D.G., Van Buskirk, H.A., Fowler, S.G. and Thomashow, M.F.** (2005) Roles of the CBF2 and ZAT12 transcription factors in configuring the low temperature transcriptome of Arabidopsis. *Plant J*, **41**, 195–211.
- Walker D.J., Leigh R.A., Miller A.J.** (1996) Potassium homeostasis in vacuolate plant

cells. *Proc Natl Acad Sci USA* 93: 10510–10514

Wang, Q.-M. and Wang, L. (2012) An evolutionary view of plant tissue culture: somaclonal variation and selection. *Plant Cell Rep*, **31**, 1535–1547.

Wang, Y., Ribot, C., Rezzonico, E. and Poirier, Y. (2004) Structure and expression profile of the Arabidopsis PHO1 gene family indicates a broad role in inorganic phosphate homeostasis. *Plant Physiol.*, **135**, 400–411.

Wasaki, J., Yonetani, R., Shinano, T., Kai, M. and Osaki, M. (2003) Expression of the OsPI1 gene, cloned from rice roots using cDNA microarray, rapidly responds to phosphorus status. *New Phytologist*, **158**, 239–248.

Williamson, L.C., Ribrioux, S.P., Fitter, A.H. and Leyser, H.M. (2001) Phosphate availability regulates root system architecture in Arabidopsis. *Plant Physiol.*, **126**, 875–882.

Woo, J., MacPherson, C.R., Liu, J., Wang, H., Kiba, T., Hannah, M., Wang, X.-J., Bajic, V.B. and Chua, N.-H. (2012) The response and recovery of the Arabidopsis thaliana transcriptome to phosphate starvation. *BMC Plant Biol.*, **12**, 62.

Wu P., Ma L.G., Hou X.L., Wang M.Y., Wu Y.R., Liu F.Y., and Deng X.W. (2003) Phosphate Starvation Triggers Distinct Alterations of Genome Expression in Arabidopsis Roots and Leaves. *Plant Physiol.*, **132**, 1260–1271.

Xiao, K., Liu, J., Dewbre, G., Harrison, M. and Wang, Z.Y. (2006) Isolation and Characterization of Root-Specific Phosphate Transporter Promoters from *Medicago truncatula*. *Plant Biology*, **8**, 439–449.

Xu, G.-H., Chague, V., Melamed-Bessudo, C., Kapulnik, Y., Jain, A., Raghothama, K.G., Levy, A.A. and Silber, A. (2007) Functional characterization of LePT4: a phosphate transporter in tomato with mycorrhiza-enhanced expression. *J. Exp. Bot.*, **58**, 2491–2501

Yu, B., Xu, C. and Benning, C. (2002) Arabidopsis disrupted in SQD2 encoding sulfolipid synthase is impaired in phosphate-limited growth. *Proc. Natl. Acad. Sci. U.S.A.*, **99**, 5732–5737.

Zhang, S.H., Lawton, M.A., Hunter, T. and Lamb, C.J. (1994) atpk1, a novel ribosomal protein kinase gene from Arabidopsis. I. Isolation, characterization, and expression. *J. Biol. Chem.*, **269**, 17586–17592.

List of tables

Table 1.1 Pht1 family in *Arabidopsis*

Table 1.2 Multiple responses of plants to phosphate deficiency

Table 2.1 Full nutrient media for *Arabidopsis* seedling growth

Table 2.2 Pi-free media for starvation treatment with *Arabidopsis* seedlings

Table 2.3 Full nutrient media for *Arabidopsis* suspension cell culture growth

Table 2.4 Pi-free media for starvation treatment with *Arabidopsis* suspension cell culture

Table 2.5 Primer sequences for *Pht1;1* promoter deletion construct

Table 2.6 Primer sequences for amplification of cDNA by Quantitative PCR

Table 4.1 Media composition of Duchefa media and classic MS media.

Table 4.2 ICP results of the commercial 0.5xMS media (Duchefa) and user-made 0.5xMS media.

Table 6.1 The list of genes encoding proteins containing EAR motif

Table 7.1 Number of regulated genes in various comparisons identified by microarray analysis.

Table 7.2 The list of selected Pi starvation induced genes from microarray data.

Table 7.3 The list of selected Pi starvation repressed genes from microarray data.

Table 7.4 Number of regulated genes in different microarray datasets after re-calculation.

Table 7.5 The list of robust rapid Pi responsive marker genes.

List of figures

Fig. 1.1 Phylogenetic analysis of *Arabidopsis* phosphate transporter protein sequences.

Fig. 1.2 Predicted topology of the tomato Pht1;1 (LePT1) Pi transporter (Daram et al., 1998) typical for Pht1;1 proteins

Fig. 1.3 An overview of Pi signalling pathway.

Fig. 1.4. Gene expression kinetics of phosphate abundance-responsive genes in *Arabidopsis* suspension-cultured cells and roots.

Fig. 1.5 Pht1;1 RNA abundance directly responds to changes in cytoplasmic phosphate homeostasis.

Fig. 1.6 Gene expression of phosphate-responsive genes after exposure of *Arabidopsis* cells to cycloheximide (CHX).

Fig. 1.7 Gene expression kinetics after exposure of Pi-deplete cells to protein proteolysis inhibitors.

Fig. 3.1 Map of the different promoter fragments of *Pht1;4* used in EMSA assays.

Fig. 3.2 EMSA using radio-labeled F1;4-2 (a) and F1;4-3 (b) fragments and total protein extracts from *Arabidopsis* roots and suspension cell cultures grown under +Pi conditions.

Fig. 3.3 EMSA using radio-labeled F1;4-3 fragments and total protein extracts from *Arabidopsis* roots and suspension cell cultures grown in +Pi conditions. Shifted bands were indicated by arrowhead.

Fig. 3.4 EMSA using radio-labeled F1;4-3 fragments and total protein extracts from *Arabidopsis* suspension cell cultures grown in +Pi conditions

Fig. 3.5 Map of the different promoter fragments of *Pht1;4* used in EMSA assays.

Fig. 3.6 EMSA using radio-labeled F1;1-1~5 fragments and total protein extract from *Arabidopsis* suspension cell cultures grown under +Pi condition.

Fig. 3.7 EMSA using radio-labeled F1;1-1~F1;1-5 fragments and total protein extract from *Arabidopsis* suspension cell culture from +Pi condition. Smear bands were indicated by arrowhead.

Fig. 3.8 EMSA using radio-labeled F1;1-1-3 (a) or F1;1-4 (b) fragments and total protein extracts from *Arabidopsis* suspension cell cultures grown in +Pi conditions.

Fig. 3.9 EMSA using radio-labeled F1;1-3 (a) or F1;1-4 (b) fragments and total protein extract from *Arabidopsis* suspension cell cultures grown in +Pi conditions.

Fig. 3.10 EMSA using radio-labeled F1;1-3 (a) or F1;1-4 (b) fragments and total protein extract from *Arabidopsis* suspension cell culture grown in +Pi conditions.

Fig. 3.11 EMSA using radio-labeled F1;1-3 fragment and total protein extract from *Arabidopsis* suspension cell cultures grown in +Pi conditions.

Fig. 3.12 EMSA using radio-labeled F1;1-3 fragment and total protein extract from *Arabidopsis* suspension cell culture and roots grown in +Pi conditions.

Fig. 3.13 EMSA using radio-labeled F1;1-3 fragment and total protein extract from *Arabidopsis* suspension cell culture grown in +Pi condition.

Fig. 3.14 EMSA using radio-labeled F1;1-3 (a) and F1;1-4 (b) fragments and total protein extract from *Arabidopsis* suspension cell culture grown in Pi sufficient (+Pi) or Pi deficient (-Pi) conditions.

Fig. 3.15 EMSA using radio-labeled F1;1-3 fragment and total protein extract from *Arabidopsis* suspension cell culture.

Fig. 3.16 Genotyping PCR result with F1;1-2 primers.

Fig. 3.17 Several *Arabidopsis* accessions showing similar genetic variations in the *Pht1;1* promoter sequence as that in Ler accession.

Fig. 4.1 RT-PCR with cDNA from *Arabidopsis* suspension cells and Col-0 roots.

Fig. 4.2 PCR reactions with genomic DNA extracted from new suspension cells (lane 1), Col-0 roots (lane 2), Ler roots (lane 3) and Ler suspension cells (lane 4).

Fig. 4.3 Gene expression kinetics in *Arabidopsis* suspension cell culture after transfer from +Pi media to -Pi media.

Fig. 4.4 Gene expression kinetics in 7-day old *Arabidopsis* suspension cell culture after transfer from +Pi media to –Pi media.

Fig. 4.5 Gene expression kinetics in 5-day old *Arabidopsis* suspension cell culture after transfer from +Pi media to –Pi media.

Fig. 4.6 Gene expression in 5-day old *Arabidopsis* suspension cell culture.

Fig. 4.7 Gene expression kinetics in 5-day old *Arabidopsis* suspension cell cultures after transfer from +Pi media to –Pi media.

Fig. 4.8 Gene expression kinetics in 5-day old *Arabidopsis* suspension cell culture after transfer from +Pi media to –Pi media.

Fig. 4.9 Gene expression kinetics of phosphate starvation responsive genes in *Arabidopsis* suspension cell culture after exposure to 20μM CHX.

Fig. 4.10 Gene expression kinetics of phosphate starvation responsive genes in Pi-deplete *Arabidopsis* suspension cells after exposure to MG132

Fig. 4.11 Gene expression kinetics in 18-DAG *Arabidopsis* seedling roots after transfer from +Pi media to –Pi media.

Fig. 4.12 Gene expression kinetics in 18-DAG *Arabidopsis* root after transfer from +Pi media to –Pi media.

Fig. 5.1 Schematic structure of the *AtPht1;1* promoter deletion constructs

Fig. 5.2 Histochemical localization of GUS activity driven by full-length *Pht1;1* promoter in *Arabidopsis* root.

Fig. 5.3 Pht1;1::GFP fusion protein localization driven by *Pht1;1* native promoter in *Arabidopsis* lateral root tip under Pi starvation.

Fig. 5.4 Histochemical localization of GUS activity driven by full-length and truncated *Pht1;1* promoter in *Arabidopsis* root.

Fig. 5.5 Histochemical localization of GUS activity driven by full-length *Pht1;1* promoter without intron (*Pht1;1-FLΔI*) in *Arabidopsis* root.

Fig. 6.1 Amino acid sequence of Zat18 (At3g53600).

Fig. 6.2 Localization of VENUS tagged Zat18 in *Arabidopsis* root hair cells.

Fig. 6.3 Gene expression in *Arabidopsis* seedling roots under +Pi and –Pi conditions

Fig. 7.1 Gene expression in *Arabidopsis* seedling roots during Pi starvation.

Fig. 7.2 Venn diagram illustrates common and unique differential gene expression in different comparisons.

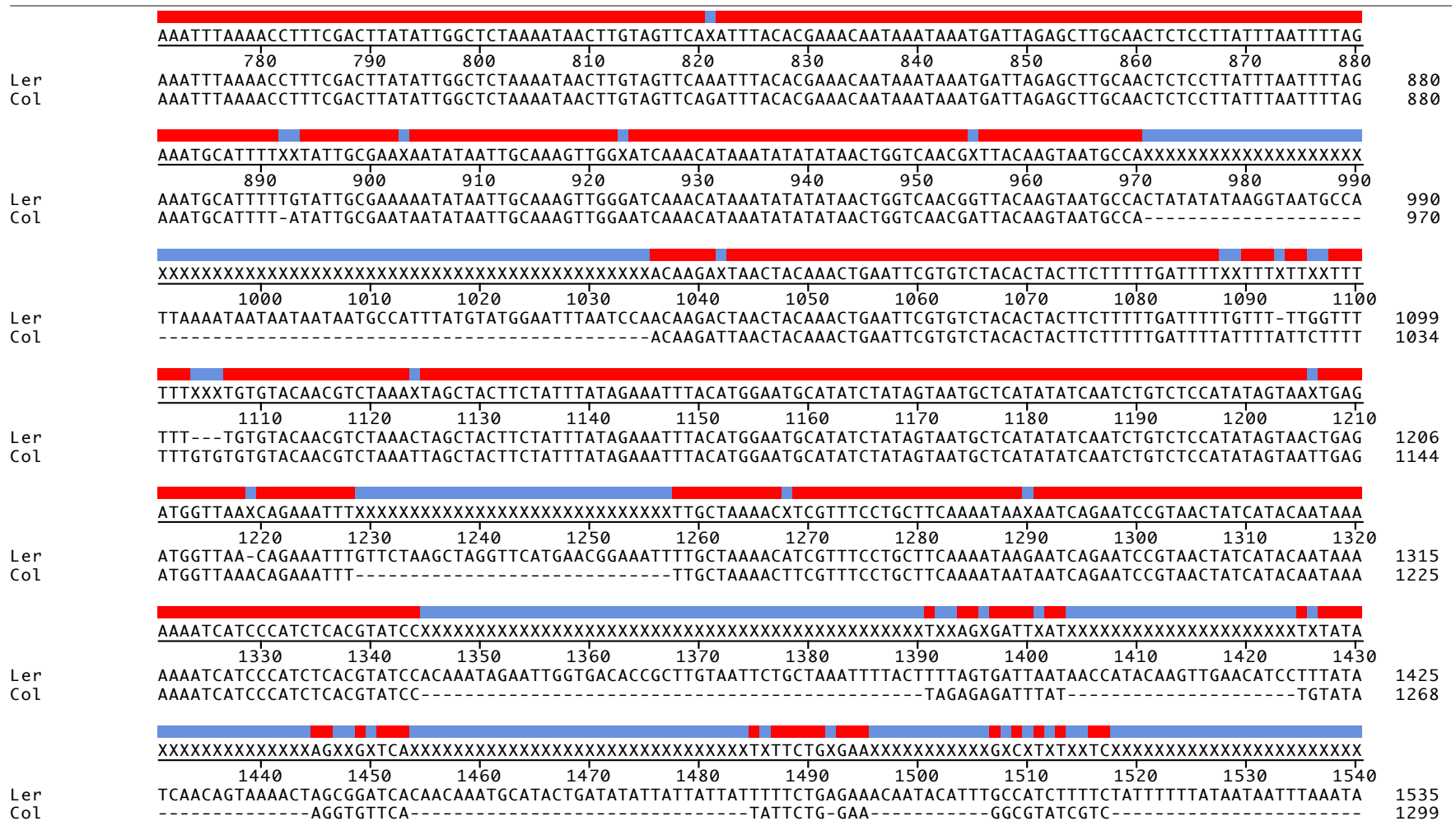
Fig. 7.3 Venn diagram illustrates common and unique differential gene expression in different comparisons.

Fig. 7.4 Venn diagram illustrates common and unique differential gene expression in different comparisons.

Appendix1: Alignment of gene sequence of Pht1;1 between Col-0 and Ler ecotype

Alignment is performed with Martinez-NW method in MegAlign package from Lasergene software V10.0 (DNASTAR inc.).

	GGCCTTTTCTTTTCTTTGCTTGTAGCCTTGTAATAATAGGAATGCCAAGGGCAAGTCCCTTGAAGAGCTCTCCGGTGAGGCTGAGGTTGAGAAATGATTACGCCATA	
	10 20 30 40 50 60 70 80 90 100 110	
Ler	GGCCTTTTCTTTTCTTTGCTTGTAGCCTTGTAATAATAGGAATGCCAAGGGCAAGTCCCTTGAAGAGCTCTCCGGTGAGGCTGAGGTTGAGAAATGATTACGCCATA	110
Col	GGCCTTTTCTTTTCTTTGCTTGTAGCCTTGTAATAATAGGAATGCCAAGGGCAAGTCCCTTGAAGAGCTCTCCGGTGAGGCTGAGGTTGAGAAATGATTACGCCATA	110
	ATATTTTCAAATTCCTTAATTGGTTCGATGAATTACATCTTCTATTACGATTTACTTTATTTTTGCGATGCGTAATGTGATATTTTCATGTTTCGTAATGGTGGATCTCTACA	
	120 130 140 150 160 170 180 190 200 210 220	
Ler	ATATTTTCAAATTCCTTAATTGGTTCGATGAATTACATCTTCTATTACGATTTACTTTATTTTTGCGATGCGTAATGTGATATTTTCATGTTTCGTAATGGTGGATCTCTACA	220
Col	ATATTTTCAAATTCCTTAATTGGTTCGATGAATTACATCTTCTATTACGATTTACTTTATTTTTGCGATGCGTAATGTGATATTTTCATGTTTCGTAATGGTGGATCTCTACA	220
	TTTATTTTTTTGTGTGACAAAATGTAATCAATCGATATTTAGTGGTCATTTATGATATTTATTTGACTGCTTATCTCTACTACACAGCTACTATCAAATTCCTAATCTTT	
	230 240 250 260 270 280 290 300 310 320 330	
Ler	TTTATTTTTTTGTGTGACAAAATGTAATCAATCGATATTTAGTGGTCATTTATGATATTTATTTGACTGCTTATCTCTACTACACAGCTACTATCAAATTCCTAATCTTT	330
Col	TTTATTTTTTTGTGTGACAAAATGTAATCAATCGATATTTAGTGGTCATTTATGATATTTATTTGACTGCTTATCTCTACTACACAGCTACTATCAAATTCCTAATCTTT	330
	GTTGTTATTATGGTTATATTTAATTTATGTCATGTAATACCTCTCGTATAACAACAAAACATTCAAACCATTTAAACATTAACGTGTACATATCGAAGTCCAGAAAACCC	
	340 350 360 370 380 390 400 410 420 430 440	
Ler	GTTGTTATTATGGTTATATTTAATTTATGTCATGTAATACCTCTCGTATAACAACAAAACATTCAAACCATTTAAACATTAACGTGTACATATCGAAGTCCAGAAAACCC	440
Col	GTTGTTATTATGGTTATATTTAATTTATGTCATGTAATACCTCTCGTATAACAACAAAACATTCAAACCATTTAAACATTAACGTGTACATATCGAAGTCCAGAAAACCC	440
	GTCATTTAAAACAAATACAATCCTCACATTTATATATATATATGGTCTGAGCTGGATTGGTTGATATTAATCCTTATTTATGTATATGTAATGGCAACTAAGTCCACTA	
	450 460 470 480 490 500 510 520 530 540 550	
Ler	GTCATTTAAAACAAATACAATCCTCACATTTATATATATATATGGTCTGAGCTGGATTGGTTGATATTAATCCTTATTTATGTATATGTAATGGCAACTAAGTCCACTA	550
Col	GTCATTTAAAACAAATACAATCCTCACATTTATATATATATATGGTCTGAGCTGGATTGGTTGATATTAATCCTTATTTATGTATATGTAATGGCAACTAAGTCCACTA	550
	AGGCATGAATTATCTGTTAAATGAATTTATGCTTATGTTCTCGCGAATATCCTATGTTTTTGAATATGCTTTTTTAAATAATGATTTTGACTTTGCTAAATGATA	
	560 570 580 590 600 610 620 630 640 650 660	
Ler	AGGCATGAATTATCTGTTAAATGAATTTATGCTTATGTTCTCGCGAATATCCTATGTTTTTGAATATGCTTTTTTAAATAATGATTTTGACTTTGCTAAATGATA	660
Col	AGGCATGAATTATCTGTTAAATGAATTTATGCTTATGTTCTCGCGAATATCCTATGTTTTTGAATATGCTTTTTTAAATAATGATTTTGACTTTGCTAAATGATA	660
	ATTAATCTTCATGACTATATGTATCCTGATTGTCACTCCTCAAATGTCAACTATTAGAGTTGAATAACTCGACTGCAAAAAACAAAACAAAGAAAACGAGGAAGATGGAG	
	670 680 690 700 710 720 730 740 750 760 770	
Ler	ATTAATCTTCATGACTATATGTATCCTGATTGTCACTCCTCAAATGTCAACTATTAGAGTTGAATAACTCGACTGCAAAAAACAAAACAAAGAAAACGAGGAAGATGGAG	770
Col	ATTAATCTTCATGACTATATGTATCCTGATTGTCACTCCTCAAATGTCAACTATTAGAGTTGAATAACTCGACTGCAAAAAACAAAACAAAGAAAACGAGGAAGATGGAG	770



146

Ler	2320	2330	2340	2350	2360	2370	2380	2390	2400	2410	2420	2402
Col	1638											
Ler	2430	2440	2450	2460	2470	2480	2490	2500	2510	2520	2530	2509
Col	1748											
Ler	2540	2550	2560	2570	2580	2590	2600	2610	2620	2630	2640	2616
Col	1856											
Ler	2650	2660	2670	2680	2690	2700	2710	2720	2730	2740	2750	2726
Col	1966											
Ler	2760	2770	2780	2790	2800	2810	2820	2830	2840	2850	2860	2836
Col	2076											
Ler	2870	2880	2890	2900	2910	2920	2930	2940	2950	2960	2970	2946
Col	2186											
Ler	2980	2990	3000									2983
Col												2223